Fall 8-10-2012

Biochemical Evaluation of SRH Analogs as Potential LuxS Inhibitors

richa gupta
rgupta5@dons.usfca.edu

Biochemical Evaluation of SRH Analogs as Potential LuxS Inhibitors

A Thesis Presented to the Faculty
of the Department of Chemistry
at the University of San Francisco, California
In Partial Fulfillment of the Requirements for the Degree of
Masters of Chemistry

Written by

Richa Gupta
07/15/12

ACKNOWLEDGEMENTS

I would never have been able to finish my research without the guidance of my graduate advisor, help from friends, and support from my family and husband.

I would like to express my deepest gratitude to my advisor, Dr. Megan Eileen Bolitho, for her excellent guidance, caring, patience, and providing me with an excellent atmosphere for doing research. I would like to thank Dr. Christina Tzagarakis-Foster, Dr. Juliet Spencer, Dr. John Sullivan, Lhia Krista Dolores and Angela S. Pletcher who helped me in resolving the issues I came across during my research work. I would like to thank Dr. Julia Van Kessel for helping me with the achievement of LuxS mutants by suggesting the use of non-overlapping primers. I would like to thank Dr. Larry Margerum and Dr. Christina Tzagarakis-Foster for their guidance and advice in writing this thesis.

I would like to thank Ruoyi Liu, who as a good friend, was always willing to help and give her best suggestions. It would have been a lonely lab without her. Many thanks to Jeff Oda, Andy Huang, Chad Schwietert, Deidre Huberty Shymanski, Yishun Qin, Keeshia Wang, Emily Showell-Rouse and others in the Department of Chemistry for helping me at various stages of my research. My research would not have been possible without their helps.

I would also like to thank my parents, two brothers, and my sister. They were always supporting me and encouraging me with their best wishes. Finally, I would like to thank my husband, Arvind Gupta. He was always there cheering me up and stood by me through the good times and bad.

TABLE OF CONTENTS

LIST OF FIGURES

LIST OF TABLES

ABSTRACT

Quorum sensing in bacteria is a process of cell-to-cell communication facilitated by small molecules called autoinducers. Interspecies quorum sensing is facilitated by the autoinducer AI-2. The enzyme LuxS catalyzes the formation of AI-2 from *S*-ribosyl homocysteine (SRH) in a wide variety of bacterial species. Inhibition of LuxS would therefore inhibit interspecies quorum sensing. The goal of this project is to establish biochemical assays for the evaluation of small molecules as potential LuxS inhibitors. The first assay is a conventional colorimetric assay that utilizes Ellman's reagent to quantify the homocysteine byproduct of DPD production by LuxS. For this assay purified enzyme (LuxS), a negative control (LuxS C84A), and the substrate (SRH) are required. His-tagged LuxS and LuxS C84A have been purified from overexpression cultures of *Escherichia coli* cells freshly transformed with a vector harboring the appropriate gene. Chemically-synthesized and quantified SRH was also acquired after extensive efforts of our fellow organic chemists. Ellman's assay was then performed to determine the activity of house-purified LuxS. This assay would be optimized in future to be performed in 96 well plate to avoid excess consumption of enzyme and substrate. In addition, a fluorescence proximity assay is envisioned for the evaluation of a subset of LuxS inhibitors that function by preventing protein dimerization. This assay requires that purified LuxS be conjugated with an appropriate fluorophore, likely via a cysteine residue. An appropriate LuxS variant i.e. LuxS Y71C to which a single fluorophore would attach was acquired after extensive troubleshooting. An appropriate fluorophore would be attached to this LuxS variant for determination of potential dimerization inhibition.

CHAPTER 1: INTRODUCTION

Behaviors such as bioluminescence, biofilm formation, and motility are examples of behaviors most effective when performed collectively by a group of bacteria.[1] The regulation of gene expression to perform these behavioral responses in response to cell population in bacteria is termed quorum sensing.[1] The basic process of quorum sensing involves three prime characters: (1) synthase, (2) signal, and (3) sensor. The synthase plays the key part because it initiates the process of quorum sensing by synthesizing small-molecule signals called autoinducers (AI). These signals, when received by the sensors at a threshold level, initiate gene expression for the aforementioned collective behavioral responses. (see Fig. 1.1)

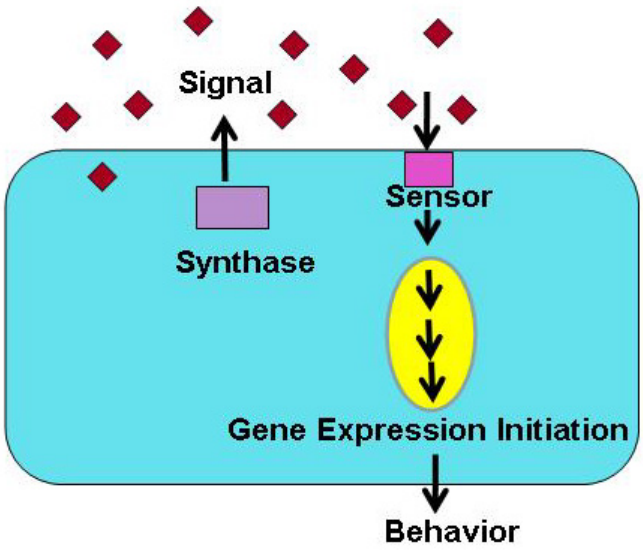

Fig. 1.1 | Quorum Sensing Model. The signals synthesized by the synthases are received by the sensor initiating a chain of reactions leading to bacterial behavioral responses.

1.1 | Quorum Sensing System Two: Interspecies Quorum Sensing. As of now, two major quorum sensing systems have been identified: System One which involves intraspecies communication and System Two involving interspecies communication.[2] System Two

quorum sensing is present in a wide variety of bacterial species.[3] Virulence expression in many human pathogens is one of the behavioral responses co-ordinated by System Two quorum sensing.[4] Virulence is the ability of bacteria to cause disease, and examples of bacterial species that utilize System Two quorum sensing for pathogenesis are listed in Table 1.1. Before targeting the host for pathogenesis interspecies quorum sensing helps these pathogenic bacteria to successfully infect the host by gathering a bacterial population density capable of overwhelming the immune system of the host. Therefore, System Two quorum sensing is a very apt target for the development of novel antimicrobial drugs against bacterial species that functions as human pathogens.

Table 1.1 | Bacterial Species Utilizing Quorum Sensing System Two for Pathogenesis. Some of the examples of the diseases caused by different bacterial species are shown.[3]

Species	Diseases
Actinobacillus actinomycetemcomitans	Periodontal disease
Borrelia burgdorferi	Lyme disease
Campylobacter jejuni	Food poisoning
Clostridium perfringens	Food poisoning
Escherichia coli	Intestinal and extra-intestinal infections
Neisseria meningitides	Bacterial meningitis (epidemic)
Porphyromonas gingivalis	Periodontal disease

To facilitate System Two quorum sensing, the enzyme *S*-ribosylhomocysteinase (LuxS), universally found in all bacterial species & involved in interspecies quorum sensing, acts as synthase to produce small molecule signals called autoinducer-2 (AI-2).[5,3] The AI-2 signal is

structurally different for different bacterial species, and the sensor which receives these small molecules as signals varies from one bacterial species to another bacterial species. Two examples of the different signals/AI-2 (*S*-THMF borate and *R*-THMF) received by different protein sensors LuxP (*Vibrio harveyi*) and LsrB (*Salmonella typhimurium*) are shown in Figure 1.2.[6]

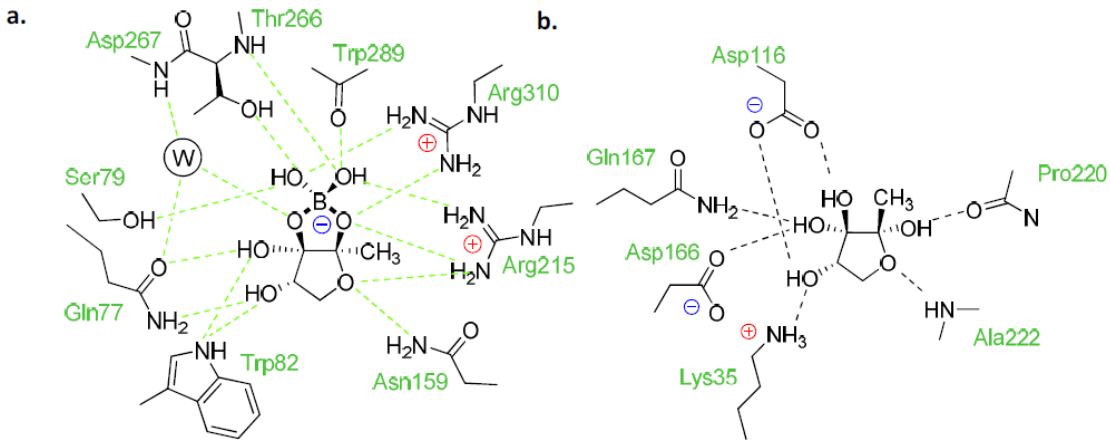

Fig. 1.2 | Sensors Bound to Autoinducer-2 Signals. a. The sensor LuxP in *Vibrio harveyi* recognizes *S*-THMF-borate as its AI-2 signal. b. The sensor LsrB in *Salmonella typhimurium* recognizes *R*-THMF as its AI-2 signal.[6b, 7]The image is taken from a paper by Chen et al.[6b]

1.2 | S-Ribosylhomocysteinase (LuxS). The goal of this research project is to develop biochemical assays capable of determining LuxS inhibition. LuxS is a 35 kDa homodimeric protein and is responsible for AI-2 biosynthesis (see Fig. 1.3).[8] The active site of this protein lies between the two identical monomers.[9]

Fig. 1.3 | Crystal Structure of LuxS. The crystal structure of *B.subtilis S*-ribosylhomocysteinase containing cobalt in place of the native iron atom (Co-BsLuxS) in complex with a catalytic intermediate (depicted in ball and stick model) is shown. The ribbon diagrams of the two monomers are shown in two colors, purple and green. The image is taken from a paper by Rajan et al.[10]

Initially, the metal ion in LuxS was proposed to be zinc (Zn^{2+}). It was later speculated by Pei et al. that due to the similarity of the environment surrounding the metal ion (i.e. presence of two histidines, a cysteine and water at the metal binding site) to another Fe^{2+} containing enzyme, peptide deformylase, the native metal ion could be Fe^{2+}.[8a, 11, 12] In order to test the identity of the metal present in LuxS, three LuxS variants containing metals Fe, Zn and Co were prepared by Pei and coworkers (see Table 1.2).[9] Based on the metal analyses and determination of catalytic activity, the native metal was Fe^{2+} in LuxS.[9] Due to the easy oxidation the Fe^{2+} ion under the aerobic conditions of enzyme purification, the iron ion is routinely replaced to cobalt by addition of cobalt chloride in the culture when bacterial cells

are in their exponential growth phase.[9] Pei and coworkers showed that the replacement of iron by cobalt in LuxS minimally affected the activity of the enzyme, yet facilitated its purification.[9] The catalytic activity of the three LuxS enzyme variants with iron, zinc, or cobalt is summarized in Table 1.2. The catalytic parameters compared were: (1) K_M: the binding affinity of substrate for the enzyme, (2) k_{cat}: the number of substrate molecules converted to product per unit time and (3) k_{cat}/K_M : the catalytic efficiency of the enzyme. As shown, the catalytic parameters of the two enzymes (i.e. Fe-LuxS-HT and Co-LuxS-HT) were comparable. The replacement of iron by cobalt did not bring any significant change in the enzyme's binding affinity (K_M), as well as the k_{cat} and catalytic efficiency (k_{cat}/K_M) values increased only by approximately two fold (see Table 1.2). Whereas the replacement of iron by zinc increased the value of K_M by approximately thirty fold and the value of k_{cat} by approx. four fold in comparison to the native iron containing LuxS (Fe-LuxS-HT). This led to decrease in overall catalytic efficieny (k_{cat}/K_M) of the enzyme (Zn-LuxS-HT) by nine fold (see Table 1.2).

Table 1.2 | Comparison of Catalytic Activity of LuxS Variants. The catalytic activities of LuxS enzymes with different metal ions present at the active sites are compared. The table is taken from a paper by Pei et al.[9]

Enzyme	K_M (μM)	k_{cat} (s^{-1})	k_{cat}/K_M ($M^{-1}s^{-1}$)
Fe-LuxS-HT	1.9 ± 0.2	0.018 ± 0.003	0.9 X 10^4
Co-LuxS-HT	2.3 ± 0.5	0.035 ± 0.003	1.6 X 10^4
Zn-LuxS-HT	58 ± 7	0.065 ± 0.008	0.1 X 10^4

The mechanism of biosynthesis of AI-2 from *S*-ribosyl homocysteine (SRH) in the presence of LuxS was first elucidated by Pei and coworkers.[9-10, 13] Figure 1.4 depicts substrate SRH, a

product of *S*-adenosyl homocysteine (SAH) (**2**) detoxification, where SAH is a byproduct of the numerous cellular methyl transfer reactions involving *S*-adenosyl methionine (SAM) (**1**). SAH is capable of inhibiting methyltransferases by competitive enzyme inhibition due to its structural similarity to SAM. Therefore, it is toxic to the cells and must be detoxified. In bacteria, SAH detoxification is done in two steps.[4, 14] First, the nucleosidase Pfs acts on SAH to give *S*-ribosyl homocysteine (SRH) (**4**) after removal of adenosine (**3**). In the second step, LuxS acts on SRH to produce 4(*S*),5-dihydroxy-2,3-pentanedione (DPD) (**5**) and homocysteine (HCys) (**6**). In eukaryotes, LuxS is absent.[15] Therefore, this detoxification is accomplished in one step by another enzyme, SAH hydrolase (SahH), with adenosine and homocysteine as the end products.[13a, 15-16]

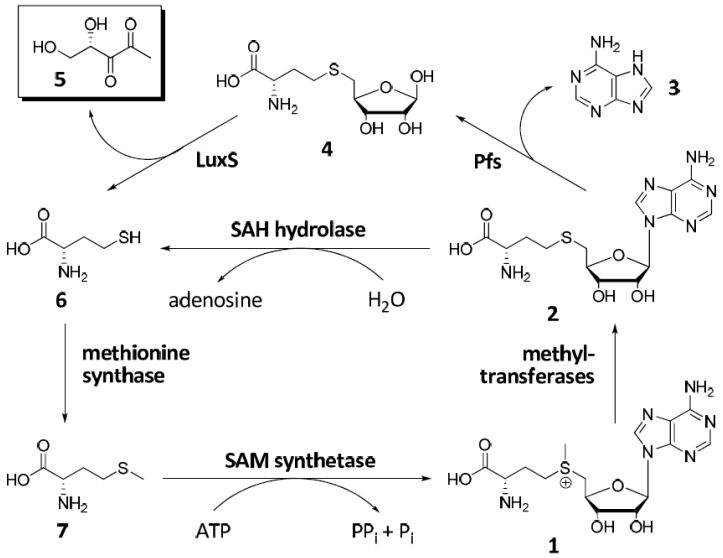

Fig. 1.4 | Biosynthetic Pathway of DPD (5). SAM (**1**) is converted to SAH (**2**) in presence of methyltransferases. Nucleosidase Pfs acts on SAH (**2**) to convert it into SRH (**4**) by removing adenosine. LuxS acts on SRH to convert it into homocysteine (**6**) and DPD (**5**). In eukaryotic cells SAH is detoxified by the action of SAH hydrolases, breaking SAH into adenosine and homocysteine (**6**). Methionine synthases acts on homocysteine to form methionine (**7**) which is converted to SAM (**1**) in presence of SAM synthetase.[5b]The image is taken from the paper by lowery et al. [14]

DPD forms the interspecies quorum sensing signal AI-2 upon cyclization.[17] The structure of AI-2 may vary from species to species and two examples of different AI-2 signals formed from DPD cyclization i.e. *Salmonella typhimurium* and *Vibrio harveyi* are given in Fig. 1.5.[2,14,18] DPD is a very unstable molecule and it polymerizes upon concentration, making it difficult to isolate from biological samples.[19]

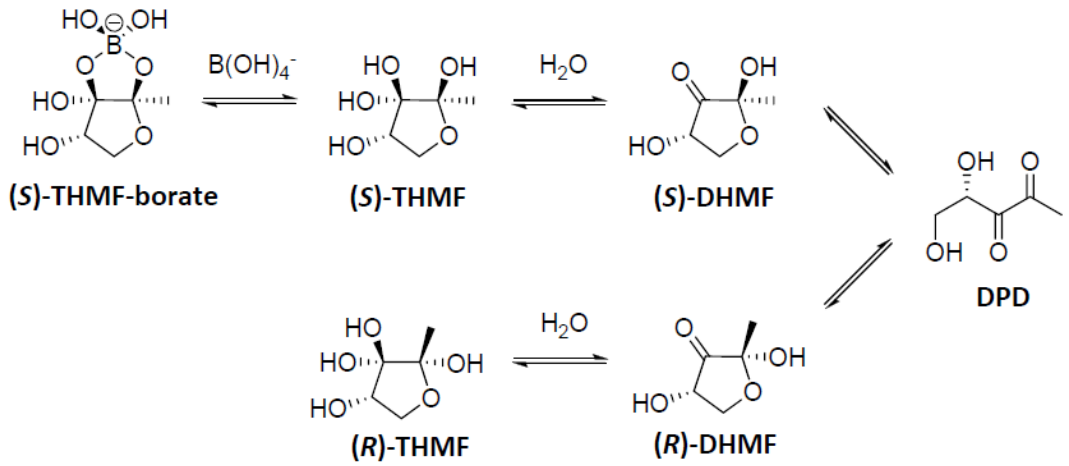

Fig. 1.5 | AI-2 Structures. *S*-THMF borate acts as AI-2 signal for *Vibrio harveyi* whereas *R*-THMF borate acts as AI-2 signal for *Salmonella typhimurium*.[5]

1.3 | LuxS Inhibition. Quorum sensing inhibition prevents virulence in some bacterial species. For example, quorum sensing deficient strains of pathogenic *Pseudomonas aeruginosa* were unable to kill nematodes and amoebas.[21] Eukaryotes were found to use natural anti-quorum sensing strategies to fight against harmful bacteria via an increase in pH and the secretion of small quorum sensing inhibitor molecules such as halogenated furanones, patulin and penicillic acid (see Fig 1.6).[20] These natural defense mechanisms of eukaryotes against bacterial infections provided inspiration for the idea of interfering with the quorum sensing systems of pathogenic bacteria for the prevention of bacterial infections in humans using small molecules.

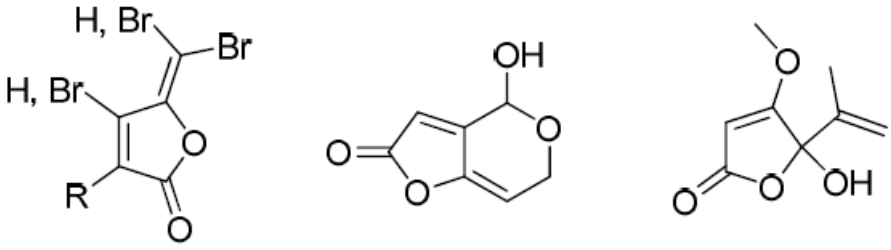

(A) **(B)** **(C)**

Fig. 1.6 | Quorum Sensing Inhibitors Found in Nature. (A) Halogenated furanones are secreted by the marine alga *Delisea pulchra*. **(B)** patulin and **(C)** penicillic acid are secreted by fungi to inhibit quorum sensing in *Pseudomonas aeruginosa*. The images are taken from the paper by Givskov et al. and Rasmussen et al. [20b,20c]

The virulence inhibition by bacteria utilizing System Two quorum sensing is envisioned by inhibiting LuxS. The *luxS* gene has been identified in over 70 species, mostly utilizing quorum sensing for virulence expression (see Table 1.1), and makes LuxS a very attractive target.[14] The inhibition of LuxS would inhibit AI-2 biosynthesis and, therefore, interspecies quorum sensing. One of the benefits of targeting LuxS is that it is absent in humans, allowing novel drugs to be designed that would inhibit LuxS and would likely be minimally toxic. In order to evaluate potential LuxS inhibition, the IC_{50} value of the inhibitor must be determined, which is the concentration of inhibitor needed to inhibit half of the maximum activity of LuxS through Ellman's assay. Research directed at accomplishing LuxS inhibition by small molecules, both *in vitro* and *in vivo* include a competitive LuxS inhibitor as in Figure 1.7. This rationally-designed molecule gave a half maximal inhibitory concentration (IC_{50}) value of 4.7 ± 1.7 μM against LuxS *in vitro*.[21]

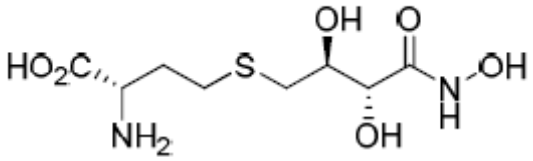

Fig. 1.7 | Example of a Competitive LuxS Inhibitor. (*S*)-2-amino-4-((2*S*, 3*R*)-2,3-dihydroxy-4-(hydroxyamino)-4-oxybutylthio)butanoic acid is shown to inhibit LuxS with an IC_{50} value of 4.7 ± 1.7 μM.[21] The image is taken from a paper by Shen et al. [21]

Organic chemists in our lab are working towards synthesizing a new class of LuxS inhibitors. These inhibitors are designed to inhibit LuxS by inhibiting its dimerization of LuxS. Dimerization inhibitors like these have been reported previously for other enzymes.[22] One example of a small molecule dimerization inhibitor is TSAO-T ([2',5'-bis-O-(tert-butyldimethylsilyl)-β-D-ribofuranosyl]-3'-spiro-5''-[4''-amino-1'',2''-oxathiole-2'',2''-dioxide]), the first inhibitor to inhibit dimerization of HIV-1 reverse transcriptase enzyme.[22a] (Figure 1.8) This is a key enzyme and plays a vital role in the life cycle of the virus (responsible for HIV). Therefore, it is a target for antiviral intervention.[22a]

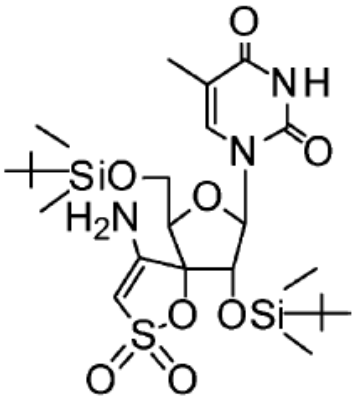

Fig. 1.8 | Example of Small Molecule Dimerization Inhibitor. TSAO-T (([2',5'-bis-O-(tert-butyldimethylsilyl)-β-D-ribofuranosyl]-3'-spiro-5''-[4''-amino-1'',2''-oxathiole-2'',2''-dioxide]) interferes with the dimerization of HIV-1 reverse transcriptase. The image is taken from the paper by Camarasa et al.[22a]

The enzyme HIV-1 reverse transcriptase (HIV-1 RT) is a heterodimer.[22b] His-tagged p51 and Flag-tagged p66 protein subunits for this enzyme were prepared and purified using Flag/His columns.[22b] The HIV-1 reverse transcriptase assay was used to assay dimerization inhibition of HIV-1 reverse transcriptase enzyme by TSAO-T through determination of IC_{50} values. In this assay an anti-FLAG detector antibody conjugated with e-tag was added to the Flag/His-tagged p66/p51 HIV-1 RT.[22b] (see Figure 1.9) In dimeric state this e-tag is released which in turn releases methylene blue, which is detected to determine potential dimerization inhibition in presence of an inhibitor as in this case TSAO-T.[22b] Dimerization inhibition of this enzyme by a TSAO-T molecule inhibits the essential role played by this enzyme in the virus, demonstrating its therapeutic use. Before performing the real assay, docking studies were also performed using PyMol to test the TSAO-T as potential inhibitor.

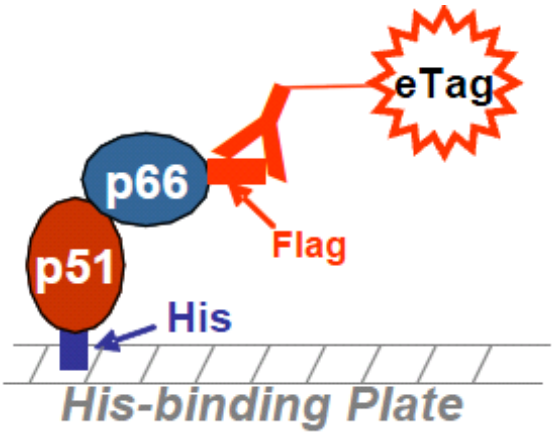

Fig. 1.9 | HIV-1 Reverse Transcriptase Assay. Anti-Flag detector antibody conjugated with e-tag is added to the His/Flag-tagged p66/p51 HIV-1 reverse trancriptase. The image is taken from the paper by Camarasa et al.[22b]

The use of dimerization inhibitors for LuxS is something that has not been attempted before. The introduction of steric bulk at the homocysteine C3 and/or C4 positions of SRH is expected to inhibit LuxS dimerization by imposing the steric bulk at the active site (see Fig.

1.10). The inability of LuxS to dimerize properly could inhibit AI-2 production and therefore interspecies quorum sensing.

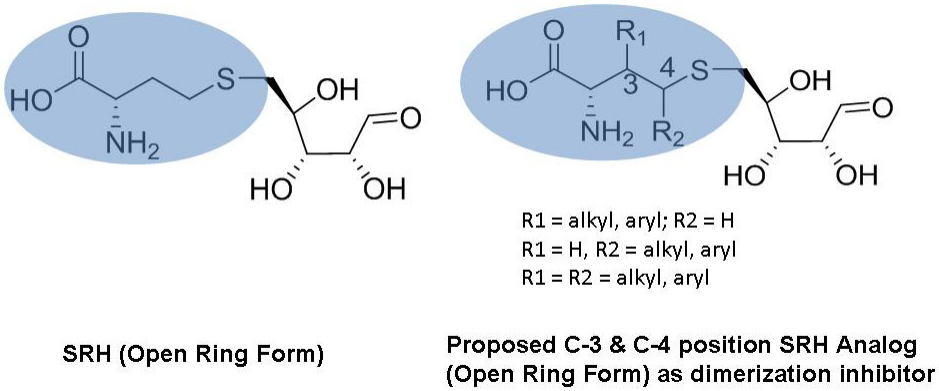

Fig. 1.10 | Proposed LuxS Dimerization Inhibitors. Introduction of a steric bulk at the HCys C3 and/or C4 positions of SRH is expected to interfere with LuxS dimerization, thereby inhibiting LuxS and interspecies quorum sensing.

The project goal is to evaluate such SRH analogs as potential LuxS inhibitors by two biochemical assays: (1) Ellman's assay, and (2) fluorescence proximity assay.

1.4 | Ellman's Assay. Ellman's assay is the measurement of protein sulfhydryls in presence of 5,5'-dithiobis(2-nitrobenzoic acid) (DTNB) at a wavelength of 412 nm (see Fig. 1.11).[24] It used as a biochemical assay for the assessment of putative SRH analogs as LuxS inhibitors.[9, 23] For example, it was used for assessment of (*S*)-2-amino-4-((2*S*, 3*R*)-2,3-dihydroxy-4-(hydroxyamino)-4-oxybutylthio) butanoic acid as potential competitive LuxS inhibitor (see Fig. 1.7). Homocysteine has thiol group (-SH), a byproduct of LuxS action on SRH, and reacts with DTNB and breaks the disulfide linkage, splitting DTNB into two halves (see Fig. 1.11). One half of this DTNB joins with the thiol group of homocysteine to form a conjugate with a disulfide linkage. The other half, 2-nitro-5-thiobenzoate, is quantified by measuring

the absorbance of visible light at 412 nm. The quantification of 2-nitro-5-thiobenzoate indicates the presence of homocysteine and therefore of DPD in the reaction mixture, thus determining LuxS activity.

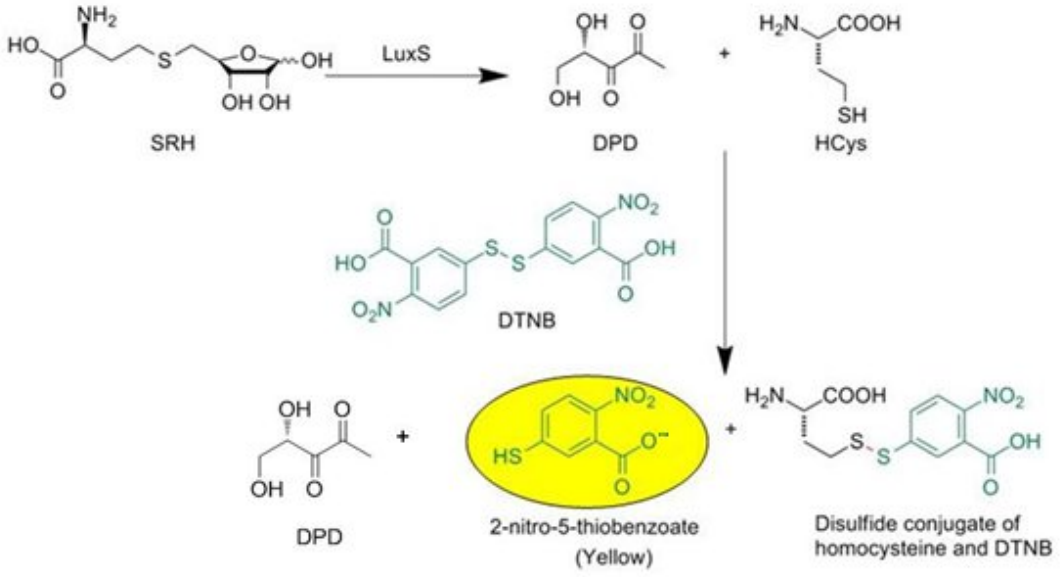

Fig. 1.11 | Ellman's Assay for Detection of LuxS Activity. SRH converts into DPD and homocysteine (HCys) in the presence of LuxS. Homocysteine reacts with DTNB to form a conjugate, whereas the remaining half of DTNB gives a yellow color to the reaction mixture which is measured at 412 nm.

The presence of an SRH analog that inhibits LuxS (e.g. *S*-anhydroribosyl-L-homocysteine) in the reaction mixture should prevent the formation of homocysteine. Therefore, there will be only a minimal increase in absorbance at 412 nm with respect to blank as compared to the increase in absorbance in the presence of SRH alone (see Fig. 1.12). This difference in recorded absorbances enables an assessment of a potential SRH analog that would be able to inhibit LuxS and therefore interspecies quorum sensing.

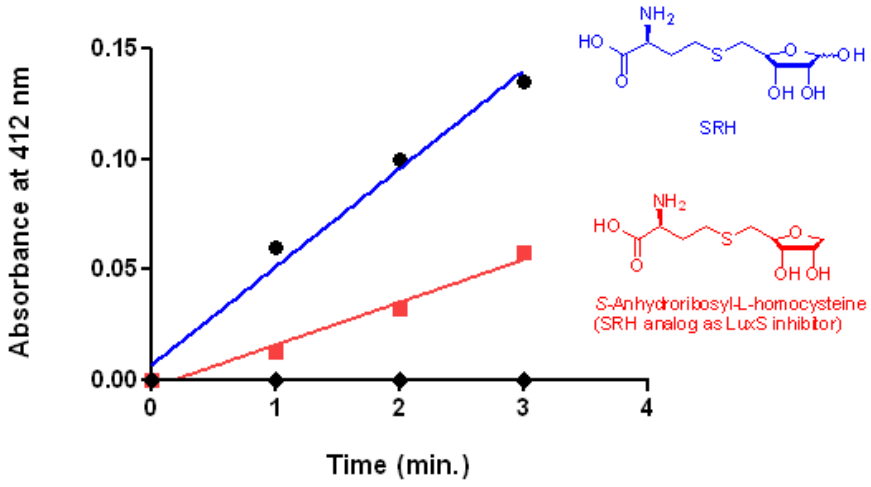

Fig. 1.12 | Ellman's Assay in the Presence of a LuxS Inhibitor. (A) Increase in absorbance at 412 nm is recorded in presence of SRH alone in the reaction mixture. (B) Minimal increase in absorbance at 412 nm is recorded in the presence of a potential LuxS inhibitor. Figure generated from raw data provided by Alfaro, et al. [25]

Ellman's assay is a reliable assay, known to work for the evaluation of LuxS inhibitors. It is time efficient because the absorbance measurements are taken over only 204 seconds. This assay also enables the determination of the catalytic parameters of the enzyme, which could be compared with the other enzyme variants for comparison of their respective catalytic efficiencies. However, there are also some drawbacks to this assay. First, surface thiols on LuxS can react with Ellman's reagent even in the absence of the substrate. Second, an active enzyme is required for this assay, but the iron containing enzyme LuxS turns inactive when purified in aerobic conditions due to oxidation of iron. Third, a high volume of the reaction mixture (1 mL) is required. To prepare a 1 mL reaction mixture requires 10 µL of the 40 µM purified enzyme and 30 µL of 680 µM purified SRH. Hence, a substantial amount of enzyme and substrate is consumed in this assay, each of which is acquired only after extensive effort. The final disadvantage of using this assay for the evaluation of LuxS inhibitors is the inability

to determine whether the inhibition was achieved by typical competitive or dimerization inhibition.

Despite its drawbacks, the Ellman's assay will be used to evaluate LuxS inhibitors because it is the standard assay in the field. The preparation of an active enzyme and a negative control for this assay as well as optimization of this assay in our lab conditions are presented in Chapter 3.

1.5 | Fluorescence Proximity Assay. To overcome one of the drawbacks of the Ellman's assay-determining the kind of inhibition by a particular inhibitor-a fluorescence proximity assay is envisioned for the evaluation of potential SRH analogs as dimerization inhibitors of LuxS. The disruption of dimerization of a dimeric protein is possible given an inhibitor that binds between two protein monomers. The dimerization disruption could be determined when artificial fluorophores are incorporated onto each monomer at appropriate positions (see Fig. 1.13).[26]

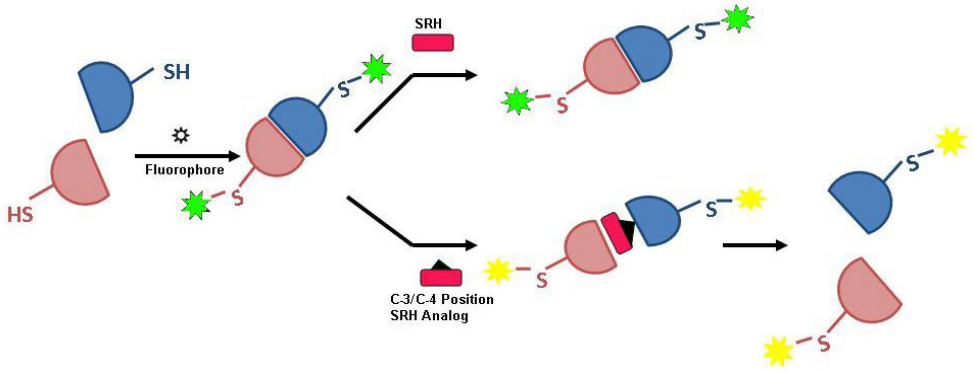

Fig. 1.13 | Fluoroscence Proximity Assay for LuxS. In the presence of SRH as substrate, a fluorophore-attached active LuxS variant would be present as a dimer. Whereas in the presence of a C-3/C-4 position SRH analog, the steric bulk present on the analog could impose hindrance in the dimerization, resulting in dimer disruption and therefore a change in proximity of the LuxS monomers.

Fluorescence proximity assays have literature precedents for other enzymes but not for LuxS.[26] For example, this type of assay was developed for the enzyme HIV-1 protease. One of the key steps in the life cycle of a human immunodeficiency virus (HIV) is the proteolytic cleavage of the viral polyprotein gene products into active structural and replicative proteins. The viral enzyme HIV protease is responsible for these precursors, and its inactivation would produce immature and non-infectious viral particles. These findings initiated a chain of intense research to inhibit this enzyme by synthetic inhibitors.[26] HIV-1 protease is a homodimer with each monomer contributing equally to the active site. The fluorescence proximity assay for HIV-1 protease was based on an HIV-1 expression assay using cyan and yellow fluorescent protein tagged monomers. Non-peptidyl small molecules including darunavir and experimental protease inhibitors were used as dimerization inhibitors for this enzyme (see Fig. 1.14). When the two HIV-1 protease monomers attached to CFP and YFP were in close proximity, a focused laser beam excitation of CFP resulted in rapid energy transfer to YFP and the fluorescence photons were emitted by YFP. In the presence of a dimerization inhibitor of HIV-1 protease, the average distance between CFP and YFP became larger, therefore the energy transfer rate decreased, and the fraction of photons emitted by YFP was lowered. The dimerization inhibition by these inhibitors was monitored and their IC_{50} (concentration of inhibitors required to inhibit viral replication by 50%) values were determined for the potential inhibitors.

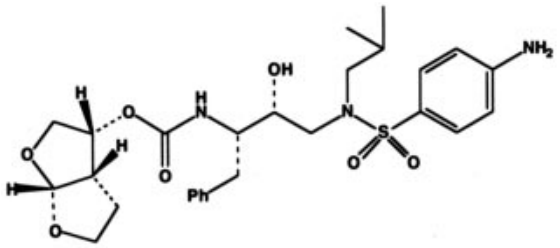

Darunavir

Fig. 1.14 | Dimerization inhibitor for HIV-1 Protease. Darunavir was one of the dimerization inhibitors used for the inhibition of HIV-1 protease. The IC_{50} value recorded for this inhibitor was 0.0034 ± 0.0005 μM.[26] The image is taken from the paper by Mitsuya, et al. [26]

In the case of LuxS, the presence of SRH in the reaction mixture would promote dimerization and therefore fluorophore proximity (see Fig. 1.13). For the evaluation of potential SRH analogs as dimerization inhibitors, change in fluorescence needs to be measured. When a C3/C4 position SRH analog binds to a fluorophore-attached LuxS variant, the steric bulk present on the inhibitor inhibits enzyme dimerization, and the resultant changed relationship between the two monomers of LuxS causes a change in fluorescence.

The measured change in fluorescence with time would be correlated to LuxS dimerization inhibition. Work towards the successful generation of a LuxS variant for use in the proposed fluorescence proximity assay is discussed in Chapter 4.

CHAPTER 2: MATERIALS AND METHODS

2.1 | Protein Purification. The requirements and the method for the purification of protein are discussed as follows:

2.1.1 | Chemical Reagents. Cobalt chloride ($CoCl_2$), sodium chloride (NaCl), ethanol, manganese chloride ($MnCl_2$), borate (H_3BO_3), ammonium molybdate ($(NH_4)_6Mo_7O_{24}$), copper sulfate ($CuSO_4$), hydrogen chloride (HCl), D-glucose, ammonium sulfate ($(NH_4)_2SO_4$), potassium phosphate dibasic (KH_2PO_4), and potassium phosphate monobasic (K_2HPO_4) were purchased from Sigma Aldrich.

2.1.2 | Biochemical Reagents, Kits and Supplies. Casamino acids and LB agar were purchased from BioWorld. Site directed mutagenesis kit and BL21(DE3) competent cells were purchased from Agilent Technologies. Ampicillin sodium salt and vacuum filtrations (nylon membranes, sterile) systems were purchased from VWR. TALON® Resin was purchased from Clontech laboratories. GeneJET™ plasmid purification kit, PageBlue™ protein staining solution, Tris EDTA (TE) buffer, PageRuler™ plus prestained protein ladder, bovine serum albumin (BSA) standard kit, Bradford dye, 1 kb DNA ladder and 100 bp DNA ladder were purchased from Fermentas.

2.1.3 | Literature Procedure for Purification of Co-BsLuxS-HT. The procedure for the purification of Co-BsLuxS-HT was reported in the paper by Pei et al. [9]

2.1.4 | Preparation of Reagents. The reagents required for the purification procedure were prepared as follows: **(a)** Co-BsLuxS-HT Minimal Media (1 L). First, 1000 X trace metals

solution was prepared by adding 500 mM $MgSO_4$, 0.5 mM NaCl, 0.1 mM $MnCl_2$, 0.5 mM H_3BO_3, 1 μM $(NH_4)_6Mo_7O_{24}$ and 10 μM $CuSO_4$ in 10 mL of 0.1 M HCl. Solution was then filtered through a stericup. 100 X sugar stock solution was prepared by adding 25% D-glucose, 200 μg/mL thiamin, 100 μg/mL D-biotin and 10% $(NH_4)_2SO_4$ in 500 mL of hot distilled water. Solution was then filtered through a Stericup. Finally, for 1 L LuxS minimal media, 5.5 g KH_2PO_4, 10.8 g K_2HPO_4, 10 g NaCl and 5 g casamino acids were mixed into 989 mL distilled water. 1 mL of 1000X trace metals stock solution was added to the solution. 10 mL of 100 X sugar stock solution was added to the solution. The media was then filtered through a stericup with 0.45 μM pore size. **(b)** LB Amp^{75} Media (1 L). To 800 mL H_2O was added the following: 10 g bacto-tryptone, 5 g yeast extract, 10 g NaCl. The pH was adjusted to 7.5 with NaOH and the volume was adjusted to 1 L with distilled water. The media was then autoclaved for 15 min. at 121°C. After media cools, add 750uL of 100mg/mL ampicillin. **(c)** 100 mM $CoCl_2$ (50 mL). To 0.65 g of $CoCl_2$ 50 mL distilled water was added and then stored for future use at room temperature. **(d)** 100 mM Isopropyl β-D-1-thiogalactopyranoside/IPTG (50 mL). IPTG was weighed 1.19 g and added to 50 mL of distilled water and mixed on a magnetic stirrer. 1 mL aliquots were prepared and kept in the freezer at -80°C for future use. **(e)** Preparation of the Freezer Stocks. To prepare freezer stocks 750 μL of the bacterial cultures grown in LB Amp^{75} media were added to 250 μL of 80% glycerol in a 1.5 mL Eppendorf tube and stored in freezer at -80^{o}C. **(f)** Buffers**.** For preparation of mechanical lysis buffer a solution of 20 mM Tris·HCl (pH 8.0), 400 mM NaCl, 5 mM imidazole (pH 8.0) was prepared. To prepare chemical lysis buffer a solution with 20 mM Tris·HCl (pH 8.0), 0.5 M NaCl, 5 mM imidazole, 1% Triton X-100, 0.5% protamine sulfate, 20 μg/mL trypsin inhibitor, 50 μg/mL p-methylbenzenesulfonyl fluoride, and 70 μg/mL chicken egg white lysozyme was prepared. The Elution Buffer was made

consisting of 20 mM Tris·HCl (pH 8.0), 400 mM NaCl, 60 mM imidazole (pH 8.0). For the preparation of 10X running buffer, 30.3 g of trizma base, 144.0 g of glycine, 10 g of SDS was added to 1000 mL of distilled water and stirred into a homogenous mixture. **(g)** Preparation of 12.5% SDS-PAGE Gels. To make a 12.5% gel, a stacking gel solution and a separating gel solution were made. For preparation of the separating gel solution, 3.35 mL of distilled water, 2.5 mL of 1.5 M Tris·HCl (pH 8.8), 55 µL of 20% SDS, 4 mL of Acrylamide/Bis, 80 µL of 10% ammonium per sulfate (APS) were added. 8 µL of tetramethylethylenediamine (TEMED) was added last. For the stacking gel solution, 6.1 mL of distilled water, 2.5 mL of 0.5 M Tris·HCl (pH 6.8), 55 µL of 20% SDS, 1.3 mL of 30% Acrylamide/Bis, 80 µL of 10% APS were added. 8 µL of TEMED was added last. Bio-Rad Mini-PROTEAN® Tetra handcast gel frame for two gels was set up. First the separating gel solution was poured up to 3/4th height of the gel frame and allowed to solidify. Isopropanol was immediately added to level the surface of the gel. After the gel was set (as could be seen from the leftover solution) isopropanol was removed by soaking into paper towels. The stacking gel was then added into the remaining space and combs were placed at the top of the gel frame. Once the gel has solidified, it was stored in the refrigerator by wrapping it in wet paper towels and parafilm.

2.1.5 | Co-BsLuxS-HT Purification. A 5 mL LB Amp^{75} media containing the desired bacterial cells (ELS 1409 with Co-BsLuxS-HT cells) was grown for 16 hours at 37°C. 5 mL culture was then backdiluted to 50 mL Co-BsLuxS-HT minimal media Amp^{75} in a ratio of 1:1000 and grown for 16 hours at 37°C. 50 mL culture was then backdiluted to 2 L of Co-BsLuxS-HT minimal media Amp^{75} in a ratio of 1:50. The 2 L culture was then grown to an OD_{600}~0.6 at 37°C. 1 mL of the media was saved as blank for the measurement of O.D. of the culture. 500 µL of the 100 mM $CoCl_2$ stock was then added and the culture was incubated for

30 min. at 30°C. After 30 min, 250 µL of 100 mM IPTG was added. The culture was incubated for 16 hours at 30°C. After 16 hours the culture was centrifuged at 5000 rpm keeping the temperature of the centrifuge at 4°C to get a big pellet. The pellet was resuspended in 35 mL mechanical lysis buffer. The resuspended cells were lysed by French press at approximately 20,000 psi and then centrifuged to get a supernatant containing the Co-BsLuxS-HT protein. To purify the protein, supernatant was passed through TALON® cobalt resin column. The column was previously washed with 10 mL each of distilled water and mechanical lysis buffer. After passing the supernatant through the cobalt resin column, the column is then washed with 35 mL mechanical lysis buffer. The 40 mL of elution buffer was added to the column to elute the desired protein. Then 40 blue fractions of 1 mL purified protein were obtained containing the desired protein in elution buffer. Later 40 mL of purified protein was concentrated using YM-10 centriprep tubes to a dark purple solution by centrifugation at temperature 4ºC and at a speed of 5000 rpm for approximately 2 to 3 hours. The purified protein was then mixed with 80% glycerol (30-33% of the entire volume) and frozen at -80°C for future use in activity assays.

2.1.6 | Measurement of Protein Concentration by Bradford Dye Assay. For measuring protein concentration by Bradford dye assay, absorbance values for the bovine serum albumin (BSA) standards were measured in triplicate to obtain a standard curve. The volume and concentrations of BSA standards used were as given in Table 2.1 below. Transparent 96 well plates with transparent bottoms were used for the assay, which were bought from Costar (part no. 3598). A volume of 300 µL of Bradford dye was added to each well and absorbance values at 595 nm are measured after a delay of 8 min using EnVision® multlilabel reader. A delay of 8.0 min gives stable color change whose absorbance could be recorded at 595 nm.

Table 2.1 | Bradford dye assay. The concentration and volumes of BSA standards to be added for the standard curve are shown in the table above.

BSA std. conc. mg/mL	Volume of BSA std used (µL)	Amount of BSA (µg)
0	0	0
0.125	4	0.5
0.25	6	1
0.25	4	1.5
0.5	5	2
0.5	4	2.5
0.75	4.67	3
0.75	4	3.5
1	4	4

The dilutions 1:10, 1:20, 1:40, 1:80 of the protein were prepared, and absorbance values were measured at 595 nm along with undiluted protein in triplicate. After recording the absorbance values in triplicate a curve was made using the averaged absorbance values of the BSA standards (corrected from blank absorbance value). The curve gave a linear equation, which was used for the calculation of the protein concentration for absorbance values falling inside the standard curve.

2.1.7 | SDS-PAGE Gel. To run a SDS-PAGE gel a 5 mL pellet of the bacterial cells (acquired during centrifugation of 2 L culture) was resuspended in 1 mL of chemical lysis buffer by pipetting up and down gently. Before sonication, 500 µL of the resuspended cells were saved as the whole cell (WC) samples. Cells were then lysed by sonication in Eppendorf tubes for 5 min at 4°C. 250 µL of the cells lysed by sonication was then centrifuged at 8000 rpm and at a temperature of 4ºC. Supernatant of the centrifuged sample was loaded on an SDS-PAGE. A volume of 12 µL of all three samples (i.e. whole cell (WC), sonicated (S) and sonicated as well as centrifuged (CS) samples) was added to 4 µL of the loading dye in PCR tubes. Samples were heated for 10 min at 95°C and loaded onto a 12.5% SDS-PAGE along

with the ladder (L). The gel was run for ~45 min at 150 V and stained with ~30 mL of PageBlue protein staining solution (Fermentas) overnight on a belly dancer/shaker. Next day the gel was destained by 10% acetic acid solution until all the excess dye washes away. The gel was then viewed using the software Quantity One program (Bio-Rad) and a gel picture is acquired using a Bio-Rad Chemi Doc.

2.2 | Negative Control Co-BsLuxS-HT C84A. The procedure for acquiring a negative control for the Ellman's assay is discussed in the following sections:

2.2.1 | Biochemical Reagents, Kits and Supplies. QuikChange® II XL Site-Directed. Mutagenesis Kit, BL21(DE3) pLys competent cells were bought from Agilent Technologies Stratagene. LB agar and ampicillin sodium salts were purchased from VWR. GeneJET™ Plasmid Miniprep Kit was purchased from Fermentas. All designed primers were sent to Integrated DNA Technologies (IDT) for synthesis. Pellet Paint® Co-Precipitant was purchased from EMD4Biosciences, SOC medium from Sigma-Aldrich.

2.2.2 | Preparation of LB Amp200 Media and Plates. For the preparation of plates 20 grams of LB agar was added to 998 mL of distilled water, which was stirred and heated until boiling. 2 mL of 100 mg/mL ampicillin stock solution was added to 998 mL of LB agar solution. The solution was then spread throughout the sterile VWR® petridishes, once it has cooled to room temperature. The media added was then allowed to solidify at room temperature. The method for preparation of LB Amp[75] Media is provided in Section 2.1.4.1.

2.2.3 | Site-Directed Mutagenesis. A wild type LuxS template was purified from a 5 mL LB Amp[75] culture using GeneJET™ plasmid purification kit. C84A overlapping primers were designed using PrimerX software. These primers were sent to be created by IDT. 100 mM stock and 10 µM working solutions of these primers were made in distilled water. In a PCR tube 36 µL of distilled water, 2 µL of DNA template (10 ng/µL), 1 µL of forward and reverse primers, 4 µL of 10X reagent buffer, 2 µL of dNTP, 3 µL of quick solution and 1 µL of DNA polymerase were added. The reaction was run in a thermal cycler for site directed mutagenesis (SDM). The initial denaturation temperature for the parent DNA template used for SDM was 95ºC for 30 s. The cycling parameters set for 16 cycles of SDM were: (1) denaturation at 95ºC for 30 s (2) annealing at 55ºC for 1 min (3) elongation at 68ºC for 6 min for Co-BsLuxS-HT (1 min/kb).

Pellet Paint® Co-Precipitant. PCR products were transferred to 1.5 mL capacity Eppendorf tube. To this, 50 µL of PCR product and 2 µL of the Pellet Paint was added along with 150 µL of 95% ethanol. This reagent mixture was frozen at -80°C for one hour. After one hour this mixture was centrifuged at 14,000 rpm for 15 minutes. After 15 minutes the supernatant was discarded. A visible pink colored pellet was saved. 200 µL of 80% ethanol was added to the pellet, which was again centrifuged at 14,000 rpm for 10 minutes. After 10 min. the supernatant was again discarded and the pellet was dried using a Eppendorf vacufuge concentrator for ~1 hour. The dried pellet was resuspended in 20 µL of distilled water.

***Dpn*-I Digestion and Transformation.** To the resuspended pellet of the PCR amplified DNA, 2 µL of *Dpn*-I was added and loaded in thermal cycler for digestion at 37ºC for 2 hours. After 2 hours of digestion, 2 µL of the digested product was added to 100 µL of

BL21(DE3) competent cells in a 15 mL BD falcon tube. This tube was incubated on ice for 30 min. The cells were heat shocked at 42°C for 20 seconds. 900 µL of SOC medium was added to the tube containing the cells. The tube was incubated at 37°C for 1 hour. After one hour the transformed mixture was spread throughout the LB Amp^{200} plates. These plates were incubated at 37°C overnight.

Plasmid Isolation and Sequencing. Next day colonies were picked and grown in 5 mL of LB Amp^{75} media at 37°C for 16 hours. After 16 hours 4.25 mL of culture was centrifuged to get a pellet, while 750 µL of added culture was used to make freezer stocks. The pellet was then used to purify the plasmid using the GeneJET™ Plasmid Miniprep Kit. Purified plasmid concentration was estimated using a Nanodrop spectrophotometer in ng/µL. This purified plasmid was then sent to either Seqwright or Sequetech for sequencing. The sequences received from Seqwright and Sequetech were then aligned against wild type LuxS sequence using Lasergene 8.0.

2.2.4 | Co-BsLuxS-HT C84A Purification. Once the desired mutation was confirmed after aligning the mutated sequences against wild type Co-BsLuxS-HT sequences, the BL21DE3 competent cells containing the desired Co-BsLuxS-HT mutant were purified using the purification method given in Section 2.1. The estimation of protein concentration by Bradford Dye Assay was performed as provided in section 2.1.6.

2.3 | SRH Quantification. The SRH synthesized by the organic chemists in our laboratory (see Fig. 3.12) was quantified by fluorescamine quantification assay. The method for the assay is discussed in detail in the following sections:

2.3.1 | Chemical Reagents and Plates. Tyrosine, alanine, threonine, fluorescamine, and dry acetone were purchased from VWR. 96 well black plates with transparent, flat bottoms were purchased from Costar (part no. 3631).

2.3.2 | Preparation of Reagents. The reagents required for the fluorescamine quantification method were **(a)** 55 mM Sodium Borate. The weighed amount of 2.097 g of sodium borate was added to 100 mL of distilled water, and the pH adjusted to 9.0 using 1 M HCl. **(b)** Tyrosine Standards (0–40 μM). Tyrosine standards of 0.5, 10, 15, 20, 25, 30, 35 and 40 μM were prepared in 55 mM of sodium borate (pH 9.0). **(c)** Fluorescamine Solution 1 mg/mL (10 mL). Fluorescamine weighing 10 mg was added to 10 mL of dry acetone. **(d)** Known Standards. A stock solution of 20 mM was prepared for amino acids alanine and threonine in 55 mM sodium borate solution (pH 9.0). **(e)** Preparation of 20 mM SRH Stock and ~1 mM SRH Working Solution. Based on the percentage yield (20%) of the final product of SRH synthesis the theoretical value of SRH determined was 0.09144 g in impure mixture (containing inorganic salts and water) of 0.9481 g. Dissolved the final product in 12 mL of distilled water to make a stock of 20 mM. For 1 mL of working solution dissolved 50 μL of 20 mM in 950 μL of 55 mM sodium borate (pH 9.0).

2.3.3 | Tyrosine Standard Curve. This assay was performed using Wallac EnVision™ multilabel reader. 125 μL of the tyrosine standards were added in triplicate to 96 well black plates with flat and transparent bottom. 62.5 μL of 1 mg/mL fluorescamine was then added to each well. The plate was shaken inside Wallac EnVision™ multilabel reader for 1 min. Emission values at 485 nm were recorded for all the tyrosine standards.

2.3.4 | Fluorescamine Quantification Assay. Several dilutions for the known and unknown samples were prepared in 55 mM sodium borate (pH 9.0). Known samples and unknown sample dilutions of 125 µL were then added to the wells in triplicate. A volume of 62.5 µL of 1 mg/mL fluorescamine was added to the test solutions. After shaking for 1 min., emission values at 485 nm were recorded for all samples. A standard curve was plotted using all the emission values for the tyrosine standards. The linear equation of the standard curve was used to calculate the concentration values of known and unknown samples. The emission values measured for 1:20, 1:400 and 1:800 dilutions of SRH (~1 mM) working solution and 20 mM known samples (alanine & threonine) were within the range of tyrosine standards. Four replicates of fluorescamine quantification were performed. Percent error values were determined for the known samples in each round.

2.4 | Ellman's Assay. The requirement and procedure for performing Ellman's assay is discussed below:

2.4.1 | Chemical Reagents. Ellman's reagent (5,5'-dithiobis-(2-nitrobenzoic acid))/ DTNB, 4-2-hydroxyethyl-1-piperazineethanesulfonic acid (HEPES) sodium salt, and NaCl were purchased from VWR.

2.4.2 | Preparation of Reagents. To perform Ellman's assay some reagents were required. The method for their preparations were: **(a)** 5X Co-BsLuxS-HT Buffer (50 mL). The 6.5 g of HEPES sodium salt (500 mM) were added to 50 mL of distilled water. The pH was adjusted to 7.0. Finally 2.1916 g of NaCl (750 mM) was added. **(b)** Co-BsLuxS-HT 40 µM (500 µL). The determined concentration of Co-BsLuxS-HT was 3.4 mM. A 100 µL volume of 5X LuxS

buffer and 6 µL Co-BsLuxS-HT stock were added to 394 µL of distilled water for a final concentration of 40 µM. **(c)** Co-BsLuxS-HT C84A 40 µM (500 µL). The determined concentration of the Co-BsLuxS-HT C84A was 2.8 mM. 100 µL of 5X LuxS buffer and 7 µL Co-BsLuxS-HT C84A stock were added to 393 µL of distilled water for a final concentration of 40 µM. **(d)** *S*-Ribosyl Homocysteine (SRH) 680 µM (1000 µL). A volume of 200 µL of 5X LuxS buffer and 34 µL SRH stock (20 mM) were added to 766 µL of distilled water. **(e)** Ellman's Reagent 15 mM (1 mL). 0.005 g DTNB was added to 1000 µL 5X LuxS buffer. **(f)** SRH Concentrations (0-68 µM). 68, 34, 17, 8.5, 4.25, 2.125 and 1.06 µM SRH solutions were diluted from a 20mM SRH stock solution in distilled water.

2.4.3 | Homocysteine Assay. A Hewlett Packard B452A Diode Array Spectrophotometer was blanked using a reaction mixture containing 200 µL of 5X Co-BsLuxS-HT buffer, 790 µL distilled water and 10 µL of 15 mM Ellman's reagent. Homocysteine standards of 30 µL (0-68 µM) were added to a reaction mixture containing 200 µL 5X Co-BsLuxS-HT buffer and 760 µL distilled water. A measured volume of 10 µL of the 15 mM Ellman's reagent was added last to the cuvette. Absorbance values were measured at 412 nm. These absorbance values were plotted to obtain a standard curve.

2.4.4 | Ellman's Assay for Co-BsLuxS-HT. All the enzymes, SRH, buffers, distilled water and reagents were added together in the volumes and concentrations given in Table 2.2 directly into 1 mL glass cuvette. 10 µL of the enzymes were added last. This was done so that the absorbance values were recorded from the beginning of the assay. Ellman's assay for Co-BsLuxS-HT was a kinetic assay. The absorbance readings at 412 nm were recorded every 17

seconds for 204 seconds. Diode array was first blanked with the blank mixture mentioned in Table 2.2.

Table 2.2 | Ellman's Assay. The concentrations, volumes of all the required reagents, buffers and enzymes to be added in a particular order are shown. 10 µL of the enzymes are added last to the cuvette and make sure there is no air bubble in the cuvette at any point while assaying.

Samples	5 X LuxS buffer (µL)	Distilled water (µL)	Ellman's reagent 15 mM (µL)	SRH 680 µM (µL)	Co-BsLuxS-HT 40 µM (µL)	Co-BsLuxS-HT C84A 40 µM (µL)
Blank	200	790	10	-	-	-
Co-BsLuxS-HT blank	200	760	10	30	-	-
SRH blank	200	780	10	-	10	-
Co-BsLuxS-HT C84A blank	200	780	10	-	-	10
Co-BsLuxS-HT test	200	750	10	30	10	-
Co-BsLuxS-HT C84A test	200	750	10	30	-	10

A Hewlett Packard B452A Diode Array Spectrophotometer was used for this kinetic assay, which was performed for 204 sec recording sample absorbance every 17 seconds. For calculating the initial reaction rates for Co-BsLuxS-HT and Co-BsLuxS-HT C84A (**S3**) Ellman's assay was performed with varying SRH concentrations from 0-68 µM. The concentration of Co-BsLuxS-HT and Co-BsLuxS-HT C84A (**S3**) was kept constant at 40 µM. The rest of the protocol was the same as Co-BsLuxS-HT test (see Table 2.2). Once the absorbance was measured at 412 nm it was used to determine the kinetic parameters K_M and V_{max} for the samples.

2.4.5 | Estimation of Kinetic Parameters. Graph Pad Prism 5.0 was used for calculation of kinetic parameters using reaction rates (µmol/mg/min), which were derived from absorbance values recorded at 412 nm (see Fig. 3.18). The constant value of $[E]_t$ used for determining the k_{cat} was 0.0008 µmole (see Section 3.4.2.2.1 and Fig. 3.18). The comparison of kinetic parameters of house-purified enzymes with the literature values were used for determining enzyme's activity.[9]

2.5 | Generation, Purification, Concentration Estimation and Activity Assay of Co-BsLuxS-HT Mutants. The procedure for the generation, purification and activity assay of mutants generated from native cysteines is discussed as follows:

2.5.1 | Biochemical Reagents, Kits and Supplies. NucleoSpin Gel and PCR clean up kit from E and K Scientific, *Nde*-I, *Xho*-I and *Pst*-I restriction enzymes from New England Biolabs, T4 DNA ligase from New England Biolabs, One step Ex Taq qRT-PCR Kit from TaKaRa, 1 kb DNA ladder, 100 bp DNA ladder and 5X loading dye from New England Biolabs, JM109 competent cells from Qiagen.

2.5.2 | Preparation of LB Amp200 Plates and LB Amp75 Media. The media and plates were prepared the same way as mentioned in Section 2.2.2.

2.5.3 | Preparation of Agarose Gel. To prepare 1% agarose gel 1 g of agarose was added to 100 mL of 0.5X Tris-Acetate-EDTA (TAE) buffer. The solution was heated, but not to the extent of boiling in order to avoid bubbles in the gel. The solution was cooled up to 60°C and then 1µL of ethidium bromide (10 mg/mL) was added and mixed thoroughly. For preparation

of running buffer for 1% agarose gel, 0.5X TAE was used was running buffer for the 1% agarose gel. To prepare 1000 mL of 0.5X TAE buffer from 100X TAE buffer, add 50 mL of 100X TAE buffer in 950 mL of distilled water.

2.5.4 | Site Directed Mutagenesis. Template plasmids were purified from 5 mL LB Amp[75] cultures using GeneJet™ plasmid purification kit. C22A, C41A and C126A overlapping primers were designed using PrimerX software as per the primer design protocol of the QuikChange® SDM kit (see Table 4.2). Non-overlapping primers were designed using PrimerSelect module of DNAStar Lasergene 8.0 (Table 4.5). The wild type Co-BsLuxS-HT sequence was used as a template for designing these primers. The primers were then ordered from IDT. The procedure for SDM was the same as mentioned in section 2.2.3. The procedures for using Pellet Paint® precipitant, *Dpn*-I digestion and transformation, plasmid isolation and sequencing were same as mentioned in Section 2.2.3.

2.5.5 | Procedure for Cloning Technique for Obtaining Double Co-BsLuxS-HT Mutants. To start cloning, a purified pET-22b(+) vector was required. A wild type Co-BsLuxS-HT was lysed by GeneJET™ plasmid purification kit to obtain a purified plasmid. Five samples were prepared for the digestion (1) **Blank**: 15 µL distilled water, 2 µL of 10X NEB buffer 4, 2 µL of 100X BSA, 1 µL of *Nde*-I, 1 µL of *Xho*-I (2) ***Nde*-I:** 5 µL of purified plasmid from wild type Co-BsLuxS-HT, 11 µL of distilled water, 2 µL of 10X NEB buffer 4, 2 µL of 100X BSA, 1 µL of *Nde*-I (3) ***Xho*-I:** 5 µL of purified plasmid from wild type Co-BsLuxS-HT, 2 µLof 10X NEB buffer 4, 11 µL of distilled water, 2 µL of 100X BSA, 1 µL of *Xho*-I (4) ***Pst*-I**: 5 µL of the purified plasmid from wild type Co-BsLuxS-HT, 11 µL of distilled water, 2 µL of 10X NEB buffer 3, 2 µL of 100X BSA, 1 µL of *Pst*-I (5) ***Nde*-I *Xho*-I:** 5 µL of purified

plasmid from wild type Co-BsLuxS-HT, 11 µL of distilled water, 2 µL of 10X NEB buffer 4, 2 µL of 100X BSA, 1 µL of *Nde*-I and *Xho*-I. All these samples were incubated for 1 hour at 37°C. During incubation, a 1% agarose gel was prepared in 100 mL 0.5X TAE buffer (see Section 4.52.1). After 1 hour, 5 µL of 5X loading dye was added to all the samples and loaded onto the 1% agarose gel. After filling the gel tank with 0.5X TAE buffer, the gel was electrophoresed for 1 hour 45 min. at 100 V. A picture of the gel was taken using using Quantity One software and Bio Rad Chemi Doc. The band for pET-22b(+) vector was isolated by cutting from the gel using a sterilized blade and purified using NucleoSpin® gel clean up kit. The cleaned pET-22b(+) solution was saved at -80°C for future use.

To obtain the DNA fragments encoding the double mutation C22AC84A (**D5**), primers were manually designed (see Table 3.4) and ordered from IDT for synthesis. 100 mM stock solutions and 10 µM working solutions of these primers were prepared. Two PCR reactions were performed : (1) 1 µL of Co-BsLuxS-HT C84A as template and 2 µL of the full length reverse and C22A forward primer (2) 1 µL of the Co-BsLuxS-HT C84A as template, 2 µL of the full length forward and C22A reverse primer. The 10X reaction buffers, dNTP's and the Taq Polymerase enzymes were used from the Ex Taq PCR kit. A second round of PCR reaction was run using 1 µL of the abovementioned PCR reaction (1) and (2) as a template and 2 µL of the full length forward and reverse primers. PCR product of 50 µL from the second round of the PCR reaction was purified using the NucleoSpin PCR cleanup kit. Then 15 µL of the 50 µL cleaned up reaction mixture was digested by the restriction enzymes *Nde*-I and *Xho*-I for one hour and 30 min at 37°C. The digested mixture was purified again using NucleoSpin PCR clean up kit. The cleaned up PCR mixture of 15 µL was then ligated with the 50 µL of the clean pET-22b(+) vector with 2 µL of the T4 DNA Polymerase at 4°C

overnight along with a blank sample. The following day ligated mixture was kept at room temperature for 45 min. After 45min. the enzyme was inactivated by heating the ligated mixture at 70° for 10 min. Immediately after heat inactivation, the ligation mixture was placed on ice for 10 min. 2 µL of the ligated mixture wass then transformed into the JM109 competent cells. This experiment was repeated 3 times; the other two times the competent cells used were XL-10 ultracompetent cells and BL21DE3 competent cells. After transformation, the mixture was spread onto LB Amp^{200} plates. The plates were incubated at 37°C overnight. The next day, colonies were isolated and grown in 5 mL of LB Amp^{75} media. The plasmids encoding the mutation present in the bacterial cells in the culture were then purified using GeneJET™ plasmid purification kit. The concentration of the purified samples was measured using ND-1000 spectrophotometer and the samples were sent to Sequetech for sequencing. The samples received from the sequencing company were aligned using SeqMan Pro module of DNAStar Lasergene 8.0 to determine if they carry the desired mutation.

2.5.6 | Purification of Co-BsLuxS-HT mutants Purification. Once the desired mutation was confirmed, the BL21(DE3) competent cells containing the desired LuxS mutant were purified using the purification method given in Section 2.1.

2.5.7 | Estimation of Protein Concentration of Co-BsLuxS-HT Mutants by Bradford Dye Assay. See section 2.1.6.

2.5.8 | Ellman's Assay for Activity Assay of Co-BsLuxS-HT Mutants. The Ellman's assay was performed similarly as mentioned in the Section above (see Section 2.4.4).

CHAPTER 3: ELLMAN'S ASSAY FOR LuxS ENZYMATIC ACTIVITY DETECTION

Small molecules having structural similarity to the LuxS substrate, SRH, have the potential to act as LuxS inhibitors, thereby preventing System Two quorum sensing. In order to be able to determine whether or not an SRH analog acts as an inhibitor of LuxS, an Ellman's assay was implemented in accordance with literature precedent.[24] Ellman's assay is a means of determining total sulfhydryl groups, including both protein-bound and free sulfhydryl groups, in biological samples using 5,5'-dithiobis-2-nitrobenzoic acid (DTNB; Ellman's reagent).[24] The assay is both stoichiometric and colorimetric, as one mole of thiol (-SH) substrate reacts with one mole of DTNB to release one mole of 2-nitro-5-thiobenzoate (NTB^-) ion, which is quantified in a spectrophotometer by measuring the absorbance of visible light at 412 nm.[24]

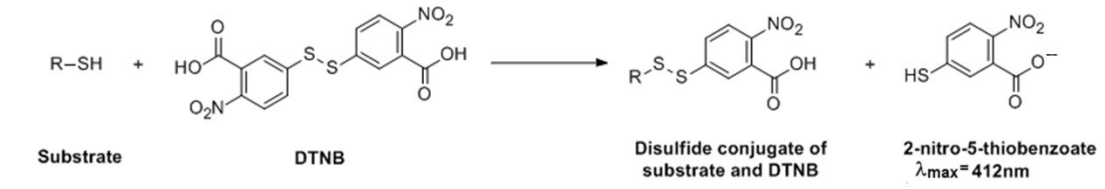

Fig. 3.1 | Ellman's Assay. The substrate (R-SH) here represents a molecule with a free sulfhydryl group. The substrate reacts with DTNB to break the disulfide linkage in DTNB. One part of the broken DTNB joins with the substrate to give a conjugate whereas the other part, 2-nitro-5-thiobenzoate (NTB^-) remains free in the solution and absorbs light at 412 nm.

Before attempting to identify any SRH analogs as potential LuxS inhibitors, Ellman's assay was first used to determine the activity of *Bacillus subtillis* LuxS enzyme with a cobalt ion in place of the native iron and a C-terminal histidine tag (Co-BsLuxS-HT). Chemically-synthesized SRH prepared in our laboratory was used as a substrate.[27] Co-BsLuxS-HT reacts with *S*-ribosyl homocysteine (SRH) to give 4(*S*),5-dihydroxy-2,3-pentanedione (DPD) as its

primary product and homocysteine as a byproduct (see Fig. 3.2). This homocysteine byproduct exhibits a free sulfhydryl group which can react with DTNB in the Ellman's assay to give 2-nitro-5-thiobenzoate (NTB^-). Absorbance of this ion at 412 nm indicates the presence of HCys in the reaction mixture and, therefore, the activity of Co-BsLuxS-HT.

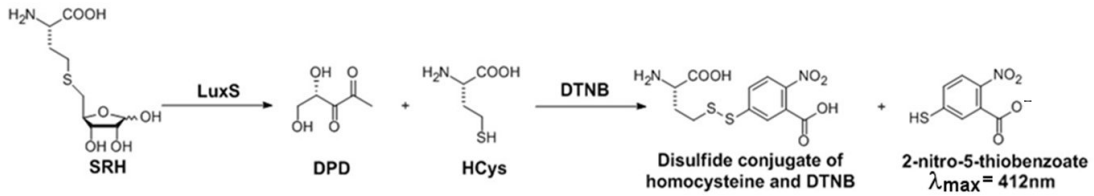

Fig 3.2 | Ellman's Assay for LuxS. Homocysteine (HCys) is formed from SRH in the presence of enzyme Co-BsLuxS-HT. HCys then reacts with the DTNB to give the NTB^- ion.

There are three basic requirements for the Ellman's assay: (1) quantified substrate, (2) purified enzyme, and (3) a negative control. Table 3.1 shows these basic requirements for an Ellman's assay in general and the requirements for the assay of Co-BsLuxS-HT in particular. The acquirement of each, for assessment of Co-BsLuxS-HT is in particular described in the following sections.

Table 3.1 | Ellman's Assay Requirements. General and specific requirements for an Ellman's assay.

General Requirements	Co-BsLuxS-HT Specific Requirements
Purified protein	Co-BsLuxS-HT
Negative control	Co-BsLuxS-HT C84A mutant
Substrate at known concentration	*S*-ribosyl homocysteine (SRH)

3.1 | Protein Purification. The Co-BsLuxS-HT enzyme was purified from the *Escherichia coli* strain ELS1409.[3] ELS1409 cells carry the expression vector pET-22b(+) containing a DNA insert coding for *Bacillus subtillis* LuxS as constructed by Pei and coworkers, from digestion of the vector by *Xho*-I and *Nde*-I.[9] To facilitate the purification of this enzyme using cobalt resin, a 'tag' of six histidine residues is incorporated at the C-terminus of the DNA insert (see Fig. 3.3). The vector also contains an ampicillin resistance gene that provides a resistance property to the bacterial cells against the antibiotic ampicillin in growth media. This enables the selective growth of ELS1409 bacterial cells containing the plasmid encoding for Co-BsLuxS-HT. The vector pET-22b(+) carries a *lacI* gene that produces a repressor that binds to the operator to inactivate transcription. An inducer, if present in the culture media, binds with the repressor to stop it from inactivating transcription, leading to rapid production of desired protein.

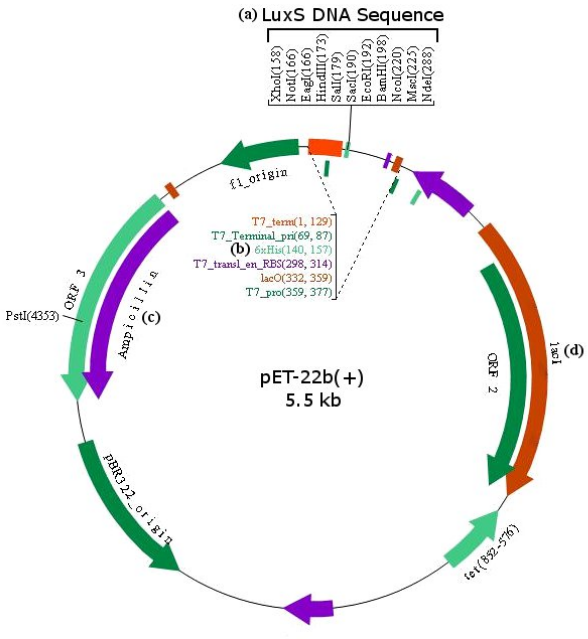

Fig. 3.3 | pET-22b(+) vector. The plasmid vector present in strain ELS1409 with **(a)** DNA insert encoding *B. subtillis* LuxS **(b)** Six histidine residues from 140-157 at the C-terminal end of the DNA insert **(c)** Ampicillin marker and **(d)** *lacI* repressor gene. The image is taken from the paper by Lee et al. [26c]

LuxS with its native iron atom is very unstable *in vitro*, oxidizing from the ferric to the ferrous state under aerobic conditions. In the Co-BsLuxS-HT variant, the native iron atom is replaced by cobalt atom. Cobalt is more stable at *in vitro* conditions, and the enzyme activity remains similar to that of the native enzyme.[9]

3.1.1 | General Parameters for Co-BsLuxS-HT Purification. For the purification of Co-BsLuxS-HT, the protein was overexpressed in a large culture of ELS1409 bacterial cells. The bacterial cells were lysed to acquire the protein. The bacterial lysate was centrifuged to obtain a supernatant containing the desired protein. The histidine-tagged protein was separated from cell debris and other proteins by affinity chromatography. The purified protein was concentrated and stored at -80°C by mixing the culture in the cryoprotectant glycerol.

3.1.2 | Co-BsLuxS-HT Protein Overexpression and Cell Harvesting. A large (2 L) culture of *Escherichia coli* ELS1409 containing the desired Co-BsLuxS-HT protein was grown in LuxS Amp[75] minimal media. The ampicillin present in the media facilitated selective growth of ELS1409 as mentioned previously (section 3.1).

3.1.2.1 | Fresh Transformation Required for Acquiring Purified Co-BsLuxS-HT. According to standard procedure, a freezer stock of ELS1409 bacterial cells stored at -80°C for a long time is used to generate a new bacterial culture.[9] However, this method was unsuccessful in our lab conditions. The long-term storage of ELS1409 was hypothesized to have caused the loss of the gene encoding for Co-BsLuxS-HT from the plasmid, leading to no Co-BsLuxS-HT expression in the cells. To ensure that the Co-BsLuxS-HT protein was expressed in the cells, a freshly transformed stock of ELS1409 (renamed as RG-f) was used.

A fresh transformation refers to the transfer of the plasmid encoding the desired protein into fresh bacterial cells. The use of freshly transformed ELS1409 ensured the presence of the vector harboring the appropriate gene for Co-BsLuxS-HT expression in the bacterial cells.

3.1.2.2 | Introduction of Cobalt and Isopropyl-β-D-thio-galactoside (IPTG) Induction. The RG-f bacterial cell culture was grown to an optical density (O.D.) at 600 nm ($O.D._{600}$) of ~0.6 at 37°C. The O.D. of a bacterial cell culture is the logarithmic ratio of the radiation incident upon the culture, to the radiation transmitted through the culture.[28] To determine the optical density at mid log phase of bacterial growth (i.e. maximal bacterial growth), the O.D. at 600 nm was measured with Diode Array spectrophotometer until an $O.D._{600}$ of ~0.6 bacterial cell growth was achieved. First 500 μL of a 100 mM solution of cobalt (II) chloride ($CoCl_2$) was added to the culture to replace the native iron in the active site of the enzyme with cobalt. In the presence of cobalt, the enzyme was blue. Next 250 μL of a 100 mM solution of isopropyl-β-D-thio-galactoside (IPTG) was added to the culture to induce rapid production of Co-BsLuxS-HT. The IPTG acts as an inducer by attaching itself to the lac repressor produced from *lacI* (see Fig. 3.3). The lac repressor releases from the lac operator (*lacO* shown in Fig. 3.3), thereby allowing the rapid transcription of the Co-BsLuxS-HT gene. After incubation at 30°C for 16 hours, the bacterial culture was centrifuged at 5000 rpm and 4°C to acquire a large pellet of bacterial cells carrying the plasmid coding for Co-BsLuxS-HT.

3.1.3 | Cell Lysis. The 2 L pellet of bacterial cells carrying plasmids encoding Co-BsLuxS-HT obtained from RG-f overexpression was lysed to acquire the desired protein. Before lysing the bacterial cells by any particular lysis technique, the pellet was resuspended in a

lysis buffer to obtain a homogenous solution of bacterial cells. There are two potential lysis methods: chemical lysis by sonication and mechanical lysis by French press. Both methods were compared for RG-f to determine the best method that lysed maximum number of cells to provide blue Co-BsLuxS-HT protein. Once the purified protein was acquired, the amount of protein concentration was measured by the Bradford dye assay (see Section 3.1.5).

3.1.3.1 | Sonication. Pei et al. used a sonication method for lysis of ELS1409 bacterial cells.[9] Applied to our case, the bacterial cell lysis by sonication required a 1 L pellet of RG-f cells to be resuspended in 35 mL of a chemical lysis buffer containing 1% Triton X-100, 0.5% protamine sulfate, 20 µg/mL trypsin inhibitor, 50 µg/mL *p*-methylbenzenesulfonyl fluoride, and 70 µg/mL chicken egg white lysozyme. The resuspended solution was divided into four parts. Each part of the resuspended cells was sonicated individually for 10 min at amplitude 75 at 4°C. After centrifugation, 1 mL of supernatant was plated on LB Amp^{200} plates to determine if the cells were lysed or not. As mentioned in Section 3.1, the ampicillin marker present in the plasmid carried by RG-f cells makes the cells resistant to ampicillin. Hence, the unlysed RG-f cells with the plasmid will grow on the plates, suggesting incomplete lysis. Therefore, the expected number of colonies after lysis and centrifugation was zero. However, the actual numbers of colonies obtained were ~300 informing incomplete lysis of the bacterial cells.

The enzyme purified from cells lysed by sonication was dark yellow in color rather than blue (see Summary Table 3.2). This indicated loss of cobalt from Co-BsLuxS-HT during the lysis procedure. The amount of the protein present in purified LuxS was later determined by Bradford dye assay to be 3.75 µg (Section 3.1.5). A summary table comparing the two

techniques i.e. sonication and French press for LuxS purification is given below (see Table 3.2).

3.1.3.2 | French Press. For cell lysis by French press, a 2 L pellet of RG-f bacterial cells was resuspended in 35 mL of mechanical lysis buffer containing 20 mM Tris-HCl, 400 mM NaCl and 5 mM imidazole. The cells were lysed by French press at 20,000 psi. After centrifugation, 1 mL of supernatant was plated on LB Amp^{200} plates. The presence of colonies suggested incomplete lysis of RG-f bacterial cells carrying the plasmid with ampicillin marker as mentioned previously, therefore no colonies were expected to grow. However, the number of colonies obtained was innumerable (i.e. separate single colonies were not obtained) suggesting incomplete lysis of bacterial cells. The protein purified from French press-lysed bacterial cells was blue (see Summary Table 3.2) as expected, presumably due to presence of cobalt in the enzyme. The amount of protein present in purified LuxS, determined by Bradford dye assay was 3.45 µg.

Table 3.2 | Summary Table. The comparison of the two lysis techniques with respect to different parameters.

Lysis Technique	Size of the Culture	Colonies Obtained	Color of Protein	Amount of Protein (µg)
Sonication	1L	~300	Yellow	3.75
French Press	2L	Innumerable	Blue	3.45

The recovery of blue enzyme from the bacterial cells lysis by French press compelled us to use French press for future lysis experiments, despite the drawbacks of high colony count and lower protein amount of purified protein.

3.1.4 | Affinity Chromatography. To purify Co-BsLuxS-HT from the mixture of other proteins present in the supernatant obtained after centrifugation, immobilized metal affinity chromatography (IMAC) was performed.[29] The TALON® resin is charged with cobalt and therefore histidine tagged Co-BsLuxS, expressed from the plasmid vector present in RG-f cells (see Section 3.1), binds with the TALON® cobalt resin facilitating the protein purification. The binding of His-tagged protein to the resin turns the color of the resin from pink to blue (see Fig. 3.4). After the centrifuged sample was applied to column, it was washed with an appropriate lysis buffer to remove any other cell debris non-specifically attached to the column, the Co-BsLuxS-HT was eluted using a buffer containing imidazole, NaCl and Tris-HCl.

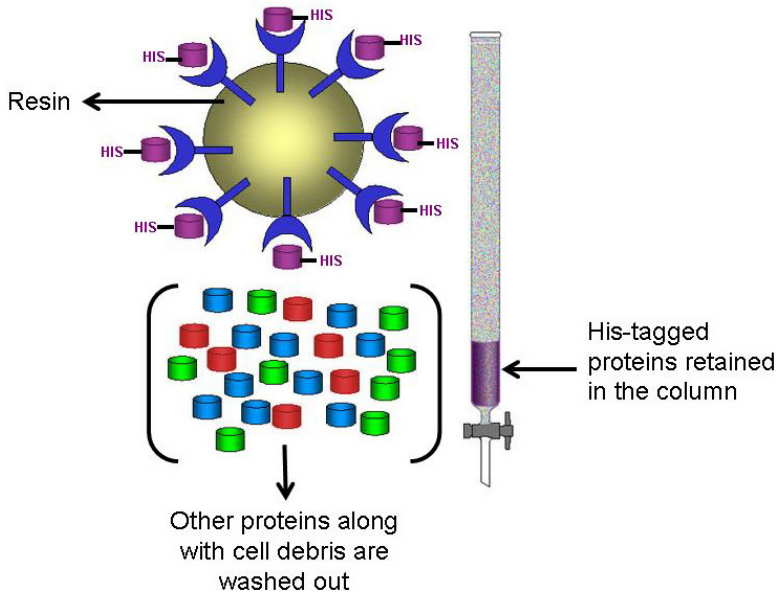

Fig. 3.4 | Affinity Chromatography for His-tagged Protein. The His-tagged protein (purple) from a mixture of proteins, binds specifically to the resin due to its affinity. The retained His-tagged protein delivers the column a purple color. The image is taken from a paper by March et al.[29]

The purified Co-BsLuxS-HT was concentrated to a dark purple solution using centriprep YM-10 tubes (MWCO 10 kDa), which retained Co-BsLuxS-HT while let other impurities along with water pass through the membrane. The purified protein mixture was immediately mixed with 80% glycerol to be stored for future use at -80°C.

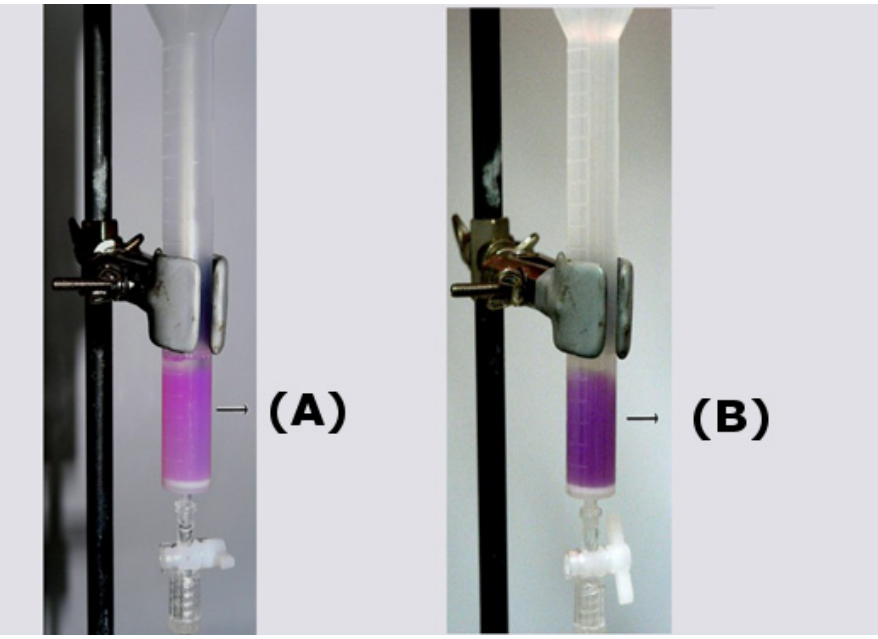

Fig. 3.5 | Talon® Cobalt Resin Column. (A) Pink colored cobalt resin before the addition of supernatant. (B) The change of color from pink to purple of the cobalt resin column on passing the supernatant of cracked cells containing Co-BsLuxS-HT.

3.1.5 | Bradford Dye Assay. The amount of protein present in the purified Co-BsLuxS-HT solution was measured by the Bradford dye assay to quantify the enzyme for the Ellman's assay. The Bradford dye assay is a colorimetric protein assay based on an absorbance shift of the dye Coomassie brilliant blue G-250 (Fig. 3.6). Under acidic conditions, the red form of the dye is converted into its blue form to bind to the protein being assayed, resulting in a shift

of the dye's absorption from the wavelength 465 nm to 595 nm.[30] The binding of the protein stabilizes the blue form of the Coomassie dye. The amount of the complex present in solution was determined by an absorbance reading at 595 nm. The absorbance values of protein standards were plotted to obtain a standard curve, and the linear trendline equation of the standard curve was used to calculate the amount of the unknown protein samples.

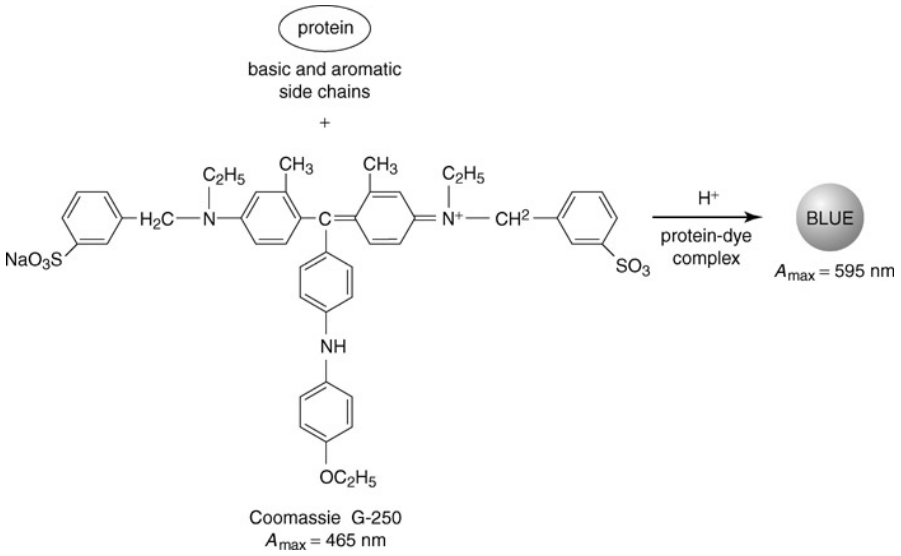

Fig. 3.6 | Bradford Dye Assay. The protein binds with the Coomassie dye to form a complex which is blue in color and the absorbance value is measured at 595 nm. The image is taken from a paper by Marion et al.[31]

3.1.5.1 | General Parameters. Standard bovine serum albumin (BSA) solutions are mixed with an appropriate amount of Bradford dye. Once a stable color is acquired, the absorbance values are measured at 595 nm in a spectrophotometer. The absorbance values are plotted to obtain a standard curve and a linear trendline. The absorbance values for unknown samples are also acquired within the range of standard curve, using dilutions of the samples if required. The linear equation from the standard curve is used to calculate the amount of protein in the unknown sample.

3.1.5.2 | Optimization of Bradford Dye Assay for Co-BsLuxS-HT. Typically the Bradford assay is performed in large volumes (i.e. 1 mL). In an effort to avoid excess consumption of Co-BsLuxS-HT enzyme solely for quantification purposes, clear 96-well transparent bottom plates with a maximum working volume of 300 µL for each well were used. Therefore, optimization of this low-volume Bradford dye assay was required beforehand. 4 µL of bovine serum albumin (BSA) standard solutions ranging from 0-2 mg/mL were used for optimization. To compare the determined unknown protein concentration results using a broad range of protein standards, BSA standards of concentrations 0-2 mg/mL were used. Different volumes of Bradford dye were also used ranging between 100 and 300 µL. The reaction mixture containing the BSA standards and the Bradford dye was kept at room temperature for 8 min in order to give a stable blue color from the protein-dye complex, which was then measured at 595 nm (see Section 3.1.5). The spectrophotometer used for absorbance measurements was Wallac EnVision™ multilabel plate reader (Perkin Elmer). The BSA standard range of 0-4 µg/mL and the 300 µL volume of Bradford dye provided a standard curve with a linear trendline and a R^2 value of 0.96 (see Fig. 3.7).

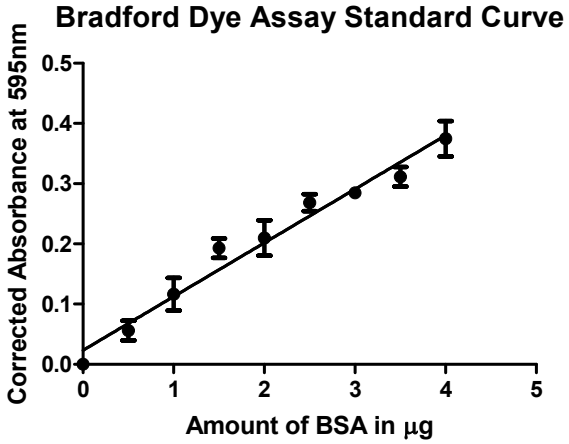

Fig. 3.7 | Bradford Standard Curve with Optimized Parameters. 0-4 µg/mL BSA standards and 300 µL volume of Bradford dye were used to acquire this standard curve with a linear trendline and small error bars.

3.1.5.3 | Protein Concentration Estimation of Unknown Sample. Once a standard curve was achieved, absorbance values for the unknown purified protein solution were determined. Serial dilutions of unknown purified Co-BsLuxS-HT samples in elution buffer (containing 20 mM Tris-HCl, 400 mM NaCl and 60 mM imidazole) were prepared to achieve an absorbance within the range of absorbance values of standard curve (0-4 µg/mL). The linear equation of the standard curve was used to calculate the amount of protein present in unknown protein samples. The final protein concentrations of purified Co-BsLuxS-HT were determined using the amount of protein obtained from the linear equation. The protein concentration determined for the blue colored Co-BsLuxS-HT (bacterial cells lysed by French press) was 0.49 mM and the concentration determined for the yellow colored Co-BsLuxS-HT (bacterial cells lysed by sonication) was 2.2 mM.

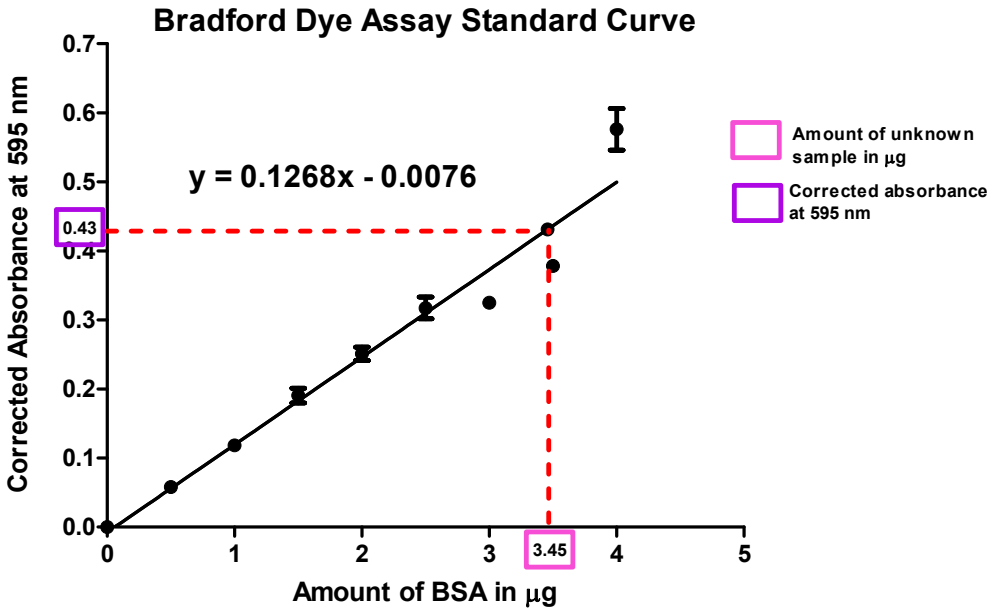

Fig. 3.8 | Bradford Assay Curve for Estimation of Amount of Protein in Purified Co-BsLuxS-HT Sample. The red dotted line in the curve shows the determined amount of protein present in 4 µL of 1:20 diluted Co-BsLuxS-HT (lysed by French press), using absorbance measured at 595 nm.

3.1.6 | Sodium Dodecyl Sulfate Polyacrylamide Gel Electrophoresis (SDS-PAGE). To check for the presence of Co-BsLuxS-HT protein in the chemically lysed bacterial cells before final purification of the enzyme, a SDS-PAGE gel was used. The technique of sodium dodecyl sulfate polyacrylamide gel electrophoresis (SDS-PAGE) is used to separate proteins based on the differences in their molecular weights.[26b] The sodium dodecyl sulfate (SDS) used for SDS-PAGE is a strong detergent agent which denatures native proteins to unfolded, individual polypeptides. SDS imparts a uniform negative charge along the length of polypeptide giving every protein same mass to charge ratio, therefore the proteins separate based only on their respective molecular weights. The gel used for this technique is a polyacrylamide gel which is susceptible to high temperatures, transparent, strong and chemically unreactive. This gel helps to separate different proteins under appropriate voltage gradients.[32] The description for the use of this technique for detection of Co-BsLuxS-HT presence, before attempting final purification, is provided in the following sections.

3.1.6.1 | General Parameters of SDS-PAGE. SDS-PAGE gels of 12.5% are prepared. The protein samples to be tested are prepared by the addition of loading dye, followed by heating at 95°C for 10 min. The samples are loaded on the gel along with an appropriate protein ladder consisting of highly purified proteins of varying molecular weight. The electrophoresis was run at 150 V for ~45 min. The proteins separate on a SDS-PAGE gel according to their molecular weights and are visualized using a Coomassie Brilliant Blue protein stain. The molecular weight of the unknown proteins is estimated by comparing their bands with respect to the bands of the protein ladder.

3.1.6.2 | SDS-PAGE Gel for Co-BsLuxS-HT. The Co-BsLuxS-HT protein is a 35 kDa homodimeric protein (see Section 3.1). As SDS denatures proteins into monomers (Section 3.1.6), the band for Co-BsLuxS-HT is expected at 17 kDa on the ladder. Whole cell (WC i.e. only resuspended), sonicated cells (RS i.e. resuspended then sonicated) and supernatant (S i.e. resuspended, sonicated and centrifuged) samples of Co-BsLuxS-HT were prepared are loaded. Multiple faint bands for different proteins were expected for WC sample because the sample was only resuspended in chemical lysis buffer. Therefore, only some of the cells were expected to be lysed due to presence of contents like lysozyme, salts etc. in the buffer. As well as for sample RS also multiple dark bands for different proteins were expected due to the maximum lysis of the cells by sonication and the presence of cell debris. The supernatant S was expected to give a dark band near 17 kDa band of the ladder, as all the cell debris was removed away and the supernatant was believed to have most of Co-BsLuxS-HT. A very faint band near 20 kDa was acquired for the WC sample. Dark bands near 20 kDa and 25 kDa bands of ladder were acquired for the RS sample. Until this time, the bands for Co-BsLuxS-HT (S) around ~20 kDa band of the ladder have been acquired. (Fig 3.9)

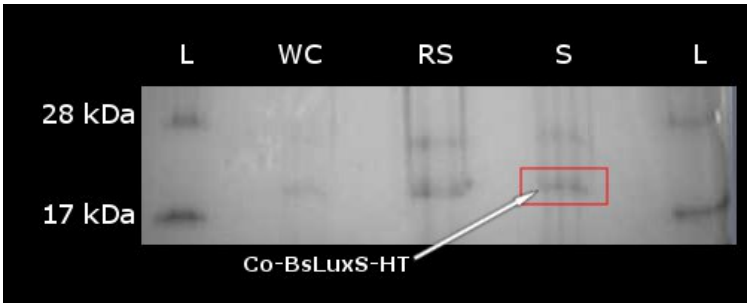

L	Ladder
WC	Whole cell (resuspended)
RS	Resuspended (resuspended & lysed)
S	Supernatant (resuspended, lysed and centrifuged culture)

Fig. 3.9 | SDS-PAGE Gel. A faint band near 17 kDa band of ladder suggests the presence of Co-BsLuxS-HT.

3.2 | Negative Control for Ellman's Assay. A negative control is exactly the same as the test sample, but no phenomenon is expected according to the theory. The mutant Co-BsLuxS-HT C84A was used as a negative control for the Ellman's assay. Based on the previous scientific work done on Co-BsLuxS-HT it is known that C84A mutation turns the enzyme inactive, as the cysteine 84 present at the active site of the enzyme plays a key role in the catalytic activity of the enzyme.[9]

3.2.1 | General Parameters. To introduce a position-specific mutation in a protein, site directed mutagenesis is performed. Site-directed mutagenesis (SDM) is a technique used to create a mutation at a defined site in a DNA molecule using primers that encode for a particular mutation.[33] After such primers are designed and prepared, a polymerase chain reaction (PCR) is run on a reaction mixture containing a DNA template, forward and reverse primers, reaction buffer, Quik solution (for dissolving all polar and non-polar compounds), deoxyribonucleotide triphosphates (dNTP's), and a DNA polymerase enzyme. The final PCR product is then transformed into competent bacterial cells. The transformed cells are spread on an appropriate agar plate containing a particular antibiotic to ensure the selective growth of the cells carrying plasmids with antibiotic resistance. This plate is incubated at a temperature suitable for the bacterial growth overnight to grow colonies. Colonies are picked, grown in an appropriate media, and then lysed to purify the plasmid. Finally, these plasmids are sequenced and aligned to determine if the desired mutation was achieved.

3.2.2 | Site Directed Mutagenesis for Co-BsLuxS-HT. The presence of a small side chain (-CH_3) in the neutral alanine made it a good choice for replacing cysteine at 84 position in

LuxS protein sequence according to Pei and coworkers.[9] This change in the enzyme's active site environment from cysteine to alanine turns the enzyme inactive.[9]

Fig. 3.10 | Site Directed Mutagenesis. Stepwise depiction of Co-BsLuxS-HT C84A mutation generation.

The primers encoding for the C84A mutation in Co-BsLuxS-HT have been designed and reported by Pei and coworkers (see Table 3.3).[9] Different primers encoding for the same C84A mutation were designed in our lab using PrimerX (see Table 3.3), according to the primer design protocol of QuikChange site-directed mutagenesis kit by Stratagene. This protocol required primers of length 25-45 bases to have the mutation site in middle with ~10-15 flanking bases. A $T_m \geq 78°C$ was required for DNA duplex stability and 40% GC content was needed to enhance the strength of the primers due to the presence of strongly bonded GC bases. Additionally, the primers were required to end with a G or C base, which helps to promote specific binding at the 3' end. The primers designed in our lab were 10 bp longer than the Pei primers and the melting temperature was 5.5°C higher, but the GC content was almost identical (see Table 3.3). The desired sequences for the abovementioned C84A primers were sent to Integrated DNA Technologies (IDT) to be synthesized. SDM using the

QuikChange® site directed mutagenesis kit was used to mutate Co-BsLuxS-HT. PCR was performed using the wild type DNA template, C84A primers, buffers, deoxyribonucleotide triphosphates (dNTP's) and *PfuTurbo*® DNA polymerase enzyme. Attempts to get colonies for Co-BsLuxS-HT C84A mutant using either pair of primers failed initially. It was hypothesized that the low concentration of the final PCR product was making it difficult for the bacterial cells to take up the plasmid during transformation, resulting in no colonies of the bacterial cells bearing the mutated plasmid.

Table 3.3 | C84A Primers Comparison. The primers for C84A mutation of Co-LuxS-HT were designed by Pei and coworkers and also by our lab.[9] The lengths and the parameters for designing the primers were different.

Primer Design	C84A Primers	Length (bp)	GC Content (%)	Melting Temp. (°C)
Pei et al [9]	5'GATATTTCTCCAATGGGCGCCCA AACAGGCTATTATC3'	37	45.95	74.1
House-designed	5'CATTGATATTTCTCCAATGGGCGC GCAGACAGGCTATTATCTAGTTG 3'	47	44.68	79.6

3.2.2.1 | Pellet Paint® Co-Precipitant. To overcome the problem of low- concentration PCR product, Pellet Paint® Co-Precipitant was used to concentrate the PCR product from 50 to 20 μL, thereby increasing the number of plasmids per unit volume available to the competent cells for uptake and leading to an increase in transformation efficiency (see Fig. 3.11). The number of colonies obtained for Co-BsLuxS-HT C84A mutation using the house-designed primers were 84. No colonies were acquired using Pei primers for the C84A mutation. Hence, Pellet Paint and the house-designed primers proved to be an important part of the protocol thereafter to acquire a mutant.

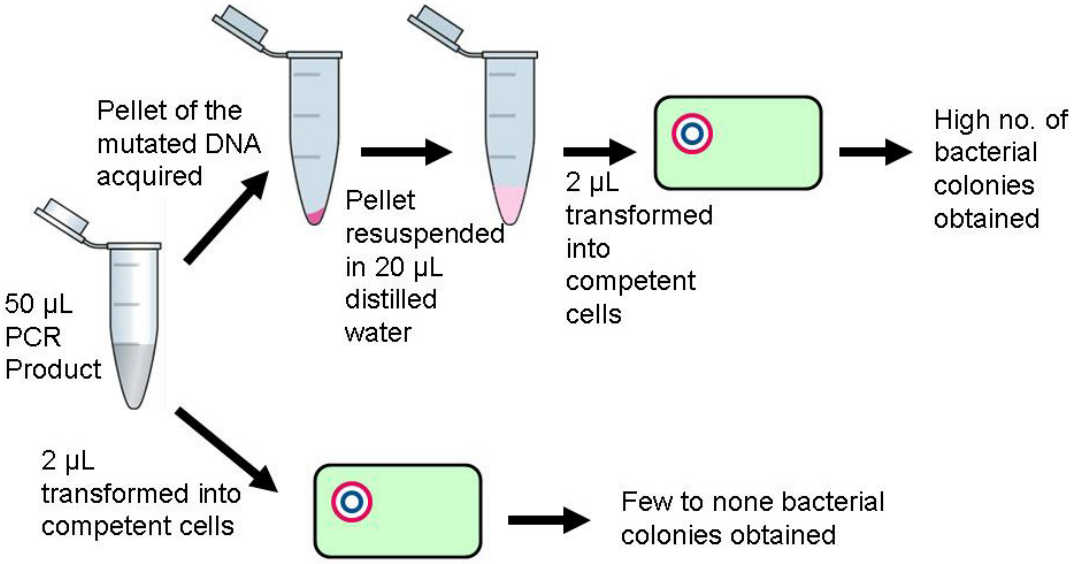

Fig. 3.11 | Procedure for Pellet Paint Paint® Co-Precipitant. To obtain higher number of colonies of bacterial cells carrying mutation the Pellet Paint Paint® Co-Precipitant was used for concentrating mutated DNA/PCR product.

3.2.2.2 | Transformation. The concentrated PCR product was digested by the restriction enzyme *Dpn*-I to digest parent DNA and transformed into *E. coli.* BL21(DE3) competent cells by heat shock. The transformation mixture was spread on LB Amp^{200} plates for selective growth of cells with the ampicillin resistance plasmid. The colonies acquired were grown in LB Amp^{75} minimal media for selective growth (see Section 3.1).

3.2.3 | Plasmid Isolation and Sequencing. The mutated plasmids from each bacterial culture grown in LB Amp^{75} minimal media were purified using Fermentas GeneJET™ Plasmid Purification Miniprep kit and the concentration of plasmid samples was estimated by UV-Vis. spectrophotometer (NanoDrop 1000). Plasmid samples of concentrations 100 ng/µL encoding for Co-BsLuxS-HT C84A were sent for sequencing to Seqwright. The alignment results

confirmed the presence of Co-BsLuxS-HT C84A encoding plasmids in the cells (see Fig. 3.10).

3.2.4 | Co-BsLuxS-HT C84A Purification. The bacterial cells containing mutated plasmid were grown and purified as mentioned in Section 3.1.

3.2.5 | Estimation of Protein Concentration. The amount of the protein was measured by Bradford dye assay as described in Section 3.1.5. The final concentration of blue-colored purified Co-BsLuxS-HT C84A protein determined was 1.1 mM (see Appendix A).

3.3 | SRH Quantification. Ellman's assay requires a known amount of substrate (SRH) in order to calculate the rate of reaction and kinetic parameters of the enzyme Co-BsLuxS-HT. Fig 3.12 shows the schematic presentation of the synthesis of SRH from homocysteine and protected ribose as initially attempted in our laboratory.[9] The final product from this scheme is a mixture of inorganic salts (e.g. NaCl), SRH, and water. In order to quantify SRH in this mixture, there are two possibilities: (1) quantify SRH in solution or (2) synthesize SRH in a different way. The amount of SRH in the final product is quantified using fluorescence proximity assay, while efforts towards synthesizing more pure SRH were ongoing.

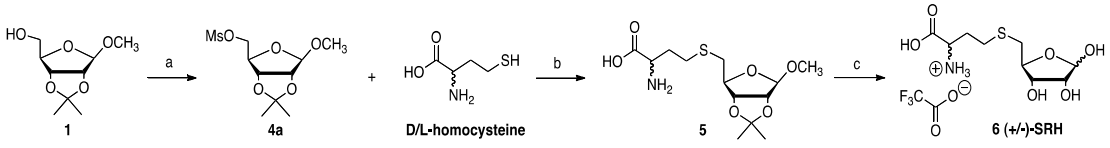

Fig. 3.12 | Synthesis Scheme for SRH. a. MsCl, Et3N, DCM, 0 °C –rt, Ar, 30 min; b. 1 M NaOH/H_2O, 60 °C, Ar, overnight; c. TFA/H_2O, 0 °C–rt, 3 hr.[27]

3.3.1 | Fluorescamine Quantification Assay. A fluorescamine quantification assay is a technique in which fluorescamine reacts with primary amines of amino acids to give fluorescent compounds. The fluorescence of these compounds is measured at an excitation of wavelength 390 nm and emission of wavelength 485 nm.[34] SRH also has a free primary amino group which reacts with fluorescamine to give a fluorophore measurable at 485 nm (see Fig. 3.13).

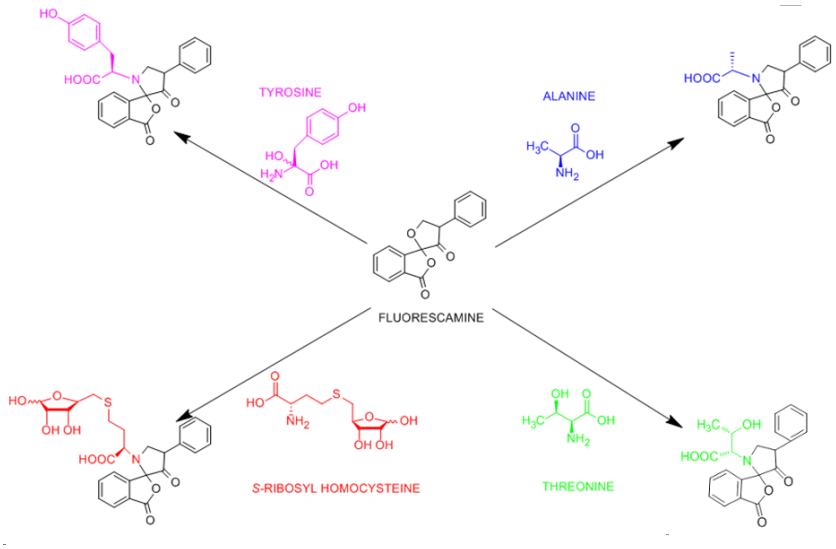

Fig. 3.13 | Fluorescamine Quantification of SRH. Fluorescamine reacts with three different amino acids tyrosine (pink), alanine (blue) and threonine (green). The fluorescamine reacts with SRH (red) in the same way due to the presence of a free amino group. Each of the reaction produces a fluorophore measured at 485 nm.

3.3.2 | Tyrosine Standard Curve. The amino acid tyrosine is the standard for fluorescamine quantification assay in accordance with literature precedent.[25] The results are demonstrated in Figure 3.14. The standard curve equation was used to calculate the amount of analyte in unknown samples.

3.3.3 | SRH Detection. To prepare the stock solution, a theoretical value of SRH was estimated from the overall yield of the chemical synthesis protocol (Fig 3.12) as 20%. The theoretical value of SRH is then 0.09144 g from 1 g of ribose, which was used to prepare "20 mM" SRH stock in distilled water. One mM working solutions of SRH were prepared from this "20 mM" SRH stock in 55 mM sodium borate buffer.

3.3.3.1 | Determination of Amount of SRH Present in the Mixture. Dilutions of SRH were made to obtain an emission values within the range of the tyrosine standard curve (0-40 μM) and were used to calculate the amount of SRH from the linear equation of the tyrosine standard curve (see Fig. 3.14 A). The concentrations of SRH determined from four replicates were 5.8, 4.4, 6.7 and 5.9 mM with a standard deviation of 0.96 (see Fig. 3.14 C), the values were four fold lower as compared to the original concentration of stock solution 20 mM of SRH.

3.3.3.2 | Estimation of Known Samples of Alanine and Threonine. The absence of a SRH standard led us to use the amino acids alanine and threonine in the fluorescamine quantification assay to determine its accuracy (see Fig. 3.13). Working solutions for the amino acids alanine and threonine of concentration 20 mM were prepared in 55 mM sodium borate buffer and the assay was performed. Emission values were recorded, applied to the standard curve, and sample concentrations were determined (see Fig 3.14 B). The concentrations of amino acids determined in the known 20 mM alanine samples were 20.9, 22, 39 and 35 mM with a standard deviation of 9.13 (see Figure 3.14 C). The percent errors for the alanine sample (of original conc. 20 mM) determined from four replicates were: 4.5, 10, 95 and 75 % respectively. The concentration of amino acids determined in the known 20

mM threonine samples was 21.2, 30, 37 and 30 mM with the standard deviation of 6.47 (see Figure 3.14 C). The percent errors for the threonine sample of known concentration (20 mM) from four replicates were: 6, 50, 85 and 50 % respectively.

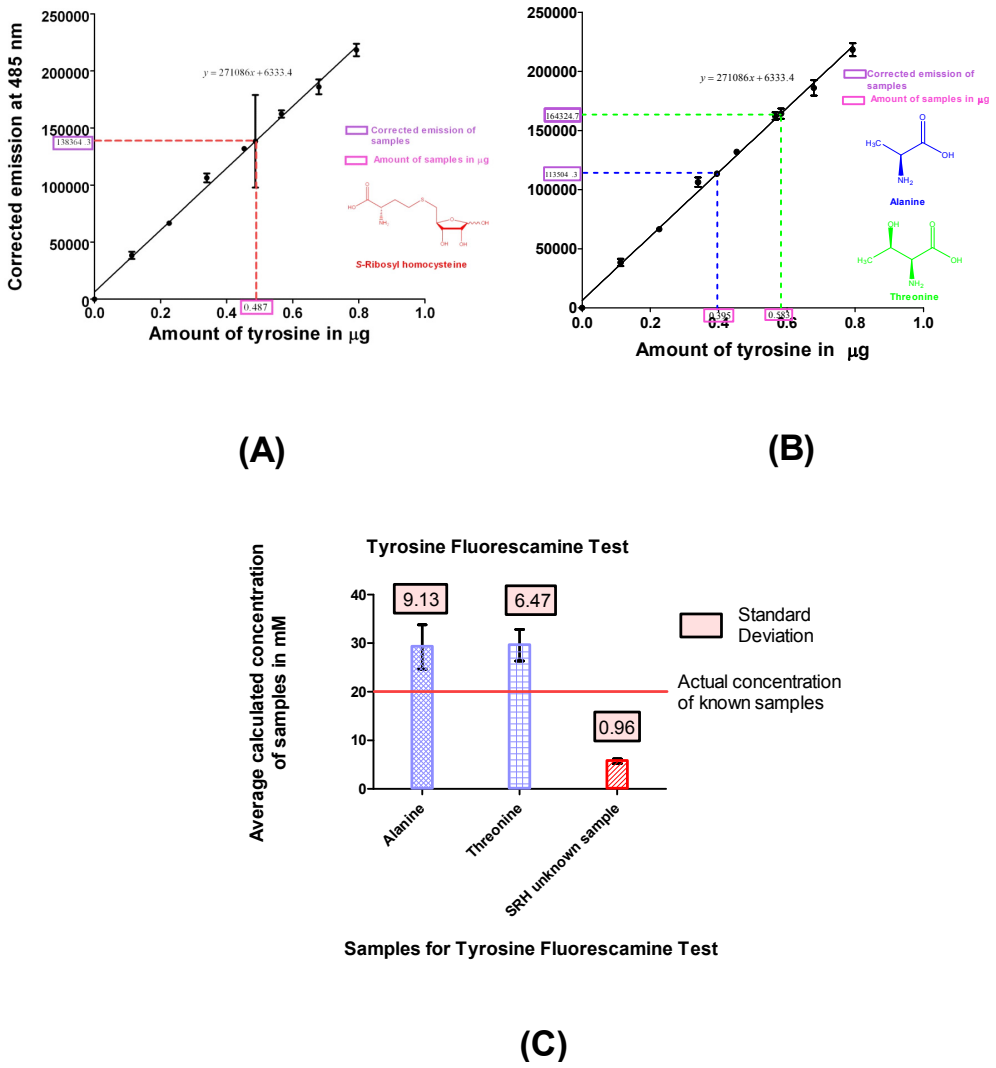

Fig. 3.14 | Tyrosine Fluorescamine Test. (A) The tyrosine standard curve and the linear equation was used to calculate the value of unknown SRH (red) sample. The red colored dotted line represents the amount of SRH determined using its emission value at 485 nm. (B) Determination of amount of alanine (blue) and threonine (green) used as known samples in one of the rounds from tyrosine standard curve. (C) Determined values of known alanine and threonine samples as well as unknown SRH samples in different replicates and their standard deviations are shown.

The high standard deviation values recorded for the known alanine and threonine samples from four replicates indicated imprecision in the method. And the high percent error values recorded for different replicates of fluorescamine quantification assay for the known amino acid standards (alanine and threonine) indicated inaccuracy. Hence, this assay was deemed to be unreliable (see Fig. 3.14). Therefore, a new synthesis scheme for SRH was devised and this new synthetic scheme provided more pure SRH without any further quantification.[27, 35]

3.4 | Ellman's Assay. As all of the required components of Ellman's Assay were acquired, activity assay for Co-BsLuxS-HT was ready to be performed.

3.4.1 | General Parameters. The assessment of the activity of an enzyme delivering an end product with a thiol group is done by an Ellman's assay. An appropriate enzyme is mixed with its substrate in a reaction mixture and the –SH group of the product reacts with DTNB to break into two equal parts (see Fig. 3.1). One of the parts reacts with the thiol group of the product to generate a conjugate. The other part (NTB^-) absorbs light at 412 nm (see Fig. 2.1). A time-dependent kinetic Ellman's assay, with varying concentrations of substrate, is performed to acquire reaction rates. These reaction rates are used to plot a Michaelis-Menten curve and to determine kinetic parameters: the maximum enzyme velocity (V_{max}), the substrate concentration at half V_{max} (K_M), and the turnover number (k_{cat}).

3.4.2 | Ellman's Assay for the Enzyme Co-BsLuxS-HT. In an effort to optimize the protocol for Ellman's assay, commercially-available homocysteine was used. As discussed previously, Ellman's reagent detects homocysteine as an indirect determination of LuxS activity (see Fig. 3.2).

3.4.2.1 | Optimizing Ellman's Assay by Homocysteine Quantification. According to the literature, an Ellman's assay for LuxS activity utilizes 30 µL of 680 µM SRH with 10 µL of 40 µM Co-BsLuxS-HT enzyme.[9] If 0.0204 µmoles of SRH (determined from 30 µL of 680 µM SRH) were completely converted to 0.0204 µmoles of homocysteine by the enzyme Co-BsLuxS-HT, the concentration of homocysteine produced in 1 mL of the reaction mixture would be 20.4 µM.

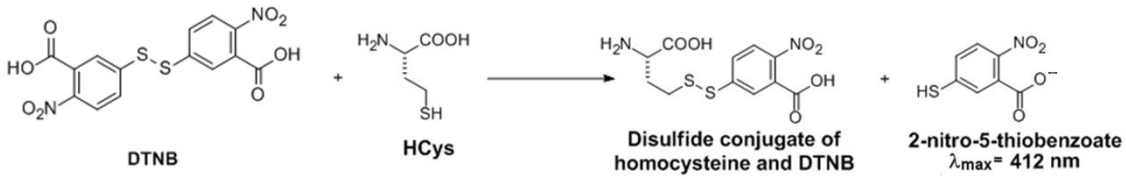

Fig. 3.15 | Homocysteine Quantification. Homocysteine reacts with 5,5'-dithiobis-(2-nitrobenzoic acid)/DTNB to give a disulfide conjugate and a yellow colored byproduct NTB^-, which is measured at 412 nm.

In order to be close to the maximum amount of homocysteine that could be produced in a true LuxS assay, homocysteine solutions of concentrations approximating 20.4 µM were prepared. Homocysteine solutions from 0-80 µM were reacted with Ellman's reagent. Six replicates of the assay were performed. The absorbance values recorded in each round were averaged, and a standard curve was plotted using these values. The error was determined as standard deviation. Linear trendline resulted in an R^2 value of 0.9996. Apart from optimizing this assay for the real Ellman's assay, this procedure also indicated a maximum absorbance that could be acquired for the enzyme in 1 mL of reaction mixture. The maximum absorbance value that could be acquired from complete conversion of 0.0204 µmoles of SRH into 0.0204 µmoles (7.8 µg) of homocysteine and DPD in a 1 mL reaction mixture was 0.840 (see Fig. 3.16).

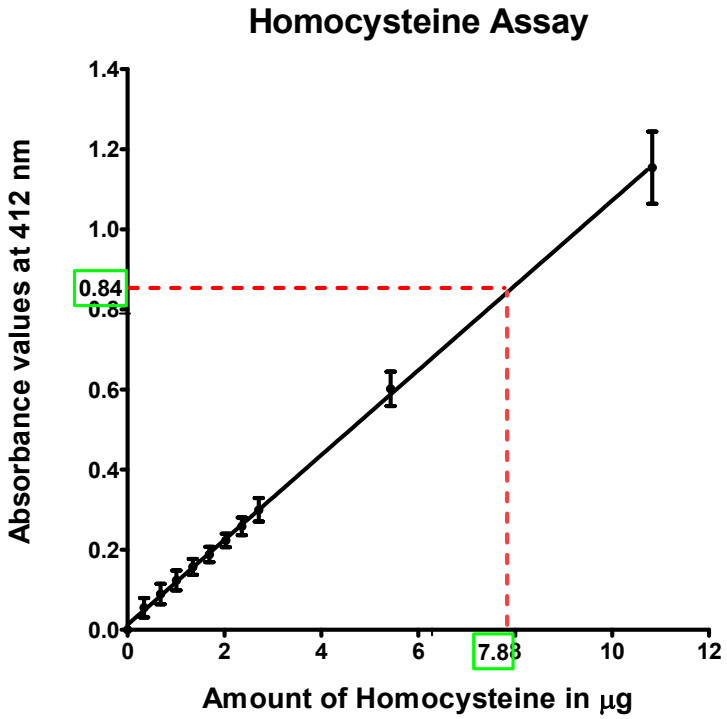

Fig. 3.16 | Homocysteine Assay. The standard curve acquired after averaging the absorbance values from the six rounds of the homocysteine assay. The error bars indicate units of standard deviation. The red dotted lines show the maximum absorbance value that could be recorded for Co-BsLuxS-HT.

3.4.2.2 | Co-BsLuxS-HT Assay. After optimizing the Ellman's assay, the activity assay for the enzyme Co-BsLuxS-HT was performed. A reaction mixture containing SRH, Ellman's reagent, distilled water, 5X LuxS buffer and Co-BsLuxS-HT was prepared (see Table 2.2). The enzymes were added at last to the cuvette with reaction mixture to ensure that absorbance values are recorded from the beginning of the enzymatic reaction. The absorbance values at 412 nm were measured every 17 seconds for a total of 204 seconds. Similarly, an Ellman's assay was performed for Co-BsLuxS-HT C84A, blank (with neither enzyme nor substrate), SRH blank (with only substrate and no enzyme), and enzyme blank (with no SRH and only enzyme). The absorbance values recorded under each set of conditions were plotted to obtain

a curve. The curves acquired for different samples were compared with each other to check the enzyme activity. Fig. 3.17 (A) shows the Co-BsLuxS-HT curve with increasing slope as compared to others depicting that the enzyme is binding with the substrate and producing homocysteine. The mutant Co-BsLuxS-HT C84A was found to be inactive (but with high background) as expected (see Section 3.2).[9]

The activities of the Co-BsLuxS-HT enzyme and its mutant were also determined as fold rate enhancement over their enzyme blanks (in absence of substrate). The linear equations of the curves for enzymes and their respective blanks (in absence of substrate) provided the slope, which was used to calculate the fold rate enhancement for the enzymes Co-BsLuxS-HT and Co-BsLuxS-HT C84A (see Fig. 3.17 (B)). A 4.7 fold increase was observed in freshly purified Co-BsLuxS-HT activity from Co-BsLuxS-HT blank. On the other hand, a 0.2 fold increase was observed for the negative control Co-BsLuxS-HT C84A from its respective blank. The fold rate enhancement values demonstrated that Co-BsLuxS-HT purified in our lab conditions was active whereas C84A mutant was inactive.

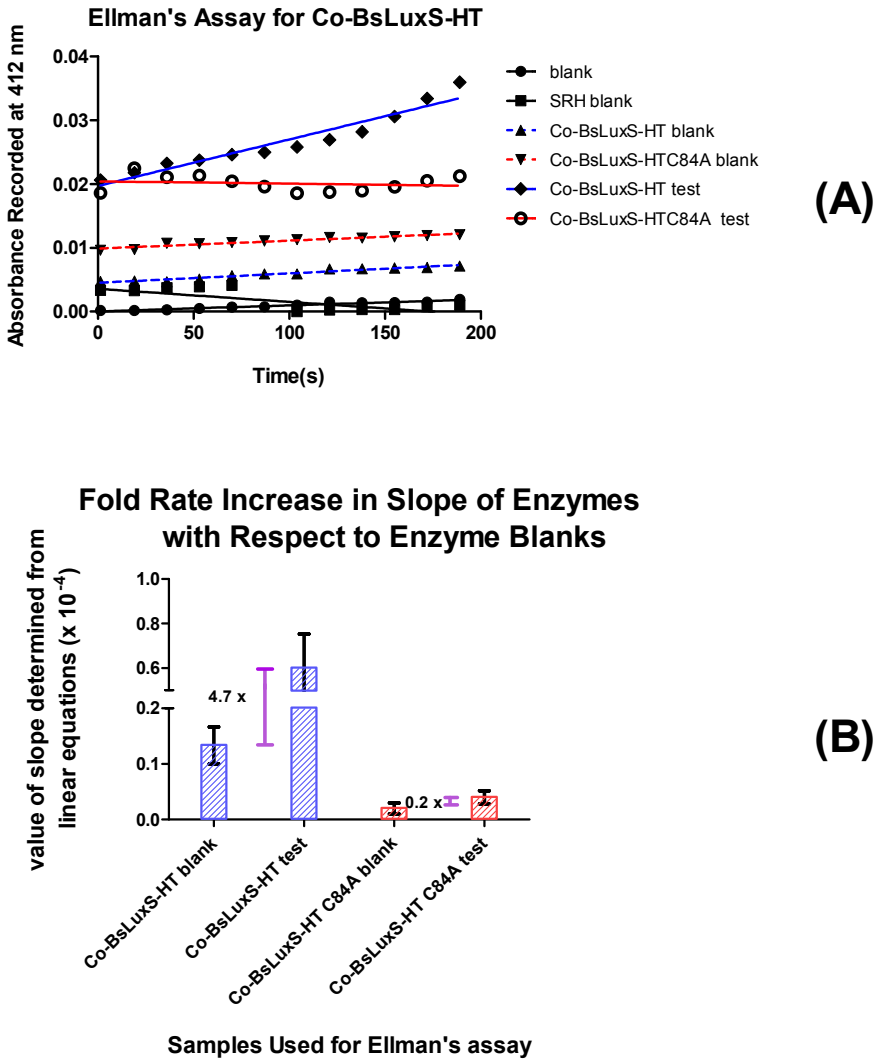

Fig. 3.17 | Ellman's Assay Curves & Fold Rate Enhancement. (A)The curves for different samples of Ellman's assay obtained from the absorbance values recorded at 412 nm. A continuous increase in the absorbance values of blue solid trendline for Co-BsLuxS-HT which depicts the rapid formation of homocysteine by the action of Co-BsLuxS-HT on SRH. (B) The fold rate increase in activity of enzyme over their respective blanks is depicted using values of slope acquired from three rounds of activity assay.

3.4.2.2.1 | Kinetic Parameters of Co-BsLuxS-HT. For the comparison of the activity of Co-BsLuxS-HT purified in our lab conditions with the Co-BsLuxS-HT purified by Pei et al., the

kinetic parameters V_{max}, K_M, k_{cat} and catalytic efficiency of the enzyme were determined.[9] V_{max} is the maximum enzyme velocity, whereas K_M, the amount of substrate at half of V_{max}, is used to evaluate the binding affinity of the enzyme. The kinetic constant k_{cat} defines the turnover number of an enzyme, i.e. the number of substrate molecules converted to product per second. The ability of an enzyme to convert the substrate into product at a high reaction rate is called its catalytic efficiency. The kinetic parameters determined by us for the house-purified Co-BsLuxS-HT were expected to be comparable with the published values by Pei et al.[9]

The parameters K_M and V_{max} of Co-BsLuxS-HT were determined via an Ellman's activity assay using variable concentrations of SRH.[a] The absorbance values (AU/s) of enzymatic reactions using 0-68 μM SRH according to the protocol set by Pei were recorded at 412 nm (see Table 2.2 for reaction composition).[9] These values were then converted to reaction rates in units of μmol/mg/min for comparison to the reaction rates provided by Pei et al.[9] The equations used for determining the amount of Co-BsLuxS-HT present in 1 mL of final reaction mixture and the conversion of units of reaction rates from AU/s to μmol/mg/min are provided in Fig 3.18 (A) & (B). A Michaelis-Menten curve was plotted using these values of reaction rates (μmol/mg/min) versus SRH concentration in Graph Pad Prism 5.0, to relate the rate of enzymatic reaction to the concentration of the substrate.[23a,36] The Michaelis-Menten curve was used to determine the kinetic parameters K_M (μM) and V_{max} (μmol/mg/min) for

[a] Initially, to acquire reaction rates for plotting the Michaelis-Menten curve, SRH concentrations from 0 μM-2000.0 μM were used (see Appendix B). The K_M values determined for Co-BsLuxS-HT purified in our lab using the above mentioned SRH concentration range was 93.5 μM, which was approximately six fold higher than the K_M value (i.e. 2.3 μM) of the Co-BsLuxS-HT reported by Pei et al.[9] Later, an SRH concentration range of 0 μM to 68 μM, as used in the published paper by Pei et al. for calculation of kinetic parameters, was used for a revision of the calculation of kinetic parameters of Co-BsLuxS-HT enzyme purified in our lab conditions. [9]

Co-BsLuxS-HT. The K_M value of 2.1 µM was comparable to the K_M value of 2.3 µM reported by Pei and coworkers (see Fig 3.19), indicating that the enzyme purified in our lab conditions binds equally well to the substrate.[9] The enzyme's maximal velocity (V_{max}) in µmol/mg/min was converted to µmol/s using the equation (D) in Fig. 3.18. The V_{max} for house-purified Co-BsLuxS-HT (1.1 x 10^{-5} µmol/s) was approximately 2.5 fold less as compared to the V_{max} value (2.8 x 10^{-5} µmol/s) of Co-BsLuxS-HT provided by Pei et al., indicating that the time taken by the house-purified enzyme to convert one mole of substrate into product was 2.5 times greater.[9]

To calculate the value of k_{cat}, the concentration of enzyme active sites in a reaction mixture $[E]_t$ was required. The enzyme Co-BsLuxS-HT is a homodimer of molecular weight 34438 g/mol with 2 active sites. Thus, the value of $[E]_t$ obtained according to equation (D) in Fig. 3.18 was 0.0008 µmoles. The value of k_{cat} for house-purified Co-BsLuxS-HT was 0.014 s^{-1} (determined using the equation (E) in Fig. 3.18) which was 2.5 fold less than the value of k_{cat} provided in literature (0.035 s^{-1}). This value indicated that one mole of substrate took 2.5 fold greater time to be converted into product, which was expected according to the lower V_{max} for the house-purified enzyme. The catalytic efficiency (determined using the equation (F) in Fig. 3.18) of house-purified LuxS was 0.67 x 10^4 M^{-1}/s^{-1}, which was 2.4 fold lower than the catalytic efficiency (1.67 x 10^4 M^{-1}/s^{-1}) of the enzyme purified by Pei and coworkers. Again because the maximal reaction rate V_{max} was lower than the literature values, it affected the catalytic efficiency of the enzyme.[9] Although the value of K_M was comparable, but the lower k_{cat}, $V_{max,}$ and catalytic efficiency values of house-purified Co-BsLuxS-HT as compared to those provided by Pei et al., depicted some discrepancies in purification procedure of house-purified Co-BsLuxS-HT. The K_M value of the house-purified enzyme demonstrated that the

enzyme and substrate bind well but somehow the conversion of substrate to product was slow. One probability for this could be that the cysteine 84 amino acid residue, that initiates catalysis in the active site, gets oxidized to some extent during the slow manual protein purification process thus impairing the overall catalytic ability of the stock solution.

(A) Determination of amount of LuxS in cuvette (mg)

$$LuxS\ in\ cuvette\ (mg) = final\ \ conc.\ of\ enzyme\ in\ cuvette\left(\frac{mol}{L}\right)\times Mol.\ wt.\ of\ LuxS\left(\frac{g}{mol}\right)\times volume\ of\ reaction\ \ mixture\ (L)\times\left(\frac{1000\ mg}{g}\right)$$

(B) Conversion of absorbance units to reaction rate (V) unit (µmol/mg/min)

$$V\ (\mu mol/mg/\min) = \frac{\left[\dfrac{absorbance\ \ (AU/s)}{molar\ absorption\ \ coefficient\ of\ DTNB^{-}\ \varepsilon\ (M^{-1}cm^{-1})}\times\left(\dfrac{60\ s}{\min}\right)\times\left(\dfrac{10^{6}\ \mu M}{M}\right)\times volume\ of\ reaction\ mixture\ (L)\right]}{amount\ of\ LuxS\ in\ cuvette\ (mg)}$$

(C) Conversion of maximum reaction velocity (V_{max}) units from µmol/mg/min to µmol/s

$$V_{\max}\ (\mu mol/s) = V_{\max}\ (\mu mol/mg/\min)\times amount\ of\ LuxS\ in\ cuvette\ (mg)\times\left(\frac{\min}{60\ s}\right)$$

(D) Determination of $[E]_t$

$$moles\ of\ LuxS\ in\ cuvette\ (\mu mol) = amount\ (mg)\times\left(\frac{g}{1000\ mg}\right)\times\left(\frac{mol}{34438\ g}\right)\times\left(\frac{10^{6}\ \mu mol}{mol}\right)$$

$$[E]_t = moles\ of\ LuxS\ in\ cuvette\ (\mu mol)\times no.\ of\ active\ sites$$

(E) Calculation of k_{cat} $\qquad k_{cat} = \dfrac{V_{\max}\ (\mu mol/s)}{E_t\ (\mu mol)}$

(F) Calculation of catalytic efficiency $\qquad Catalytic\ efficiency\ of\ LuxS = \dfrac{k_{cat}\ (s^{-1})}{K_M\ (\mu M)}$

Fig. 3.18 | Calculations and Unit Conversions for Determination of Kinetic Parameters of Co-BsLuxS-HT. The equations used for determination of LuxS (mg) **(A)**, $[E]_t$ **(D),** k_{cat} **(E)**, catalytic efficiency for Co-BsLuxS-HT **(F)** and unit conversions of recorded absorbances at 412 nm **(B)** and V_{max} **(C).** Where no. of active sites in Co-BsLuxS-HT is 2, molecular weight of Co-BsLuxS-HT is 34882 g/mol and molar absorption efficient coefficient for $DNTB^{-}$ (ε) is14150 $M^{-1}cm^{-1}$.

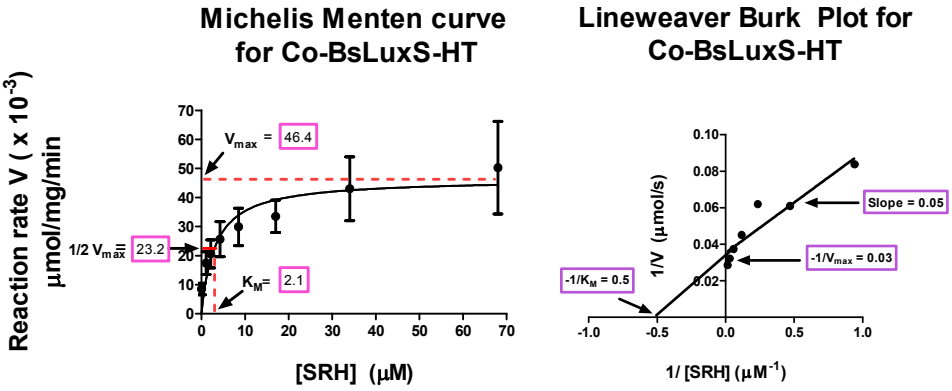

(A) (B)

Enzyme	K_M (µM)	V_{max} (µmol/s)	k_{cat} (s^{-1})	k_{cat} / K_M (M^{-1}/ s^{-1})
Co-Bs-LuxS-HT House-purified	2.1 ± 1.4	1.1 x 10^{-5}	0.014 ± 0.002	0.67 x 10^4
Co-Bs-LuxS-HT (by Pei et al.)[9]	2.3 ± 0.5	2.8 x 10^{-5}	0.035± 0.003	1.6 X 10^4

(C)

Fig 3.19 | Michaelis-Menten curve, Lineweaver Burk Plot and Comparison of Kinetic Parameters. (A) Michaelis-Menten curve for Co-BsLuxS-HT purified in our lab conditions with error bars depicting the absorbance values recorded in triplicate. The Michaelis-Menten curves for each individual round are provided in Appendix B. (B) Lineweaver Burk plot for calculation of kinetic parameters (C) Kinetic parameters of the two Co-BsLuxS-HT enzymes.

3.5 | Conclusion and Future Directions. The Ellman's assay is ready to be used for determination of potential SRH analogs as inhibitors of the enzyme Co-BsLuxS-HT. Before determination of the activity of putative Co-BsLuxS-HT inhibitors, the Ellman's assay was also used for activity assay of other Co-BsLuxS-HT mutants (See Chapter 4). This assay proved to be a useful tool to determine the activity of Co-BsLuxS-HT mutants which were

required for fluorescence proximity assay discussed in Chapter 4. In future this assay will be optimized for 96 well plate, for minimizing excessive use of enzymes and substrates.

CHAPTER 4: FLUORESCENCE PROXIMITY ASSAY

Several types of inhibitors of LuxS have been designed and tested in the literature, including SRH analogs modified at the ribosyl C3 position, analogs with a [4-aza] ribose ring and (*S*)-2-amino-4-((2*S*, 3*R*)-2,3-dihydroxy-4-(hydroxyamino)-4-oxybutylthio) butanoic acid.[21,23b,25,35] The SRH analogs proposed by our lab are a new class of LuxS inhibitors, and are expected to inhibit LuxS by disrupting its dimerization (see Fig. 3.2). These analogs are structurally similar to SRH except an alkyl or aryl group will be introduced at the homocysteine C3 position (see Fig. 4.1). This is expected to inhibit the Co-BsLuxS-HT enzyme monomers from dimerizing correctly, as has been previously reported for other enzymes.[26]

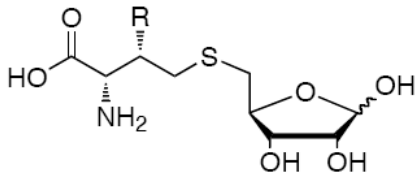

SRH Homocysteine C3 analogs (R = alkyl or aryl)

Fig. 4.1 | Proposed SRH Homocysteine C3 Analogs as LuxS Dimerization Inhibitors. The addition of bulky groups at the 3rd position of SRH is expected to disrupt LuxS dimerization. [27, 35]

As discussed earlier, the LuxS enzyme is a 35 kDa homodimeric protein. SRH positions itself at the active site, present in between the two monomers, and is catalytically converted to DPD and homocysteine (see Fig. 4.2). The DPD produced from SRH cyclizes to form the interspecies quorum sensing AI-2, which initiates System Two quorum sensing (see Introduction). The replacement of SRH by a potential dimerization inhibitor at the active site would inhibit DPD production and therefore AI-2. This results in an inhibition of quorum sensing and its related behavioral responses (virulence, etc.).

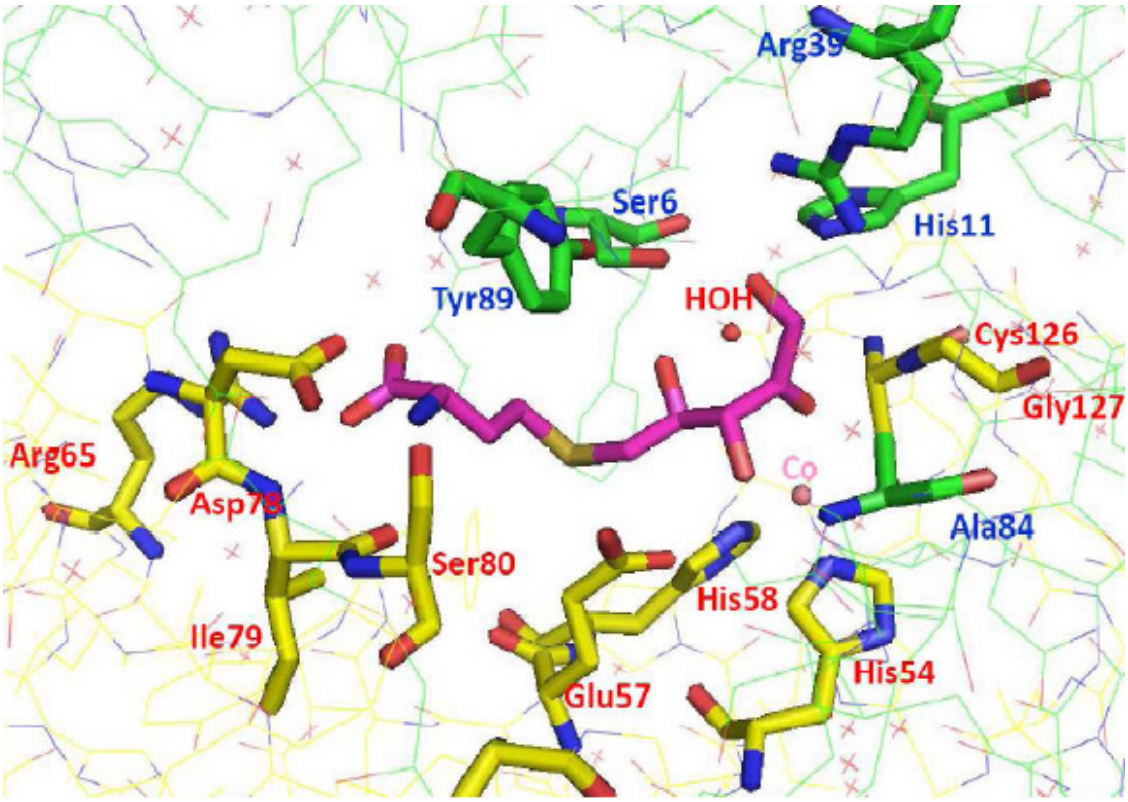

Fig. 4.2 | Co-BsLuxS-HT Binding Site. The binding site of Co-BsLuxS-HT C84A, with a catalytic 2-ketone intermediate (magenta) present at the position where SRH binds. One monomer is shown in yellow with names of the amino acid residues in red, and the other monomer is shown in green with the names of amino acid residues in blue. The structures of the major residues in the active site are enhanced (other residues are depicted by thin sticks).

Fluorescence proximity assay would be used for the detection of dimerization inhibition of LuxS by the abovementioned dimerization inhibitors. A fluorescence proximity assay is a technique used to assess the inhibition of a dimeric protein in the presence of a potential dimerization inhibitor by measuring the change in fluorescence upon monomer separation.[37] Assays of this general type have been used previously for enzymes like DNA polymerase III and HIV protease (see section 1.5).[26]

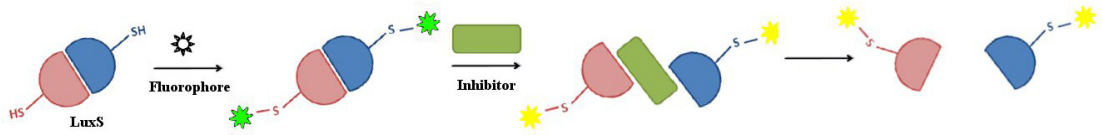

Fig. 4.3 | Fluorescence Proximity Assay for Co-BsLuxS-HT. A fluorophore is attached to the Co-BsLuxS-HT active mutant. The fluorescence changes when a dimerization inhibitor comes in between the two monomers of homodimeric Co-BsLuxS-HT. This change in fluorescence could be measured over time for detection of dimerization inhibition.

The fluorescence of a Co-BsLuxS-HT variant conjugated with a fluorophore remains unaltered when the protein is in its dimeric state (see Fig. 4.3). If a dimerization inhibitor comes in between the two monomers of the enzyme, the result is a change in proximity between the monomers, which leads to a change in fluorescence. The measurement of this change in fluorescence over time could help to detect the dimerization inhibition. To detect the inhibition of Co-BsLuxS-HT enzyme by potential inhibitors, there are two basic requirements: (1) a fluorophore-attached active Co-BsLuxS-HT mutant and (2) SRH analogs as potential dimerization inhibitors. The organic chemists in our laboratory are currently working towards synthesizing a SRH analog which could act as a dimerization inhibitor.[18,35,38] In the meantime, experimental work towards acquiring a fluorophore-attached Co-BsLuxS-HT mutant was performed.

The fluorescence proximity assay requires a thiol reactive fluorophore (see Fig. 4.4) attached to a properly-folded Co-BsLuxS-HT variant. For the attachment of a thiol-reactive fluorophore without any obstruction, a single surface accessible cysteine (–SH) is required on the Co-BsLuxS-HT enzyme. In order to keep the enzyme variant in its native folded form, the position of the cysteine for the attachment of the fluorophore should not be at either the active

site or the dimer interface. A catalytically misfolded Co-BsLuxS-HT enzyme could deter dimerization on its own and in that case it would be difficult to determine if the inhibitor was responsible for dimerization inhibition.

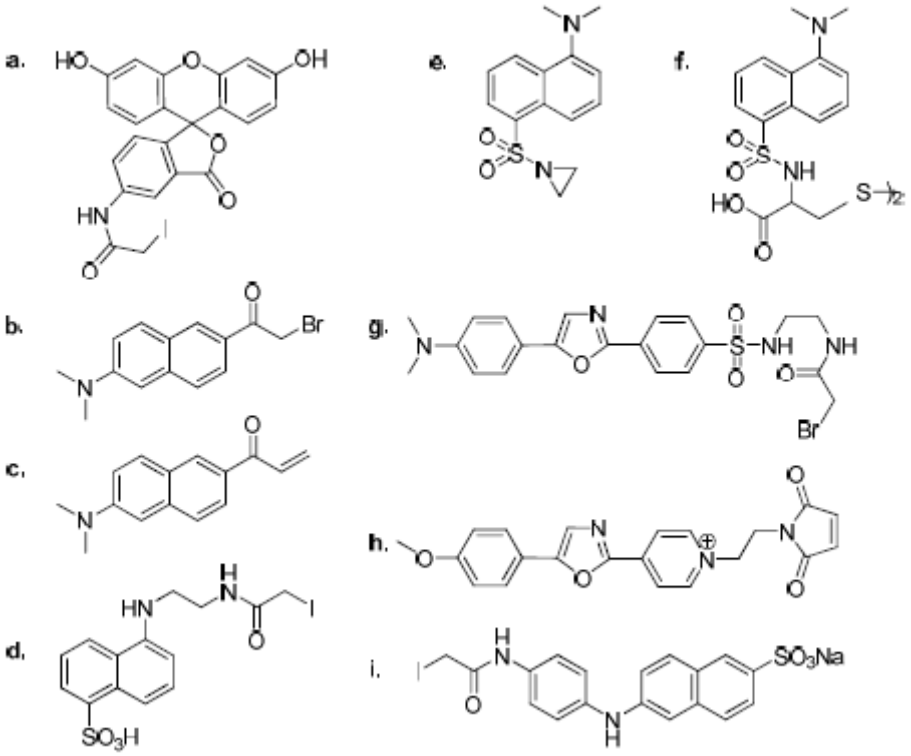

Fig. 4.4 | Examples of Thiol-Reactive Fluorophores. (a) 5-iodoacetamidofluorescein (b) Dansyl aziridine (c) DDC (d) Badan (e) Acrylodan (f) IAEDANS (g) Dapoxyl (h) PyMPO (i) IAANS.

The two steps to synthesize a fluorophore-attached, properly-folded single-cysteine Co-BsLuxS-HT mutant: (1) prepare a catalytically active Co-BsLuxS-HT variant with a single surface accessible cysteine and (2) attach a fluorophore to the active Co-BsLuxS-HT mutant. Efforts towards achieving an active Co-BsLuxS-HT variant for eventual fluorophore attachment (step 1) are explained in the following sections.

The wild type Co-BsLuxS-HT enzyme protein has four native cysteines at positions 22, 41, 84 and 126. The C84 position was not an appropriate option for fluorophore attachment because it is known to reside in the enzyme active site at the dimer interface.[10] Therefore, possibilities for a fluorophore-attachment site on Co-BsLuxS-HT include either: (a) one of the three native cysteines at positions 22, 41 and 126 (see Fig. 4.5) or (b) an amino acid elsewhere which could be mutated to cysteine keeping the catalytic properties of the enzyme intact. The following sections describe in detail the efforts made towards preparing a Co-BsLuxS-HT variant having a single surface-accessible cysteine residue that retains wild type catalytic activity.

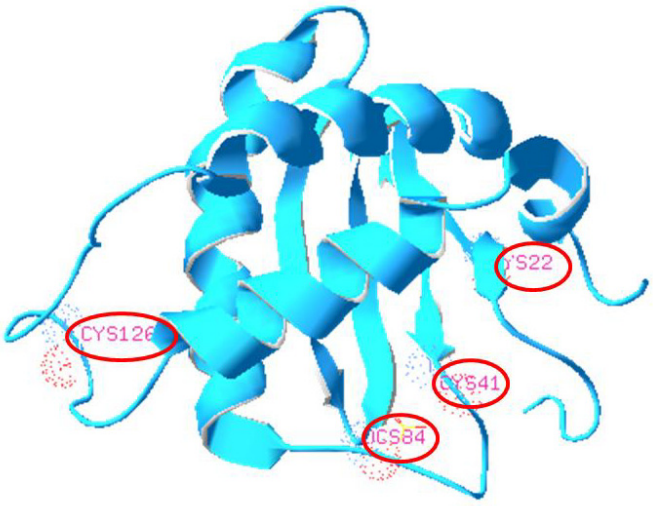

Fig. 4.5 | Structure of BsLuxS Monomer showing the Position of the Three Native Cysteines. The cysteines positioned at 22, 41, 84 and 126 (encircled in red) in a LuxS monomer of *Bacillus subtillis.* Alpha chains, beta sheets, loops are shown in orange, yellow and white color respectively. This figure was generated using the DeepView software program.

4.1 | Preparing an Active Co-BsLuxS-HT Variant with a Single Surface Accessible Cysteine from Three Native Cysteines (22, 41, and 126). The four native cysteines present

in a wild type Co-BsLuxS-HT are at positions 22, 41, 84 and 126. The best possible option of using a native cysteine for fluorophore attachment was hypothesized to be cysteine 41 because of its presence on the outer loop of the protein and it is not involved in either active site or dimer interface. The other three positions of native cysteine were not expected to be suitable for fluorophore attachment. The cysteine at 84 position, resides in the enzyme's active site (see Section 4.4), therefore a mutation here turns the enzyme inactive which has been demonstrated by Pei et al.[9] Cysteine 22 is present on a β-strand at the dimer interface and derivatization at this position could therefore hamper enzyme dimerization. The cysteine 126 is positioned in the ligation sphere of the metal ion of Co-BsLuxS-HT, making this a largely inaccessible cysteine for fluorophore attachment. The derivatization at 126 position might dislocate the cobalt ion leading to the loss of metal ion from the enzyme, turning the enzyme catalytically inactive (and yellow instead of its native blue color). Mutations at all three of these native cysteine positions were attempted in order to analyze all the available possibilities in the wild type Co-BsLuxS-HT enzyme. If the enzyme was found catalytically active even after the mutations at any of these three abovementioned native positions, it would be used for fluorophore attachment for detection of dimerization inhibitors.

4.1.1 | Generation of Co-BsLuxS-HT Mutants by Site-Directed Mutagenesis. Different combinations of mutants using the native cysteines were generated, to acquire a catalytically active enzyme mutant with a single surface accessible cysteine available for fluorophore attachment. Table 4.1 shows the Co-BsLuxS-HT mutants, some of them were expected to be catalytically active with a surface accessible cysteine. The Co-BsLuxS-HT mutants with a C84A mutation were expected to turn the enzyme catalytically inactive, but they were still generated to be used as a negative control.

Table 4.1 | Co-BsLuxS-HT mutants. The four types of mutations to be performed and the different Co-BsLuxS-HT mutants required. The mutants with C84A mutation were prepared to be used as negative controls. The presence of C126A and C22A at the active site and dimer interface made it little unsure that mutation at these sites would still render the enzyme active.

Co-BsLuxS-HT Mutants	Native Cysteine Positions				Expected to be Catalytically Active
	22	41	84	126	
Single Co-BsLuxS-HT Mutants					
S1	A	C	C	C	May be
S2	C	A	C	C	Yes
S3	C	C	A	C	No
S4	C	C	C	A	May be
Double Co-BsLuxS-HT Mutants					
D1	A	A	C	C	May be
D2	C	A	A	C	No
D3	C	C	A	A	No
D4	A	C	C	A	May be
D5	A	C	A	C	No
D6	C	A	C	A	May be
Triple Co-BsLuxS-HT Mutants					
T1	A	A	A	C	No
T2	C	A	A	A	No
T3	A	C	A	A	No
T4	A	A	C	A	May be
Quadruple Co-BsLuxS-HT Mutant					
Q	A	A	A	A	No

4.1.1.1 | General Parameters for Generation of Mutants by Site-Directed Mutagenesis. The general parameters for the generation of mutants were the same as mentioned previously (see Section 3.2.1).

4.1.1.2 | Generation of Co-BsLuxS-HT Mutants by Site-Directed Mutagenesis. The generation of a single mutant Co-BsLuxS-HT C84A (**S3**) and its use as a negative control in the activity assay of Co-BsLuxS-HT has been discussed previously in Chapter 3 (see Section 3.2).

Appropriate primer pairs encoding for the mutations C22A, C41A and C126A were designed using PrimerX. The primer design guidelines of QuikChange® site directed mutagenesis kit, such as GC% (the strength of the fragment based on the number of triple bonded G and C nucleotides present should be minimum 40%), T_m (melting temperature ≥75°C) and length (25-45 bp), were used for the design of these primers to ensure their integrity at varying PCR conditions (see Table 4.2). The purified plasmid encoding for the wild type Co-BsLuxS-HT was used as a template. The SDM, Pellet Paint® Co-Precipitant and transformation procedures and conditions were the same as previously mentioned (see Section 3.2.2).

Table 4.2 | Primers Encoding Single Mutations. The primers designed using PrimerX for the synthesis of single mutants along with their characteristics is shown.

Primers Encoding Mutation	Primers	Length (bp)	GC %	Melting Temp. (°C)
C22A	5'GTTGCTCCATATGTAAGACATGCG GGCGTGCATAAAGTGGGAAC 3'	44	50.0	79.7
C41A	5'GTTGTAAATAAATTTGACATTCGT TTTGCGCAGCCAAATAAACAGGCG ATGAAGCC 3'	56	39.3	80.4
C126A	5'GCTGCGAATGAAAAGCAGGCGGG CCAAGCGAAGCTTCATG 3'	40	57.5	80.0

Once the colonies of transformed cells were selected and grown, the purified plasmids containing the desired mutations were sent for sequencing (Sequetech).[b] The sequences were aligned using the SeqMan Pro module of DNAStar Lasergene 8.0 to determine if the single Co-BsLuxS-HT mutations were achieved. All the desired single Co-BsLuxS-HT mutations **S1**, **S2** and **S4** (see Table 4.1) were successfully made.

Initially, Co-BsLuxS-HT C84A (**S3**) was used as template for the generation of the double Co-BsLuxS-HT C41AC84A (**D2**) mutant because it was the first mutant to be generated and purified. The C41A primers used for the mutation are shown in Table 4.2. The method for synthesis of the double Co-BsLuxS-HT C41AC84A (**D2**) mutant was also the same as provided in Section 3.2.2. The colonies acquired after transformation of the plasmids (expected to encode for mutation **D2)** into competent bacterial cells were grown in LB Amp[75] media for selective growth of bacterial cells carrying the plasmid with ampicillin resistance

[b] Due to easy delivery of samples and prompt sequencing results received from Sequetech, the sequences were sent for sequencing to Sequetech instead of Seqwright where the sequences have been sent previously (see Section 2.2).

(see Section 3.1). The plasmids purified from the bacterial cells present in the culture, using Fermentas GeneJET™ plasmid purification miniprep kit, were sent for sequencing. The sequences were found to contain only the single C41A (**S2**) mutation (see Table 4.3) instead of the expected and desired Co-BsLuxS-HT C41AC84A (**D2**) mutation. This suggested that in the presence of C84A mutation makes it difficult to incorporate another mutation because the C84A mutation reverted itself back to the C84C, delivering a sequence only with a single mutation. The reason for this reversion is unknown. When this method failed to produce the desired results, two new techniques were used to achieve double mutants again using Co-BsLuxS-HT C84A (**S3**) as template and to confirm our hypothesis of C84A reversion.

The new techniques employed for acquiring double mutants using Co-BsLuxS-C84A (**S3**) as template were (a) cloning and (b) use of non-overlapping primers instead of overlapping primers. However, both the techniques also resulted in a reversion of the C84A to C84C when the second mutation was attempted to be incorporated (see Table 4.3). Efforts toward acquiring the double Co-BsLuxS-HT C22AC84A (**D5**) mutant using Co-BsLuxS-HT C84A (**S3**) mutant as template by cloning technique is described in detail in the following sections.

Table 4.3 | Reversion of C84A mutation. The Co-BsLuxS-HT C84A (**S3**) mutant when used as the template for the generation of the double Co-BsLuxS-HT mutants were found to revert to C84C. The attempts for achieving the double Co-BsLuxS-HT mutants using C84A (**S3**) as a template and new techiniques (cloning and use of non-overlapping primers) are explained in Sections 4.1.1.2.1 and 4.1.1.2.2, repectively.

Mutation desired	Template Used	Primer Used	Technique used	Mutant achieved
C41AC84A (**D2**)	C84A (**S3**)	C41A Overlapping	SDM	C41A (**S2**)
C22AC84A (**D5**)	C84A (**S3**)	C22A Overlapping	SDM	C22A (**S1**)
C22AC84A (**D5**)	C84A (**S3**)	C22A Overlapping	Cloning	C22A (**S1**)
C22AC84A (**D5**)	C84A (**S3**)	C22A Non-overlapping	SDM	C22A (**S1**)
C126AC84A (**D3**)	C84A (**S3**)	C126A Non-overlapping	SDM	C126A (**S4**)
C41AC84A (**D2**)	C84A (**S3**)	C41A Non-overlapping	SDM	No mutation found

4.1.1.2.1 | Cloning Technique for Achieving a Double Co-BsLuxS-HT Mutant. The term 'cloning' here refers to molecular cloning which involves processes used to create copies of small molecules, e.g. DNA fragments. Due to failed attempts of achieving double mutants by site directed mutagenesis using **S3** mutant as template, cloning of the mutated DNA fragments encoding the double mutation and incorporation into the plasmid vector pET-22b(+) was expected to deliver results. Initially, cloning technique was used to acquire a double Co-BsLuxS-HT C84AC22A (**D5**) mutant. This was done in order to determine if the cloning technique worked. If this technique was successful in obtaining the **D5** mutant, it was planned to be eventually used for acquirement of other double, triple and quadruple variants.

For the incorporation of the cloned DNA fragment containing the desired mutation, a pET-22b(+) plasmid vector was required (see Section 3.1). This was acquired using wild type

purified Co-BsLuxS-HT plasmid. The wild type purified Co-BsLuxS-HT plasmid was digested with the restriction enzymes *Nde*-I and *Xho*-I. As mentioned previously (Section 3.1), these restriction enzymes had been used to incorporate the DNA fragment coding for the *Bacillus subtillis* LuxS by Pei & coworkers.[9] Therefore, these enzymes were used to remove that DNA fragment from the vector.[9] Along with the *Nde*-I and *Xho*-I digested wild type Co-BsLuxS-HT plasmid, five other samples were prepared: (a) supercoiled/undigested plasmid (wild type Co-BsLuxS-HT), (b) *Nde*-I digested plasmid (linear Co-BsLuxS-HT plasmid because of a single cut near DNA insert), (c) *Xho*-I digested plasmid (linear Co-BsLuxS-HT plasmid because of a single cut near DNA insert), (d) *Pst*-I digested plasmid (linear Co-BsLuxS-HT plasmid because of a single cut away from the DNA insert), (e) blank containing no plasmid. The digested products along with the blank were loaded on a 1% agarose gel as good resolution of DNA fragments of size 0.5-10 kb is usually achieved using 1% agarose gels. The other samples were electrophoresed along with doubly-digested plasmid to compare the bands and to determine if the plasmid was doubly-digested by both *Nde*-I and *Xho*-I. The expected band for sample (a) was a thick band near 5-6 kb bands of ladder as the Co-BsLuxS-HT protein is 5.5 kb and circular. The samples (b), (c), and (d) when digested by the enzymes were expected to turn the circular DNA to linear form. The linear form of DNA travels faster in comparison to circular form of DNA hence the bands for these samples were expected to lie near and little farther from the band of sample (a). The band for the double digested plasmid was expected near ~5.4 kb due to removal of the DNA insert of ~500 bp. A small band of ~500 bp for the removed DNA insert from the plasmid vector pET-22b(+) was also expected. For the blank sample no band was expected as it did not contain DNA.

The bands on the gel were visualized with UV light because the ethidium bromide dye present in the gel fluoresces under UV light when intercalated into DNA. Two bands were acquired for supercoiled Co-BsLuxS-HT (sample a), as obtained previously by SDS-PAGE gels (see Fig. 4.6 & 3.9). Thin bands for the singly digested plasmids (samples b, c and d) were also obtained near 5 kb band of ladder, as expected (see Fig. 4.6). No band for blank was obtained. A broad band near 5 kb band of ladder was acquired for the pET-22b(+) vector (doubly digested sample), as expected (see Fig. 4.6). A small band near ~500 bp band of ladder for the removed DNA insert from the plasmid vector was not obtained. The possible reason could be the use of 1% agarose gel for resolution as resolution of tiny DNA fragments a gel of higher percentage of agarose is typically used. Assuming that the double-digest worked despite the absence of the 500 bp band, the band for the vector was cut from the gel using a sterilized blade. The gel fragment containing the desired plasmid was purified using NucleoSpin® gel extraction kit and stored at -80°C in an Eppendorf tube. This kit helps in extracting the DNA from the gel fragment by solubilizing the gel and removing it from the solution containing DNA. The purified pET-22b(+) plasmid vector was saved at -80°C until the clones of DNA fragment encoding for double mutation were acquired.

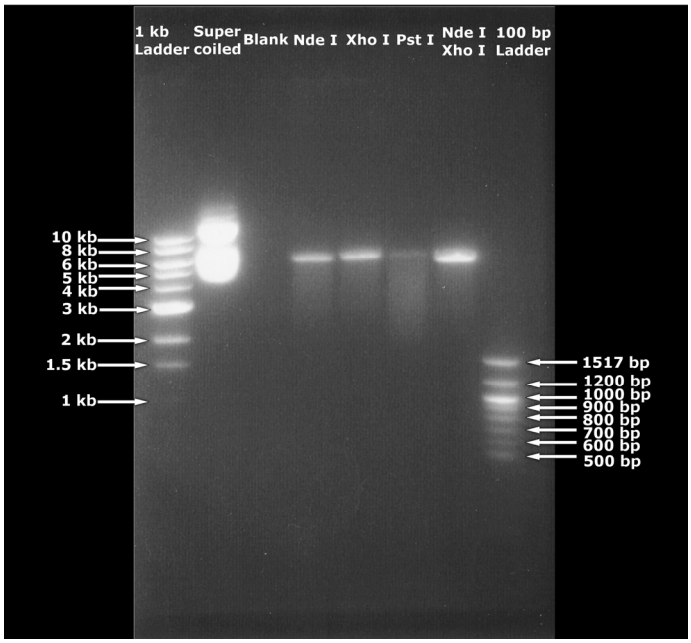

Fig. 4.6 | Agarose Gel Electrophoresis of pET-22b(+) Vector Digests. The picture shows the bands for different samples such as undigested Co-BsLuxS-HT/supercoiled, blank, *Nde*-I digested plasmid sample, *Xho*-I digested plasmid sample, *Pst*-I digested plasmid sample and plasmid vector pET-22b(+) obtained after digestion by two the restriction enzymes *Nde*-I and *Xho*-I.

The DNA fragment coding for the desired LuxS mutation was generated after acquiring a purified plasmid vector pET-22b(+). Two kinds of primers were required: a full length primer coding for the template Co-BsLuxS-HT C84A, and a C22A primer. These were designed manually using the DNA sequence of *Bacillus subtillis* coding for LuxS. The primers and their characteristics are listed in the Table 4.4. The designed primers for cloning technique were sent to IDT for synthesis.

Table 4.4 | Cloning Primers. The primers manually designed for cloning technique to incorporate the C22A mutation into Co-BsLuxS-HT C84A template.

Primers encoding for mutation	Primers	Length (bp)	GC %	Melting Temp. (°C)
Full Length Primers	5'GGAAGGCCATATGCCTTCAG TAGAAAGTTTTGAG 3'	34	44.1	66.6
C22A	5'GTAAGACATGCCGGCGTGCA TAAAG 3'	25	52	62.4

Two PCR reactions were performed. One reaction was run with full length reverse primer and C22A forward primer in order to obtain DNA fragments with C22A mutation on the 5'→3' strand (see Fig. 4.7). The second PCR reaction was run using full length forward primer and C22A reverse primer to obtain DNA with C22A mutation on the 3'→5' strand. Reaction buffer, distilled water, dNTP's and the Ex Taq™ DNA polymerase enzyme were added to both reaction mixtures. The SDM kit used for this mutagenesis was TaKaRa Ex Taq™ RT-PCR kit. Both reactions were performed in parallel. After this PCR round, a second round of PCR was performed using 1 µL of the PCR product each from the abovementioned PCR reactions as template and full length forward and reverse primers to obtain DNA fragments with C22A mutation on both the strands of DNA. Running different rounds of PCR reactions increased the efficiency and chance of obtaining the DNA fragments encoding C84AC22A mutation. 50 µL of the PCR product acquired from the second round of PCR was purified using NucleoSpin® PCR clean-up kit. This step ensured removal of any other impurities (e.g. dNTP's or unused primers and template from the PCR product), which would eventually increase the efficiency by increasing amount of DNA incorporation in to the plasmid vector. A volume of 15 µL of the clean PCR product was then digested by the restriction enzymes

Nde-I and *Xho*-I. This was done to create sticky ends in the DNA fragment, which would assist in proper incorporation into the plasmid vector (see Fig. 4.7).

The pET-22b(+) vector was ligated with the DNA fragment coding for the desired mutation using the ligation enzyme T4 DNA polymerase at 4°C overnight along with a blank sample containing distilled water instead of DNA in the reaction mixture (see Fig. 4.7). The next day, the ligated mixture was incubated at room temperature for 45 min. to denature the T4 DNA polymerase enzyme. To remove any remaining enzyme from the ligation mixture, heat inactivation was done at 70°C for 10 min. Immediately after heat inactivation, the reaction mixture was kept on ice and 2 µL of the transformation mixture was transformed into no heat shock Z-Competent™ cells. This transformation mixture was spread on LB Amp^{200} plates for selective growth of the bacterial cells (see Section 3.1) and incubated overnight at 37°C. No colonies were achieved. After three rounds of cloning using different competent cells (such as JM109 competent cells, BL21(DE3) competent cells and XL-10 ultracompetent cells), 27 colonies were acquired in last round using BL21(DE3) competent cells. Out of 27 colonies, 3 colonies were picked and their plasmids were purified by the GeneJET™ plasmid purification kit to be sent for sequencing. The sequences were aligned with the wild type Co-BsLuxS-HT sequence to determine if they had any mutations. One of the plasmid samples out of three, encoded for the C22A (**S1**) mutation. Eventually, after all the efforts, the described cloning approach failed to deliver a double mutated Co-BsLuxS-HT C84AC22A (**D5**) mutant.

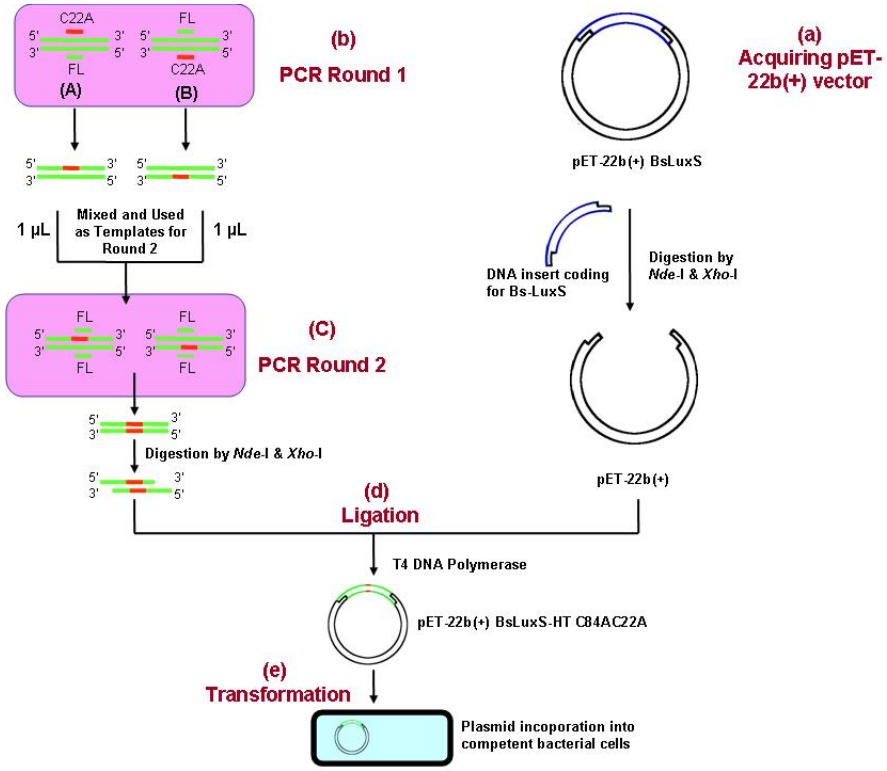

Fig. 4.7 | Cloning Technique. (a) A purified pET-22b(+) vector was acquired by removing the LuxS DNA insert from wild type Co-BsLuxS-HT plasmid (with DNA insert coding for BsLuxS in blue). **(b)** Two reactions were run in first round of PCR with Co-BsLuxS-HT C84A (green) as template and primers used were C22A (red) and full length (FL in green). **(C)** The PCR products from PCR round 1 were mixed in 1:1 ratio and used as templates with full length (FL) primers to get full length DNA fragments encoding for double C22AC84A mutation. The PCR product was then digested by *Nde*I and *Xho*I to create sticky ends in the DNA fragment. **(d)** The purified vector and the DNA fragment with C84AC22A mutation was ligated in presence of T4 DNA Polymerase at 4°C. **(e)** The plasmid resulting from the ligation encoding for the double mutation C22AC84A was transformed into competent cells.

While the efforts towards obtaining a double mutated Co-BsLuxS-HT by cloning technique were ongoing, the design and synthesis of non-overlapping primers was also in progress. The following sections provide detailed analysis of the idea and usage of non-overlapping primers for achieving Co-BsLuxS-HT double mutant.[39]

4.1.1.2.2 | Using Non-Overlapping Primers for Acquiring a Double Co-BsLuxS-HT Mutant. The idea of achieving the Co-BsLuxS-HT double mutant using the non-overlapping primers was acquired from a methodology article.[39] This article mentions using non-overlapping primers for increasing the efficiency of site directed mutagenesis using QuikChange® SDM kit. The problem associated with using overlapping primers is the possibility of self-annealing and the inability to use newly synthesized DNA strands as templates for the next rounds due to presence of nick/break (see Fig. 4.8). The presence of nick in newly formed DNA strands hampers the rapid synthesis of new DNA fragment and this leads to decreased efficiency of the site directed mutagenesis. Addition of more DNA template to combat this problem, increases the chances of synthesis of hemi-methylated DNA (newly synthesized strands complexed with a parental strand), which are not able to be digested by *Dpn*-I, resulting in recovery of non-mutated DNA.

Non-overlapping primers are short DNA sequences with overlapping sequences at their 5' end and non-overlapping sequences at their 3' end. The melting temperature of these primers is 5 to 10°C higher than the melting temperature of overlapping primers.[39] These primers don't have a length restriction, and mutation sites could be present in both the overlapping and non-overlapping regions of the primer. The use of non-overlapping primers increases the mutation efficiency by decreasing primer self-annealing and also by using of newly-formed

DNA as templates in PCR amplification cycles.[39] The nick in the newly synthesized DNA is bridged by the non-overlapping sequences, thereby rendering newly formed full length DNA fragments capable of acting as templates. The promising experimental results, reduction in cost and ease of using an additional one step in mutagenesis protocol, compelled us to use this technique for acquiring a double Co-BsLuxS-HT mutant.

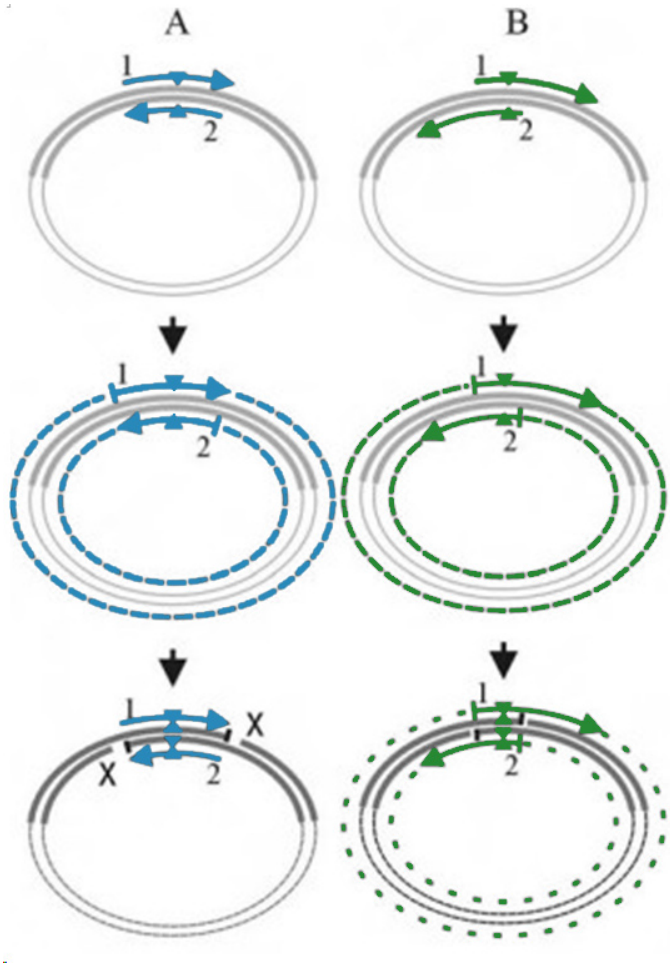

Fig 4.8 | Overlapping Primers vs. Non-overlapping Primers. (A) Using overlapping primers (depicted by black arrows) designed as mentioned in QuikChange™ protocol, fail to generate a new DNA from a newly synthesized DNA strand due to presence of a nick. (B) Using non-overlapping primers (depicted by black non-overlapping arrows) for the generation of DNA from a newly synthesized strand works well due to the absence of a nick.[39]

The non-overlapping primers for Co-BsLuxS-HT were designed using the PrimerSelect module of Lasergene 8.0. The DNA sequence of Co-BsLuxS-HT was used as the template for designing of these non-overlapping primers. All forward and reverse sequences were designed individually and therefore they all had different melting temperatures, GC contents and lengths (see Table 4.5). The designed non-overlapping primers were sent to IDT for synthesis and used later for the generation of double mutated Co-BsLuxS-HT by site directed mutagenesis.

Table 4.5 | Non-Overlapping Primers. The non-overlapping primers designed with non overlapping 3' end sequences and their parameters.

Primers encoding for mutation	Primers	Tm no	GC %	Length (bp)
C84AF	5'CAATGGGCGCGCAGACAGGCTAT TATCTAGTTGTGAGCGGAGAG 3'	79.3	53.5	43
C84AR	5'CTGTCTGCGCGCCCATTGGAGAA ATATCAATGATATCAAAATG 3'	76.7	40.9	43
C126AF	5'AAAAGCAGGCGGGCCAAGCGAA GCTTCATGATCTGGAAGGCG 3'	83.4	52.4	42
C126AR	5'GCTTGGCCCGCCTGCTTTTCATTCGC AGCAGGTATTTCTGTA 3'	80	52.4	42
C22AF	5'TAAGACATGCGGGCGTGCATAA AGTGGGAACAGAC 3'	73.4	51.4	35
C22AR	5'TGCACGCCCGCATGTCTTACAT ATGGAGCAACAAC 3'	75.1	51.4	35
C41AF	5'CATTCGTTTTGCGCAGCCAAATAA ACAGGCGATGAAGCCTGACACCA 3'	83	48.9	47
C41AR	5'GTTTATTTGGCTGCGCAAAACGAATG TCAAATTTATTTACAACGCCG3'	77.1	38.3	47

At first, the single Co-BsLxS-HT C84A (**S3**) mutant was used as template for the generation of double mutated Co-BsLuxS-HT (**D2**, **D3** and **D5**) using non-overlapping primers. But, as mentioned previously, the C84A mutation reverted back to C84C (see Table 4.3). These results confirmed that C84A mutation reverts back on incorporation of other mutations. Henceforth, for the generation of the next batch of mutants, the C84A mutation was incorporated last in those variants with a C84A requirement.

For the generation of double Co-BsLuxS-HT mutants **D1, D2, D3, D4**, **D5** and **D6**, the single mutants **S1**, **S2** and **S3** were used as templates. To make a comparison between the mutation results from the use of two kinds of primers, both overlapping and non-overlapping primers were used in the SDM protocol. The method of site directed mutagenesis was the same as discussed earlier in Section 3.2.2.

Most of the Co-BsLuxS-HT double mutants were acquired using the non-overlapping primers except C22AC41A (**D1**), C22AC126A (**D5**) and C22AC84A (**D4**) (see Table 4.6), although they were achieved using overlapping primers. The presence of a common C22A mutation in all the above mentioned three sequences suggests some correlation. It is hard to deduce some possible reasons at this time, but this fact might be considered useful while generating a mutant with a C22A mutation for later site directed mutagenesis experiments. However, the double Co-BsLuxS-HT mutants were finally achieved after extensive troubleshooting.

Table 4.6 | Results of Double Mutation. The Co-BsLuxS-HT double mutants achieved using non-overlapping primers and overlapping primers.

Double Mutants Required	Primers Used	Total no. of sequences sent for sequencing	Sequences containing mutation	Co-BsLuxS-HT Double Mutant Achieved
D1	Non-overlapping	2	0	no
D1	Overlapping	2	1	yes
D2	Non-overlapping	2	2	yes
D3	Non-overlapping	2	1	yes
D4	Overlapping	2	1	yes
D5	Non-overlapping	2	0	no
D5	Overlapping	2	2	yes
D6	Non-overlapping	2	2	yes
D6	Overlapping	2	2	yes

*No colonies were achieved in an attempt to get LuxSC126AC84A and LuxSC41AC84A mutations using overlapping primers. No colonies were achieved for C22AC84A using non-overlapping primers. Therefore they are not mentioned in the table above.

For the synthesis of triple-mutant Co-BsLuxS-HT variants, again both overlapping and non-overlapping primers were used (see Table 4.2 and 4.5). The doubly-mutated templates used for acquiring these double mutants were **D1**, **D5** and **D6**. These double mutants did not contain the C84A mutation to ensure no C84C reversion as previously discussed (see Table 4.3). The method for the synthesis of these triple mutants using site directed mutagenesis was the same as discussed in the Section 3.2.2. The non-overlapping primers again proved to be an important part of site directed mutagenesis protocol in acquiring the desired mutations (see Table 4.7) by delivering three triple mutants (**T1**, **T2** and **T3**).

Even after performing several rounds of site directed mutagenesis and using both kinds of primers, it became difficult to acquire one of the four triple mutants C22AC126AC41A (**T4**). The reason for the continuous failures is still unknown.

Table 4.7 | Triple Co-BsLuxS-HT Results. The use of non-overlapping primers delivered three triple mutation out of four.

Triple Mutants Required	Primers Used	Total no. of sequences sent for sequencing	Sequences containing mutation	Co-BsLuxS-HT Triple Mutant Achieved
T1	Non-overlapping	2	2	yes
T1	Overlapping	2	0	no
T2	Non-overlapping	2	1	yes
T2	Overlapping	2	0	no
T3	Non-overlapping	2	1	yes
T3	Overlapping	2	0	no
T4	Non-overlapping	N/A	N/A	N/A
T4	Overlapping	N/A	N/A	N/A

*For Triple Co-BsLuxS-HT C22AC41AC126A no colonies were achieved using either of the kinds of the primers.

A quadruple mutant was also designed containing all native cysteines mutated to be used as negative control. The non-overlapping primers and overlapping primers (C22A, C41A and C126A) were used to generate the quadruple mutant, and the three triple mutants acquired (**T1**, **T2** and **T3**) were used as templates. The method used for site directed mutagenesis was the same as mentioned previously in Section 3.2.2. No colonies were achieved using all the kinds of primers and triple mutants as templates. Hence, no further efforts were made towards achieving this mutant.

4.1.2 | Overexpression and Purification of Mutant Proteins. After acquiring almost all the desired Co-BsLuxS-HT mutations (except **T4** and **Q** mutations) the bacterial cells carrying plasmids encoding for the mutations were overexpressed and purified. The details and discussion for overexpression and purification of these mutants is provided in the following sections.

4.1.2.1 | General Parameters for Protein Purification. The general parameters for the overexpression and purification of the mutant proteins is the same as described previously (see Section 3.1.2 & 3.1.3).

4.1.2.2 | Purification of the Co-BsLuxS-HT Mutants. While single Co-BsLuxS-HT mutants were overexpressed and purified by the method discussed earlier (see Section 3.1.2 and 3.1.3), an interesting observation was made. The pellets for single Co-BsLuxS-HT mutants obtained after overexpression were different in color. Some of the pellets were yellow whereas some of them were grayish blue. The pellets for enzyme variants with the C126A mutation (**D3**, **D4** and **D6**) were yellow, as well as the protein purified using some of these pellets was also yellow (see Table 4.8). The probable reason for this was the presence of cysteine 126 in the ligation sphere of the metal, where a mutation was likely to make the metal unstable. Presumably the metal is not able to bind as it does in a wild type Co-BsLuxS-HT, and this result in the discoloration of the protein. Whereas the protein purified from a grayish blue colored pellet was always blue, possibly due to the presence of cobalt bound enzyme (see Section 3.1). These observations helped to determine the presence of a blue natively-folded enzyme protein before continuing with the purification procedure.

Table 4.8 | Color of the Pellet Indicating Presence of the Metal Bound Enzyme. The experimental results demonstrating that the blue colored pellet delivers a cobalt metal bound Co-BsLuxS-HT enzyme.

Co-BsLuxS-HT Mutant	Color of pellet	Color of the Purified Protein
S1	Grayish blue	Dark blue
S2	Yellow	Yellow
S4	Yellow	Yellow

Because this observation was made while purifying the pellets for single Co-BsLuxS-HT mutants, typically only pellets with a grayish blue color were purified. The BL21(DE3) competent cells carrying the plasmid coding for the double mutations **D1**, **D2**, **D3**, **D4**, **D5** and **D6** were overexpressed and 2L pellets were obtained (see Section 3.1.2).

Considering the C84A mutation renders the enzyme inactive, only the three double Co-BsLuxS-HT mutants (**D1**, **D4** and **D6**) without C84A mutation were purified (see Table 4.9). Although the pellets for the double mutations **D4** and **D6** were yellow, suggesting misfolded protein, they were still purified to analyze activity because the color of the pellet did not indicate any information about enzyme's activity. The method for purification of these double mutants was similar to the method discussed previously (see Section 3.1.3).

Table 4.9 | Purification of Double Co-BsLuxS-HT Mutants. The mutants were lysed and purified based on the pellet color indicating the presence of properly-folded protein. **D2** was not purified, although the color of the pellet acquired was grayish blue, because it had C84A mutation which was known to turn the enzyme inactive.[9]

Co-BsLuxS-HT Double Mutants	Color of the Pellet	Protein Purification Performed
D1	Grayish blue	Yes
D2	Grayish blue	No
D3	Yellow	No
D4	Yellow	Yes
D5	Yellow	No
D6	Yellow	Yes

The bacterial cells containing the plasmid coding for the triple mutants were grown and overexpressed by the same method as mentioned in Section 3.1.2. A blue pellet obtained for C22AC41AC84A (**T1**) suggested proper folding of the metal bound protein (see Table 4.10). The other two mutants (**T2** and **T3**) were yellow in color, probably due to misfolding of the

native protein and loss of cobalt metal from the enzyme as discussed in the previous sections. Two triple mutants (**T1** & **T2**) of the three mutants were lysed and purified. Although these mutants had C84A mutation, they were purified and assayed to be used as negative control and to determine if the mutation allows proper protein folding.

Table 4.10 | Purification of Triple Co-BsLuxS-HT Mutants. The triple Co-BsLuxS-HT mutants were lysed and purified based on their pellet color indicating the presence of properly folded protein.

Co-BsLuxS-HT Triple Mutants	Color of the Pellet	Protein Purification Performed
T1	Grayish blue	Yes
T2	Yellow	Yes
T3	Yellow	No

The method for purification of Co-BsLuxS-HT triple mutants was the same as discussed in section 3.1.3.

Table 4.11 | Summary Table. The primers used to get Co-BsLuxS-HT mutants, the color of the 2 L pellets of the mutants, the determined protein concentration of the mutants and the results of the activity assay of the purified mutants is shown in the table. None of the mutants generated using native cysteines present on Co-BsLuxS-HT were found to be active as explained in Section 4.1.4. The mutant **D2** was not purified, although the color of the pellet acquired was grayish blue, because it had C84A mutation which was known to turn the enzyme inactive.[9]

Co-BsLuxS-HT mutant	Primer used to achieve mutant	Pellet color	Protein purified	Protein conc. mM	Catalytic activity detected
S1	Overlapping	Grayish blue	Yes	0.877	No
S2	Overlapping	Yellow	Yes	0.121	No
S3	Overlapping	Grayish blue	Yes	0.923	No
S4	Overlapping	Yellow	Yes	2.16	No
D1	Overlapping	Grayish blue	Yes	2.96	No
D2	Non-overlapping	Grayish blue	No	N/A	N/D
D3	Non-overlapping	Yellow	No	N/A	N/D
D4	Overlapping	Yellow	Yes	1.79	No
D5	Overlapping	Yellow	No	N/A	N/D
D6	Overlapping	N/A	N/A	N/A	N/D
D6	Non-overlapping	Yellow	Yes	0.4	No
T1	Non-overlapping	Grayish blue	Yes	0.423	No
T2	Non-overlapping	Yellow	Yes	0.434	No
T3	Non-overlapping	Yellow	No	N/A	N/D

4.1.3 | Estimation of Protein Concentration by Bradford Dye Assay. The amount of the mutant enzyme proteins in the purified protein mixture was measured by the optimized Bradford dye assay using transparent-bottom 96-well plates (Section 3.1.5). The linear equation of the standard curve was used to determine the amount of protein in the purified mixture (see Appendix A) and the units were converted from µg to mM to determine concentration.

4.1.4 | Ellman's Assay for Activity Detection of Co-BsLuxS-HT Mutants. The Ellman's assay was performed to determine the catalytic activity of the mutants, as described previously (see Section 3.4). None of the Co-BsLuxS-HT mutants generated from the native cysteines was found to be active by the activity assay. The Michaelis-Menten curve for each of the mutants tested is provided in the Appendix B.

Because none of the Co-BsLuxS-HT mutants generated from the native cysteines were active, the focus shifted to find some peripheral amino acids which could be mutated to cysteine, keeping the enzyme active and properly-folded while providing surface accessibility to the fluorophores to be atttached. The work towards obtaining an active Co-BsLuxS-HT mutant using non-native cysteines is explained in the following section.

4.2 | Acquiring an Active Co-BsLuxS-HT Mutant with One Surface Accessible Cysteine from Non-native Cysteine Residues. After the failed attempts to obtain an active Co-BsLuxS-HT mutant using native cysteines, the other option was to mutate a non-cysteine amino acid present on the surface of the enzyme to cysteine. The technique involving use of non-native cysteines for attachment of fluorophores to an enzyme with no native surface

cysteines have been previously reported by Zhu and Pei.[40] The DeepView program Swiss PDB was used to find the best possible amino acid present on the periphery of Co-BsLuxS-HT enzyme for substitution (PDB code: 1IE0). The first requirement was that this amino acid should be surface accessible for the successful attachment of a fluorophore. Ideally, this amino acid should be non-polar so that its mutation to cysteine is conservative but it was very likely that an amino acid present on the surface of enzyme will be polar. However, considering that the presence of one non-polar amino acid on the surface of enzyme may not make much difference in enzyme's overall environment, native polar amino acids were considered for substitution in addition to non polar ones. Finally, such an amino acid would have a side chain with no intermolecular interactions with other side chains to decrease the risk of misfolding of the enzyme after mutation. Ultimately, three amino acids identified according to these requirements for substitution were: threonine at position 29, tyrosine at position 71, and threonine at position 116 of the Co-BsLuxS-HT enzyme (see Fig. 4.9).

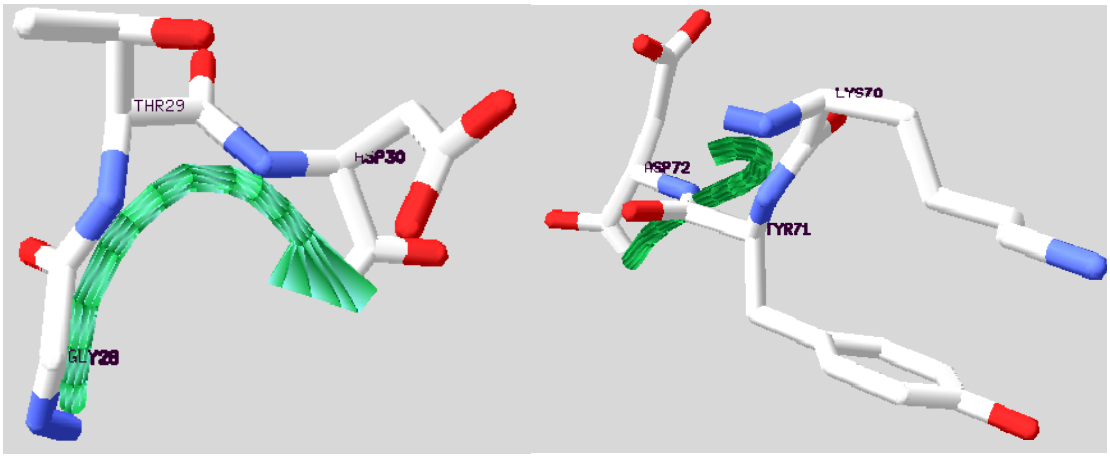

(A) **(B)**

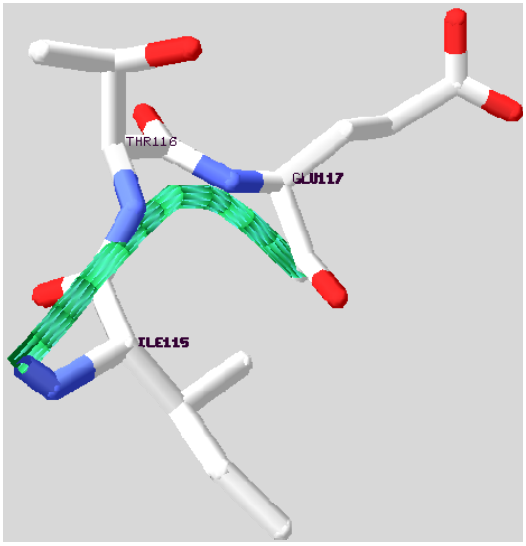

(C)

Fig. 4.9 | Possible Sites on Surface of Co-BsLuxS-HT for Mutation to Cysteine. (A) Threonine at 29 position (B) Tyrosine at 71 position (C) Threonine at 116 position. All the three amino acids are present in different loops of the enzyme and on the periphery making them surface accessible. The loop is shown in green, carbon in white, oxygen in red and hydrogen in blue. This figure was generated using DeepView.

The surface accessibility of the threonine at position 29 determined by DeepView was 52.1%, DeepView also determined that the side chain of threonine 29 was not involved in any intermolecular bonding. This was the most surface accessible amino acid of the three originally identified. The neighboring amino acids are neutral glycine with the smallest side chain and aspartate with a bulky polar side chain.

The surface accessibility of tyrosine 71 was 13% (which was the least of the three amino acids selected) and its side chain was also not involved in any molecular interactions as determined by DeepView. The presence of neighboring aspartate and lysine residues with bulky side chains made this position potentially unsuitable for mutation. This was due to possible steric bulk imposed by the neighboring residues, and this position would be used for fluorophore attachment.

The surface accessibility of threonine 116 was 47% and also had a free side chain. Its neighboring amino acids were glutamate and isoleucine. The issues with using this position for fluorophore attachment was the same as discussed for tyrosine 71, which is the presence of neighboring amino acids with bulky side chains.

4.2.1 | Generation of Co-BsLuxS-HT Mutants. Only non-overlapping primers were designed for achieving these mutations due to the promising results acquired by using them for attaining Co-BsLuxS-HT mutants from native cysteines (see Section 4.1.2). The non-overlapping primers for T29C, Y71C and T116C were designed using the PrimerSelect module of DNAStar Lasergene 8.0 (see Table 4.12). A wild type Co-BsLuxS-HT purified plasmid was used as the template for the generation of these mutants. The method for site

directed mutagenesis using QuikChange SDM kit, Pellet Paint for concentration of PCR product, transformation into BL21(DE3) competent cells and plating on to LB Amp^{200} plates was the same as mentioned previously (see Section 3.3).

Table 4.12 | Non-overlapping Primers Designed for Non-native Cysteine Mutants. The non-overlapping primers designed using PrimerSelect Module of DNA star Lasergene 8.0 to obtain T29C, Y71Cand T116C mutants.

Primers encoding mutation	Primers	Tm no	GC %	Length (bp)
T29CF	5'GTGCATAAAGTGGGATGCGACGGCGTTG TAAATAAATTTGACATTCG3'	78.1	42.6	47
T29CR	5'TTTACAACGCCGTCGCATCCCACTTTATG CACGCCGCAATGTCTTACATATG3'	66.6	48.1	52
Y71CF	5'GTTTACGATTCGTTCTCACGCTGAGAAA TGCGATCATTTTGATATC3'	74.8	39.1	46
Y71CR	5'GGAGAAATATCAATGATATCAAAATGAT CGCATTTCTCAGCGTGAG3'	73.8	37	46
T116CF	5'GACACAATGAAGGAAGCGGTAGAGATT TGCGAAATACCTGCTGCG3'	78.4	48.9	45
T116CR	5'GGCCGCACTGCTTTTCATTCGCAGCAGG TATTTCGCAAATCTCTACCGCTTC3'	68.2	51.9	52

No colonies were achieved for the T116C mutation. Colonies acquired for the other two mutants (T29C and Y71C) were grown in 5 mL of LB Amp^{75} media. The bacterial cells carrying the plasmids encoding for the T29C and Y71C mutations were lysed and purified using GeneJET™ plasmid purification kit. The purified plasmids were sent to Sequetech for sequencing, and the sequences received were aligned using the SeqMan Pro module of

DNAStar Lasergene 8.0 to determine the presence of the mutations (see Table 4.13). Each of the samples sent for sequencing had the desired T29C and Y71C mutations.

Table 4.13 | Sequencing Results. The samples sent for sequencing had the desired T29C and Y71C mutations.

Co-BsLuxS-HT Mutants	Primers Used	Total no. of sequences sent for sequencing	Sequences containing mutation	Co-BsLuxS-HT Mutant Achieved
T29C	Non-overlapping	2	2	Yes
Y71C	Non-overlapping	2	2	Yes

4.2.2 | Purification of the Co-BsLuxS-HT Mutants. The bacterial cells carrying the plasmid encoding for T29C and Y71C mutations were overexpressed and a 2 L pellet was acquired as mentioned previously (see Section 3.1). The color of the 2 L pellet for both of these mutations was grayish blue (see Table 4.14) and both proteins were purified after lysis from French press by the same method as previously described (see Section 3.1.3).

Table 4.14 | Color of Pellets Acquired after Overexpression. The pellet color for both of them was grayish blue and hence protein purification was performed for both of them.

Co-BsLuxS-HT Mutants	Color of the Pellet	Protein Purification Performed
T29C	Grayish blue	Yes
Y71C	Grayish blue	Yes

4.2.3 | Estimation of Protein Concentration by Bradford Dye Assay. The amount of protein present in the purified protein concentrate was measured by the Bradford dye assay as mentioned previously (see Section 4.1.4). The Bradford dye assay standard curves and the amount of protein determined for the purified proteins (shown in Table 4.15) are provided in the Appendix A.

4.2.4 | Ellman's Assay for Activity Detection of Co-BsLuxS-HT Mutants. Once purified protein was acquired for the two Co-BsLuxS-HT non-native cysteine variants T29C and Y71C, their activities were assayed by Ellman's assay according to the standard protocol provided in literature (see Section 2.4).[9]

Table 4.15 | Summary Table. A summary of all the three mutants designed, purified and their activities assayed by Ellman's assay.

Co-BsLuxS-HT mutant	Primer used to achieve mutant	Pellet color	Protein purified	Protein conc. mM	Catalytic activity detected
T29C	Non-overlapping	Grayish blue	Yes	1.668	No
Y71C	Non-overlapping	Grayish blue	Yes	1.480	Yes
T116C	Non-overlapping	N/A*	N/A*	N/A*	N/A*

* No colonies were acquired for the Co-BsLuxS-HT T116C mutant.

The mutant Co-BsLuxS-HT T29C was found to be inactive in the Ellman's assay (see Appendix B), whereas the other mutant Co-BsLuxS-HT Y71C was found to be active. To ensure that the mutant Co-BsLuxS-HT Y71C was indeed active, three replicates of activity assays were performed for this enzyme. The Michaelis-Menten curve including the reaction rate values from all three replicates of Co-BsLuxS-HT Y71C mutant is shown in Fig. 4.10. (The Michaelis-Menten curves for individual trials are provided in Appendix B). The kinetic parameters for Co-BsLuxS-HT Y71C were determined as discussed in Section 3.4.2.2.1 for Co-BsLuxS-HT.

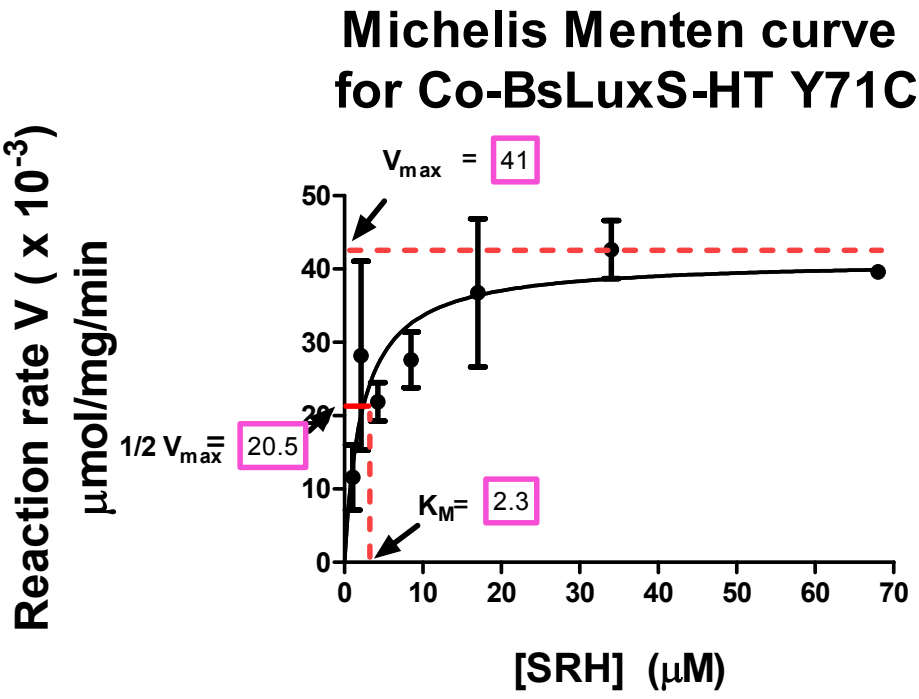

Fig. 4.10 | Michaelis-Menten Curve for Co-BsLuxS-HT Y71C. The Michaelis-Menten curve for the active Co-BsLuxS-HT Y71C mutant. The values of the K_M and V_{max} are shown on the curve.

The kinetic parameters of this variant were compared to those determined for house-purified Co-BsLuxS-HT (see Table 4.16) to determine its activity. The K_M value for the active Co-BsLuxS-HT variant (Y71C) was 2.3 µM, which is comparable to the house-purified Co-BsLuxS-HT enzyme value of 2.1 µM. The K_M value achieved for this variant suggested that the enzyme binds equally well with substrate as compared to the wild type Co-BsLuxS-HT.[9] The V_{max} value determined for the Co-BsLuxS-HT was 0.1 x 10^{-5} µmol/s, which was approximately 11 fold lower as compared to house-purified Co-BsLuxS-HT (1.1 x 10^{-5} µmol/s). This indicated that this variant converted one mole of substrate to product in 11 fold greater time as compared to house-purified Co-BsLuxS-HT.

Table 4.16 | Comparison of Kinetic Parameters of Enzyme. The determined kinetic parameters of Co-BsLuxS-HT enzyme and its variant Y71C are compared with the literature values for Co-BsLuxS-HT enzyme.[9]

Enzymes	K_M (µM)	V_{max} (µmol/sec.)	k_{cat} (s^{-1})	k_{cat}/K_M (M^{-1} s^{-1})
Co-BsLuxS-HT Y71C	2.3 ± 1.1	0.1 x 10^{-5}	0.001 ± 0.004	0.05 x 10^4
Co-BsLuxS-HT **(house-purified)**	2.1 ± 1.4	1.1 x 10^{-5}	0.014 ± 0.002	0.67 x 10^4
Co-LuxS-HT **(Pei and Coworkers)[9]**	2.3 ± 0.5	2.8 x 10^{-5}	0.035 ± 0.003	1.6 x 10^4

The k_{cat} value for the variant Co-BsLuxS-HT Y71C from three replicates of activity assay was 0.001 s^{-1}, which was 14 fold lower than the house-purified Co-BsLuxS-HT (0.014 ± 0.002 s^{-1}), indicating that this variant converts one mole of substrate into product in 14 fold higher time than house purified wild type Co-BsLuxS-HT. The lower value of V_{max} and k_{cat} affected the catalytic efficiency for Co-BsLuxS-HT Y71C (0.05 x 10^4 $M^{-1}s^{-1}$); it was 12 times lower as compared to the catalytic efficiency of house-purified Co-BsLuxS-HT (0.67 x 10^4 $M^{-1}s^{-1}$).

Although the K_M values for this variant suggested high binding ability of this enzyme with substrate, the considerably lower k_{cat}, V_{max}, and catalytic efficiency values acquired for this variant show that it was slow to convert substrate into product as compared to wild type Co-BsLuxS-HT (house-purified). A similar conclusion was previously derived for the house-purified Co-BsLuxS-HT as compared to literature values (chapter 3), and therefore this Y71C variant is even less catalytically active as compared to the Co-BsLuxS-HT enzyme purified by Pei and coworkers (see Table 4.16).[9]

4.3 | Conclusion and Future Directions. Based on the surface accessibility determined using Deep View Swiss PDB, threonine 29 (52.1 %) was found to be more surface accessible as compared to tyrosine 71 (13 %). Threonine has a smaller side chain in comparison to tyrosine as well. Therefore, out of the two options, threonine 29 was predicted the best possible amino acid to mutate to cysteine and for fluorophore attachment. However, the Ellman's activity assay demonstrated that Co-BsLuxS-HT T29C was found to be inactive whereas Co-BsLuxS-HT Y71C was able to bind well with the substrate (K_M = 2.3 ± 1.1 μM). Although Co-BsLuxS-HT Y71C binds well with the substrate, it is not as catalytically active as the house-purified wild type Co-BsLuxS-HT enzyme. It could be speculated that because the binding strength (K_M values) of the Y71C variant and the wild type Co-BsLuxS-HT (K_M = 2.1 ± 1.4 μM) were equivalent, the Y71C variant was folding in the native wild type form. As mentioned earlier, some discrepancies in the purification protocol regarding oxidation of cysteine 84 may have led to loss of catalytic ability of the stock solution to some extent. Finally the presence of a new surface accessible cysteine on Y71C variant could have had some confounding effect upon the assay, although nothing in particular is readily obvious at this time. To troubleshoot, if the mutation of tyrosine 71 to cysteine is a reason for its lower catalytic activity, another mutant with Y71A mutation could be made. The comparison of activities of the two mutants i.e. Co-BsLuxS-HT Y71C and Co-BsLuxS-HT Y71A would help determine if the presence of the surface accessible cysteine was responsible for the absorbance values recorded. Additionally, if this variant is purified eliminating all the discrepancies resulting from oxidation of cysteine 84, possibly by using degassed buffers and keeping the enzyme secluded from aerobic conditions at all times (see section 3.4.2.2.1), there are chances to acquire a Y71C variant as active as wild type Co-BsLuxS-HT.

Appendix A: Bradford Dye Assay Curves

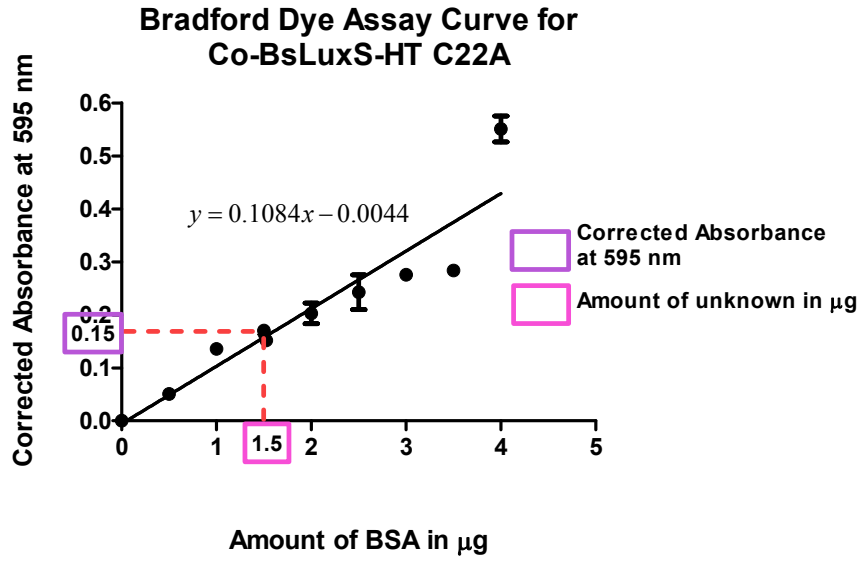

Fig. 1 | Bradford Dye Assay Curve for C22A. The standard curve for Bradford dye assay with the amount of protein determined for 1:80 diluted C22A purified protein. The protein concentration determined was 0.877 mM.

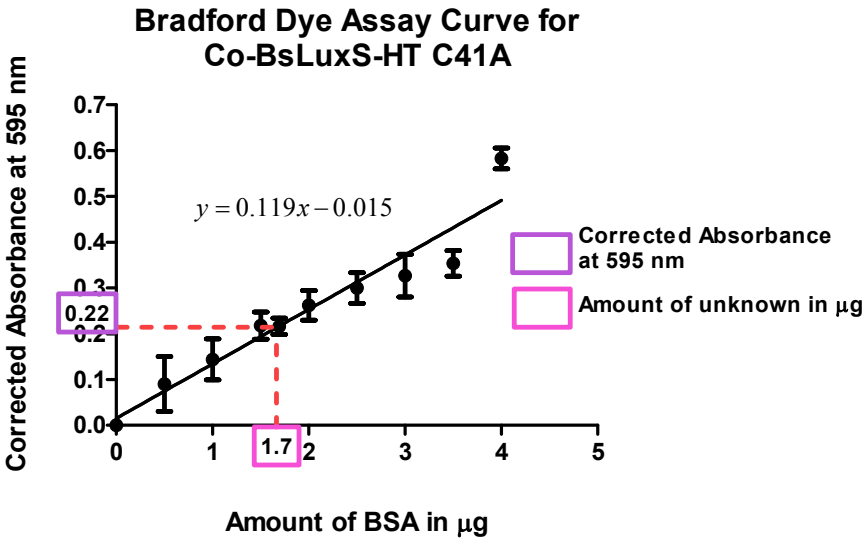

Fig. 2 | Bradford Dye Assay Curve for C41A. The standard curve for Bradford dye assay with the amount of protein determined for 1:10 diluted C41A purified protein. The protein concentration determined was 0.121 mM.

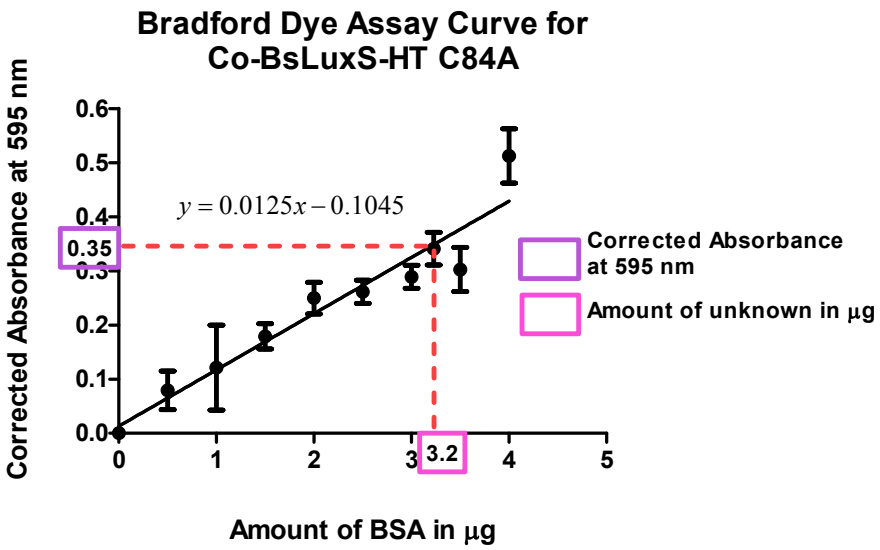

Fig. 3 | Bradford Dye Assay Curve for C84A. The standard curve for Bradford dye assay with the amount of protein determined for 1:40 diluted C84A purified protein. The protein concentration determined was 0.923 mM.

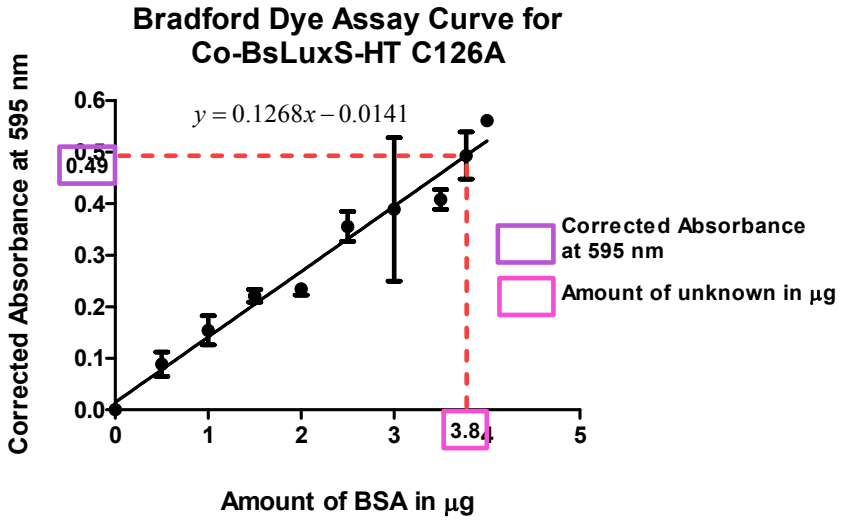

Fig.4 | Bradford Dye Assay Curve for C126A. The standard curve for Bradford dye assay with the amount of protein determined for 1:80 diluted C84A purified protein. The concentration of protein determined was 2.16 mM.

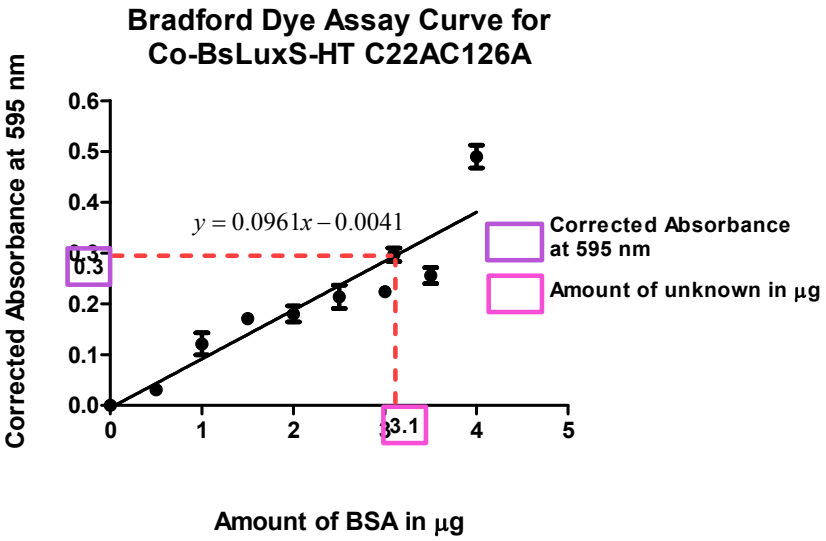

Fig. 5 | Bradford Dye Assay Curve for C22AC126A. The standard curve for Bradford dye assay with the amount of protein determined for 1:80 diluted C22AC126A purified protein. The protein concentration determined was 1.79 mM.

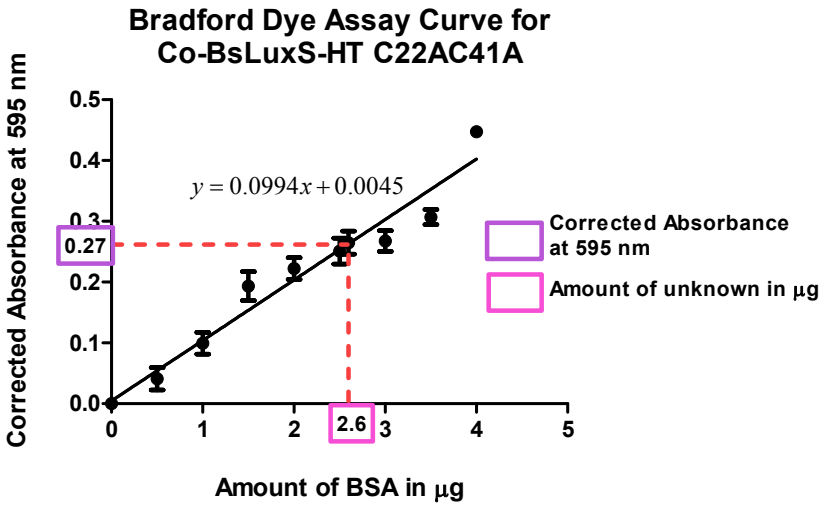

Fig. 6 | Bradford Dye Assay Curve for C22AC41A. The standard curve for Bradford dye assay with the amount of protein determined for 1:80 diluted C22AC41A purified protein. The protein concentration determined was 2.96 mM.

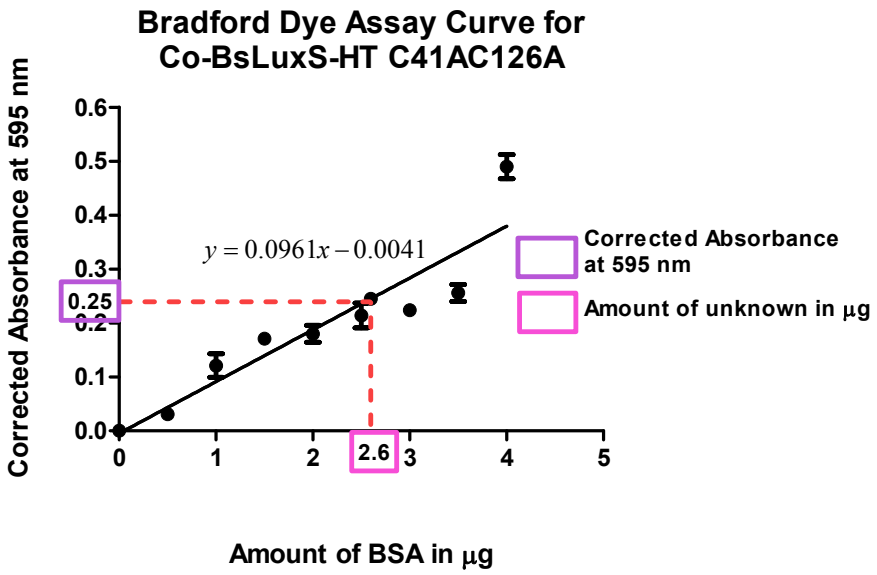

Fig. 7 | Bradford Dye Assay Curve for C41AC126A. The standard curve for Bradford dye assay with the amount of protein determined for 1:20 diluted C41AC126A purified protein. The protein concentration determined was 0.4 mM.

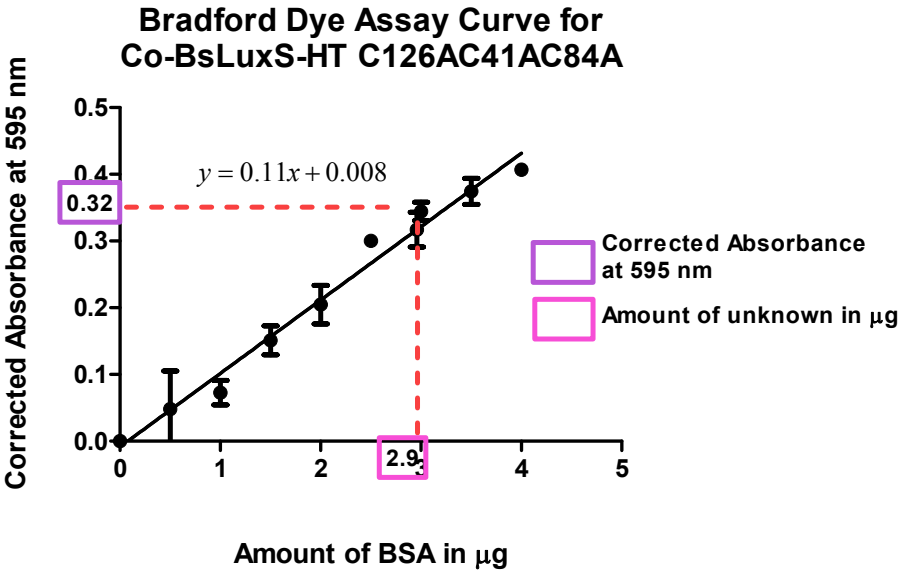

Fig. 8 | Bradford Dye Assay Curve for C126AC41AC84A. The standard curve for Bradford dye assay with the amount of protein determined for 1:20 diluted C126AC41AC84A purified protein. The protein concentration determined was 0.4 mM.

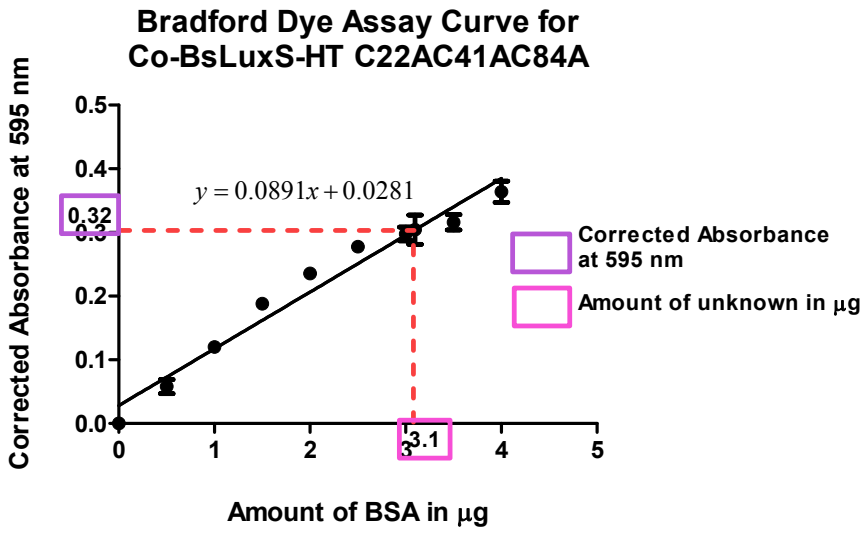

Fig.9 | Bradford Dye Assay Curve for C22AC41AC84A. The standard curve for Bradford dye assay with the amount of protein determined for 1:20 diluted C22AC41AC84A purified protein. The protein concentration determined was 0.4228 mM.

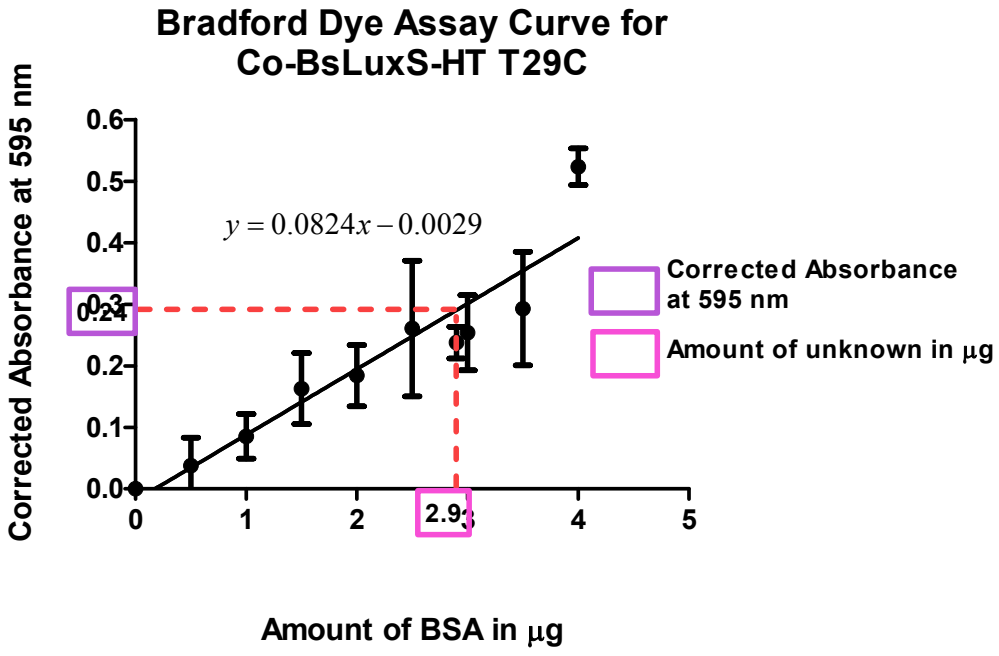

Fig. 10 | Bradford Dye Assay Curve for T29C. The standard curve for Bradford dye assay with the amount of protein determined for 1:80 diluted T29C purified protein. The protein concentration determined was 1.668 mM

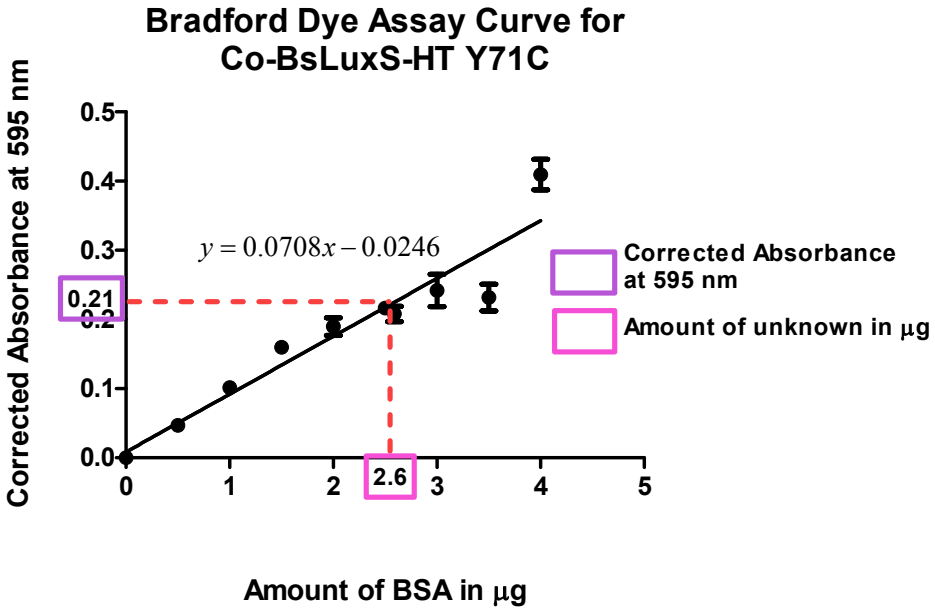

Fig. 11 | Bradford Dye Assay Curve for Y71C. The standard curve for Bradford dye assay with the amount of protein determined for 1:80 diluted Y71C purified protein. The protein concentration determined was 1.480 mM.

Appendix B: Michaelis-Menten Analysis

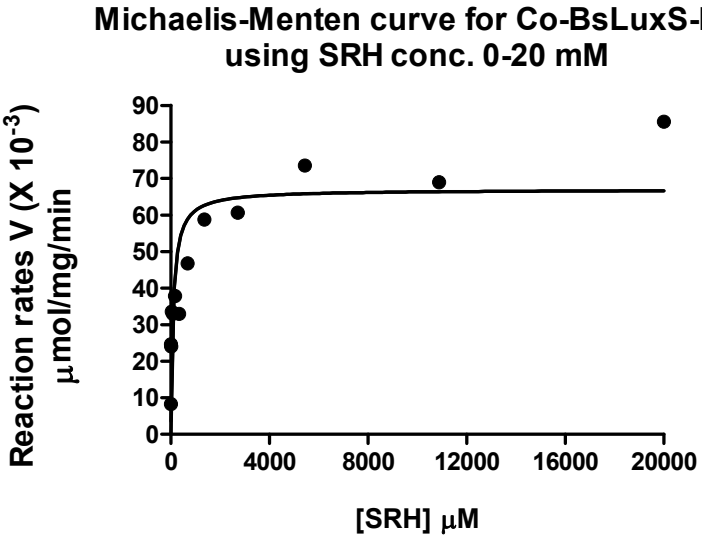

Fig. 1 | Michaelis-Menten curve for Co-BsLuxS-HT using SRH conc. 0-20 mM. The Michaelis-Menten curve for Co-BsLuxS-HT using a wide range (0-20 mM) of SRH concentrations is shown. The kinetic parameters determined were: K_M = 93.5 ± 47.1 µM, V_{max} = 1.5 x 10^{-5} µmol/s and the k_{cat} = 0.02 ± 0.06 $M^{-1}s^{-1}$.

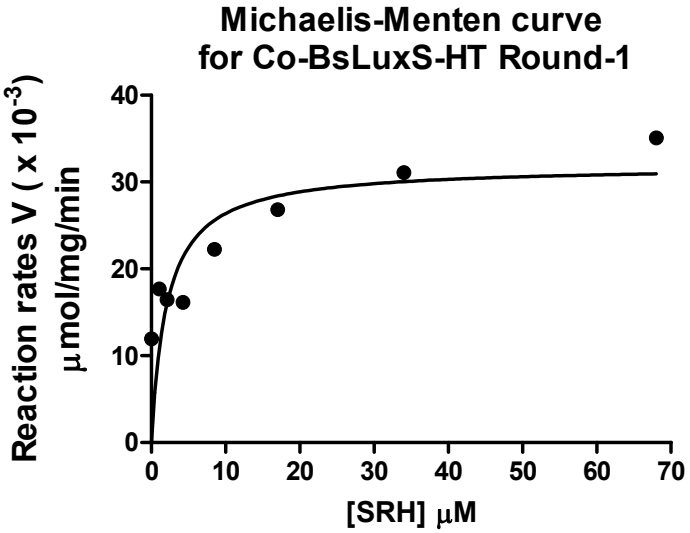

Fig. 2 | Michaelis-Menten curve for Co-BsLuxS-HT using SRH conc. 0-68 µM. The Michaelis-Menten curve for Co-BsLuxS-HT using 0-68 µM of SRH concentrations in round 1 is shown. The kinetic parameters determined were: K_M = 2.3 ± 1.4 µM, V_{max} = 0.7 x 10^{-5} µmol/s and the k_{cat} = 0.01 ± 0.04 $M^{-1}s^{-1}$.

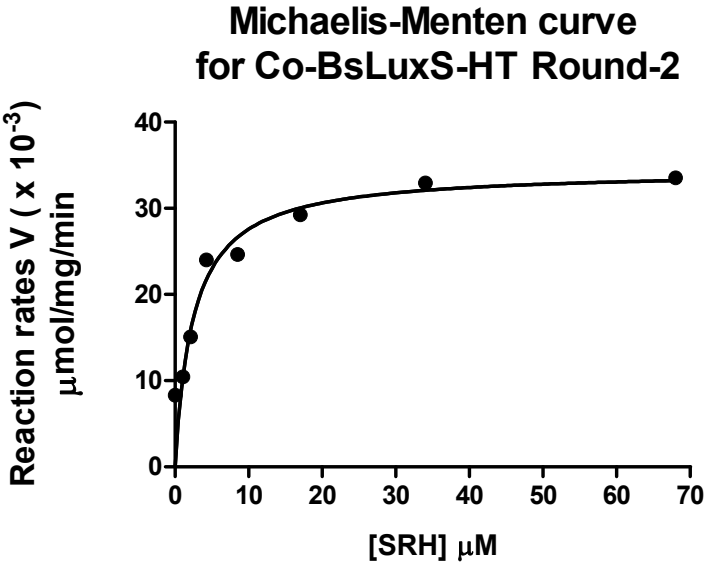

Fig. 3 | Michaelis-Menten curve for Co-BsLuxS-HT using SRH conc. 0-68 µM. The Michaelis-Menten curve for Co-BsLuxS-HT using 0-68 µM of SRH concentrations for round-2 is shown. The kinetic parameters determined were: K_M value = 2.4 ± 0.4 µM, V_{max}= 0.8 x 10^{-5} µmol/s and the k_{cat} = 0.01 ± 0.03 $M^{-1}s^{-1}$.

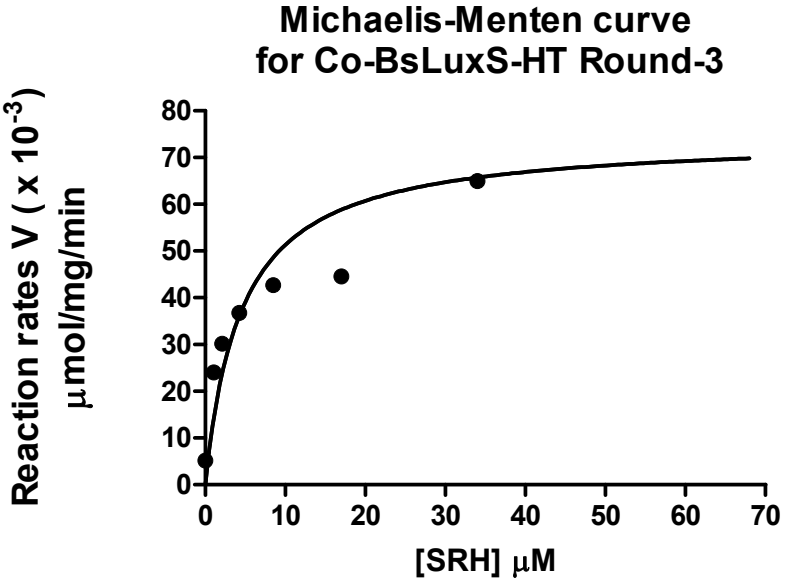

Fig. 4 | Michaelis-Menten curve for Co-BsLuxS-HT using SRH conc. 0-68 µM. The Michaelis-Menten curve for Co-BsLuxS-HT using 0-68 µM of SRH concentrations for round-3 is shown. The kinetic parameters determined were: K_M value = 1.6 ± 1.9 µM, V_{max} = 0.2 x 10^{-5} µmol/s and the k_{cat} = 0.02 ± 0.08 $M^{-1}s^{-1}$.

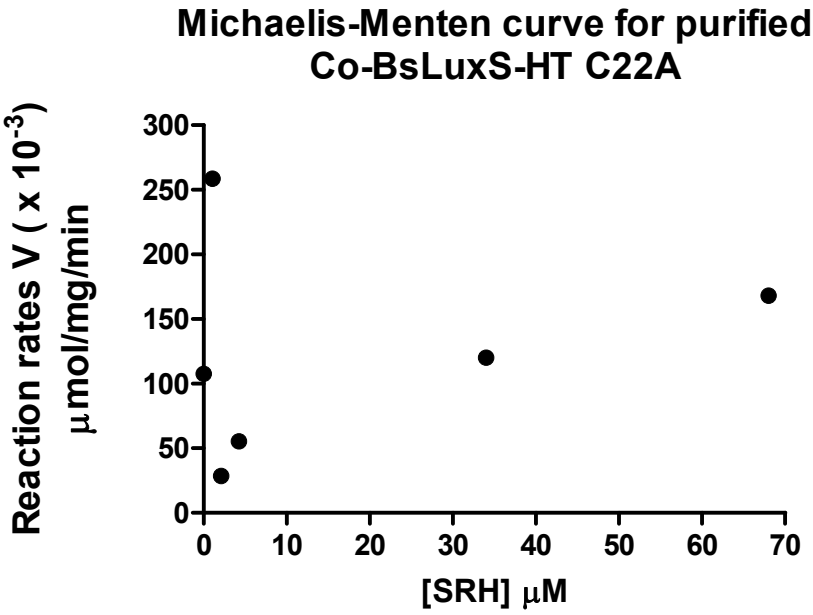

Fig. 5 | Michaelis-Menten curve for Co-BsLuxS-HT C22A. The Michaelis-Menten curve for the mutant Co-BsLuxS-HT C22A is shown. Mutant was determined to have no enzymatic activity.

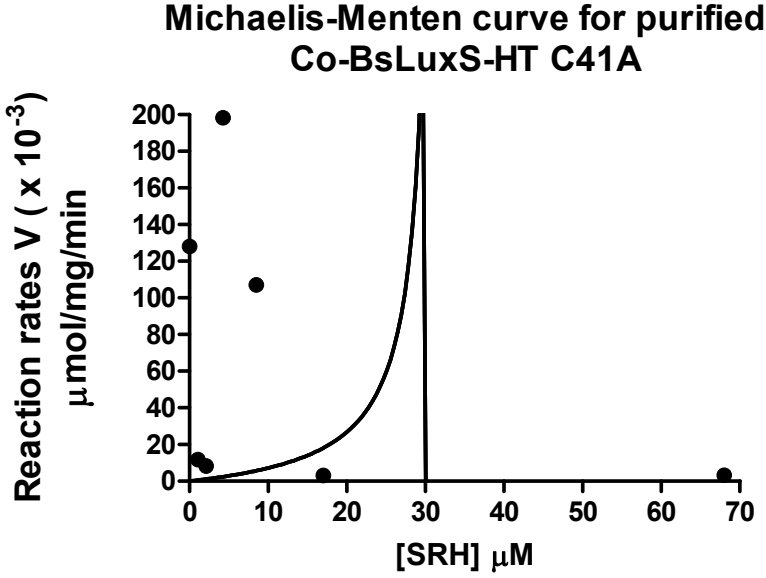

Fig. 6 | Michaelis-Menten curve for Co-BsLuxS-HT C41A. The Michaelis-Menten curve for the mutant Co-BsLuxS-HT C41A is shown. Mutant was determined to have no enzymatic activity.

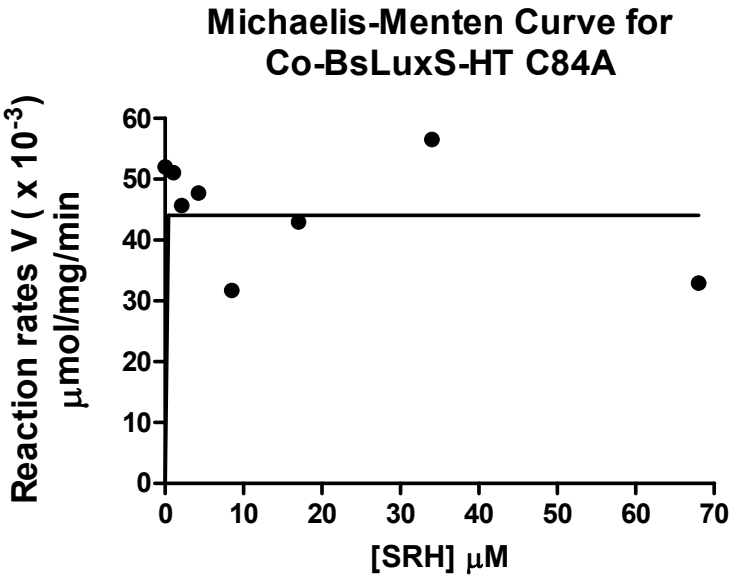

Fig. 7 | Michaelis-Menten curve for Co-BsLuxS-HT C84A. The Michaelis-Menten curve for the mutant Co-BsLuxS-HT C84A is shown. Mutant was determined to have no enzymatic activity.

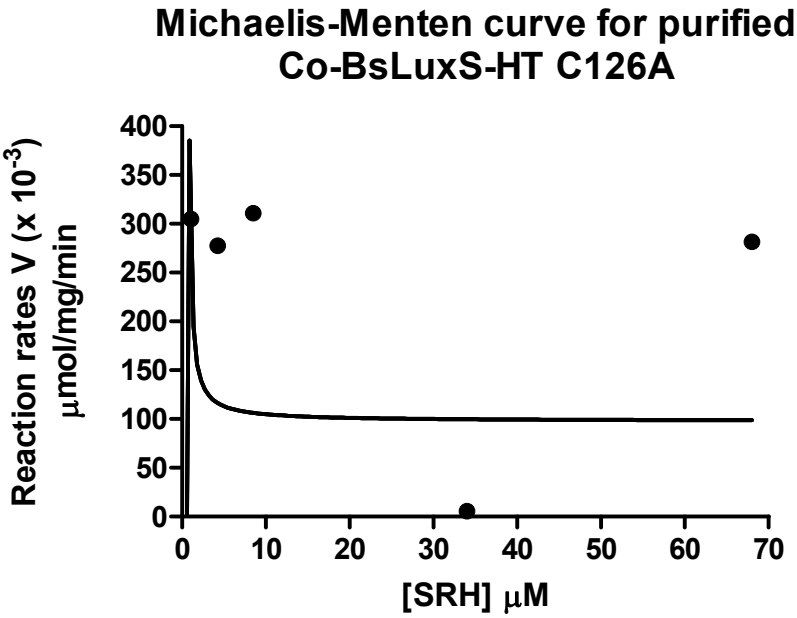

Fig. 8 | Michaelis-Menten curve for Co-BsLuxS-HT C126A. The Michaelis-Menten curve for the mutant Co-BsLuxS-HT C126A is shown. Mutant was determined to have no enzymatic activity.

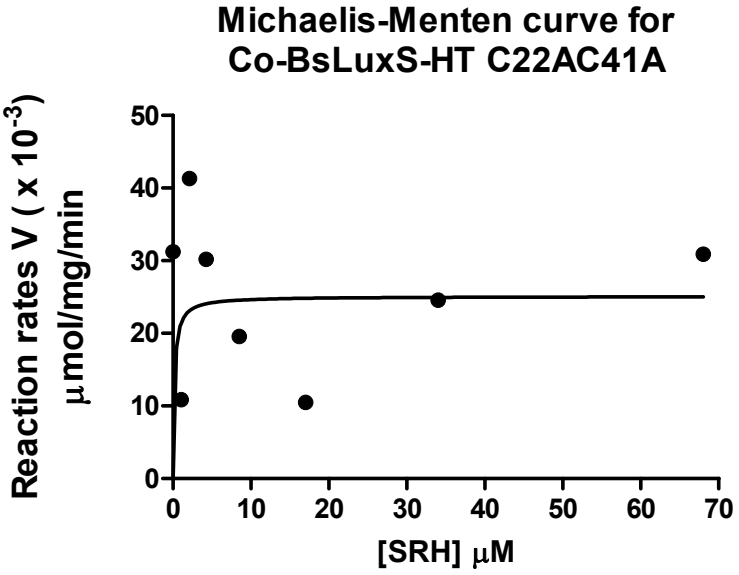

Fig. 9 | Michaelis-Menten curve for Co-BsLuxS-HT C22AC41A. The Michaelis-Menten curve for the mutant Co-BsLuxS-HT C22AC41A is shown. The kinetic parameters determined were: K_M value = 0.1 ± 1.1 μM, V_{max} = 0.6 x 10^{-5} μmol/s and the k_{cat} = 0.001 ± 0.08 $M^{-1}s^{-1}$.

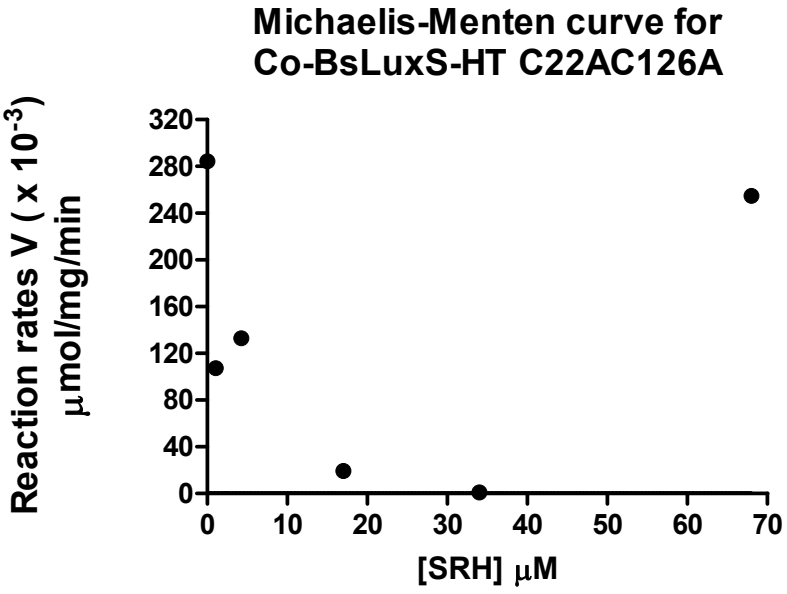

Fig. 10 | Michaelis-Menten curve for Co-BsLuxS-HT C22AC126A. The Michaelis-Menten curve for the mutant Co-BsLuxS-HT C22AC126A. Mutant was determined to have no enzymatic activity.

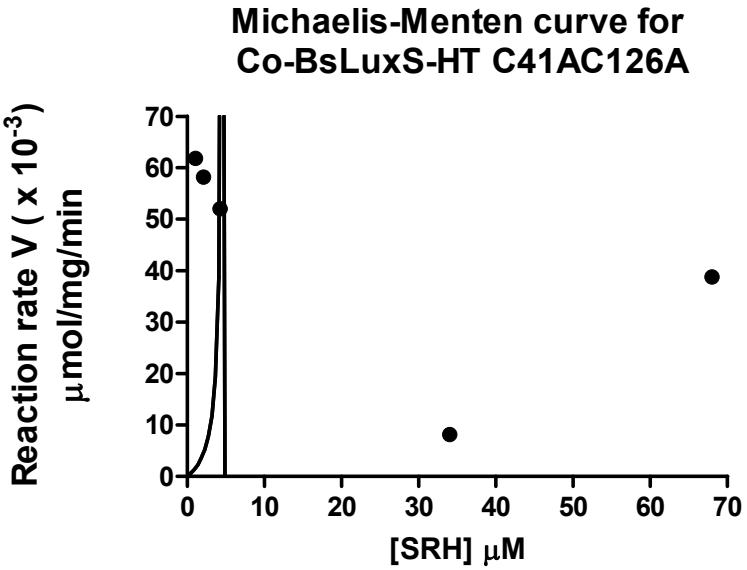

Fig. 11 | Michaelis-Menten curve for Co-BsLuxS-HT C41AC126A. The Michaelis-Menten curve for the mutant Co-BsLuxS-HT C22AC126A is shown. Mutant was determined to have no enzymatic activity.

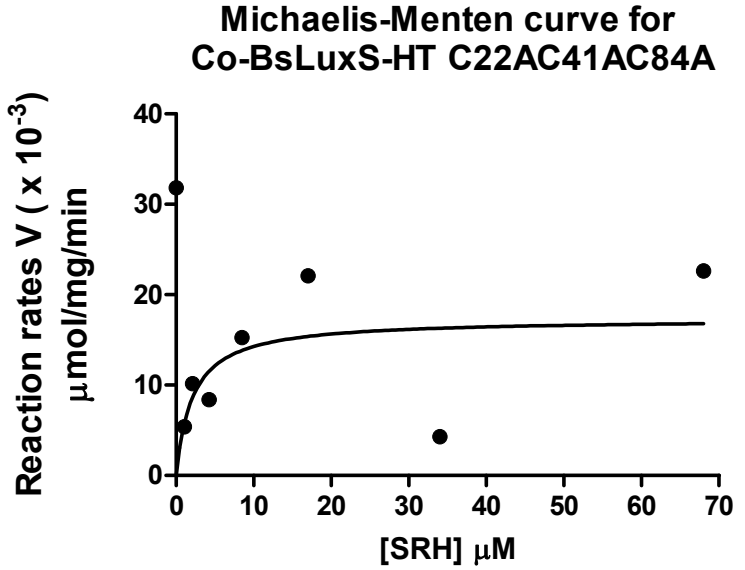

Fig. 12 | Michaelis-Menten curve for Co-BsLuxS-HT C22AC41AC84A. The Michaelis-Menten curve for Co-BsLuxS-HT C22AC41A C84A is shown. The kinetic parameters determined were: K_M value = 2.1 ± 5.6 µM, V_{max} = 0.4 x 10^{-5} µmol/s and the k_{cat} = 0.005 ± 0.002 $M^{-1}s^{-1}$.

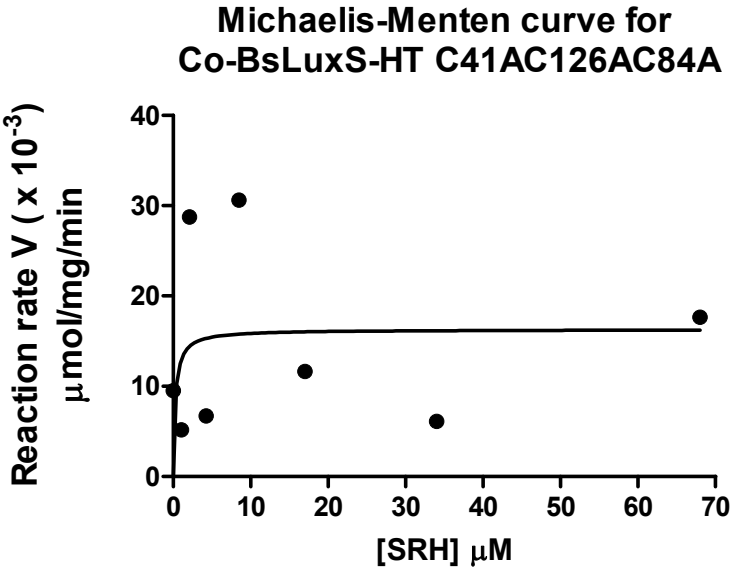

Fig. 13 | Michaelis-Menten curve for Co-BsLuxS-HT C41AC126AC84A. The Michaelis-Menten curve for the mutant Co-BsLuxS-HT C41AC126A C84A is shown. The determined kinetic parameters were: K_M value = 0.3 ± 1.2 μM, V_{max} = 0.4 x 10^{-5} μmol/s and the k_{cat} = 0.005 ± 0.002 $M^{-1}s^{-1}$.

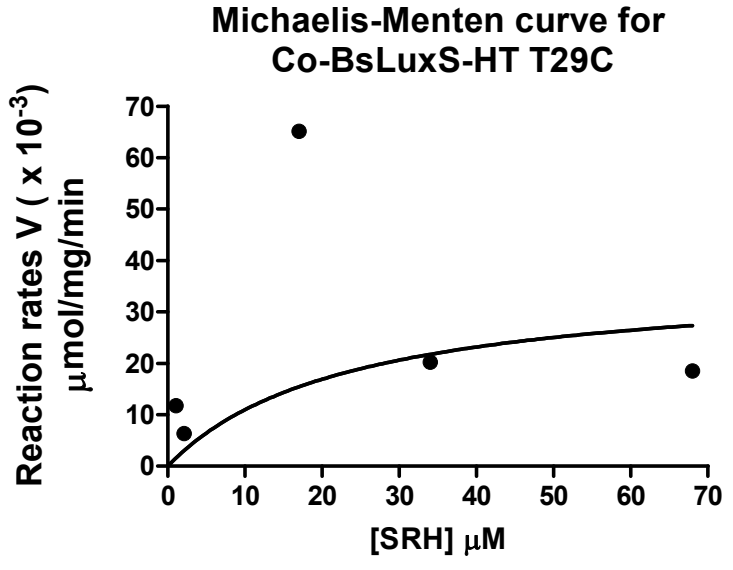

Fig. 14 | Michaelis-Menten curve for Co-BsLuxS-HT T29C. The Michaelis-Menten curve for the mutant Co-BsLuxS-HT T29C is shown. The kinetic parameters determined were: K_M = 24 ± 112 μM, V_{max} = 0.8 x 10^{-5} μmol/s and the k_{cat} = 0.012 ± 0.002 $M^{-1}s^{-1}$.

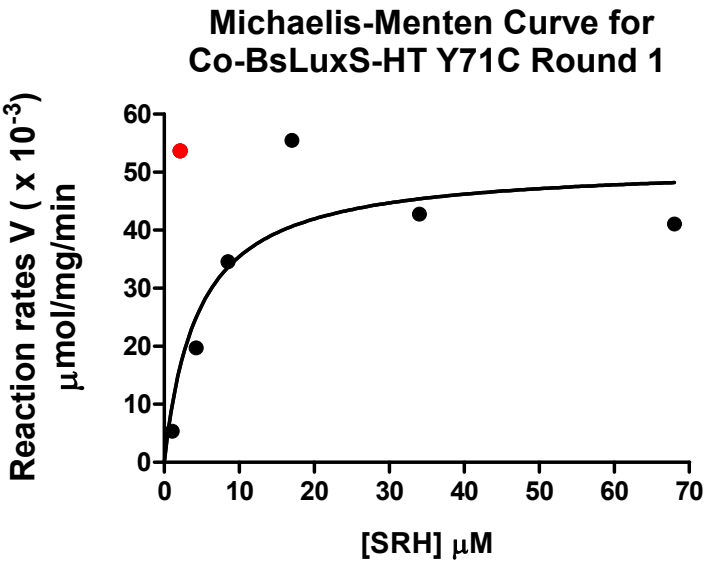

Fig. 15 | Michaelis-Menten curve for Co-BsLuxS-HT Y71C Round 1. The Michaelis-Menten curve for Co-BsLuxS-HT Y71C in round 1 is shown. The kinetic parameters determined were: $K_M = 4.5 \pm 2.8$ µM, $V_{max} = 1.12 \times 10^{-5}$ µmol/s and $k_{cat} = 0.015 \pm 0.05$ $M^{-1}s^{-1}$. The red dot is an outlier determined by graph pad prism 5.0.

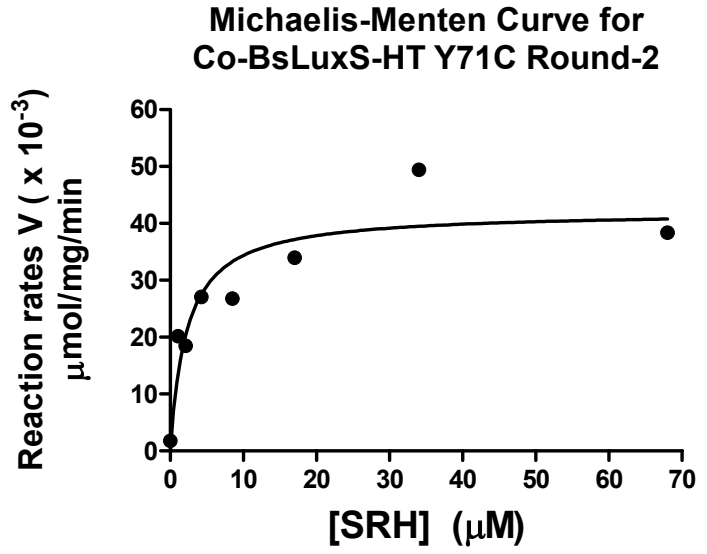

Fig. 16 | Michaelis-Menten curve for Co-BsLuxS-HT Y71C Round 2. The Michaelis-Menten curve for Co-BsLuxS-HT Y71C in round 2 is shown. The kinetic parameters determined were: $K_M = 2 \pm 1$ µM , $V_{max} = 0.9 \times 10^{-5}$ µmol/s and $k_{cat} = 0.012 \pm 0.05$ $M^{-1}s^{-1}$.

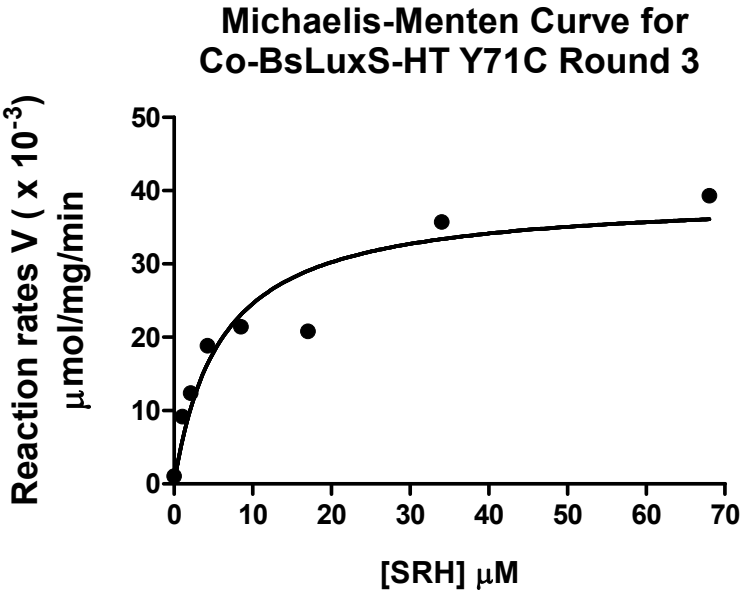

Fig. 17 | Michaelis-Menten curve for Co-BsLuxS-HT Y71C Round 3. The Michaelis-Menten's curve for the mutant Co-BsLuxS-HT Y71C in round 3 is shown. The kinetic parameters determined were: K_M= 5.9 ± 2.2 μM, V_{max} = 0.9 x 10^{-5} μmol/s and k_{cat} = 0.01 ± 0.03 $M^{-1}s^{-1}$.

REFERENCES

1. Waters, C. M.; Bassler, B. L. Quorum sensing: cell-to-cell communication in bacteria. *Ann. Rev. Cell Dev. Biol.* **2005**, *21*, 319-346.

2. Mok, K. C.; Wingreen, N. S.; Bassler, B. L. *Vibrio harveyi* quorum sensing: a coincidence detector for two autoinducers controls gene expression. *EMBO J.* **2003**, *22*, 870-881.

3. Xavier, K. B.; Bassler, B. L. LuxS quorum sensing: more than just a numbers game. *Curr. Opin. Microbiol.* **2003**, *6*, 191-197.

4. Winzer, K.; Hardie, K. R.; Williams, P. LuxS and autoinducer-2: their contribution to quorum sensing and metabolism in bacteria. *Adv. App. Microbiol.* **2003**, *53*, 291-396.

5. Surette, M. G.; Miller, M. B.; Bassler, B. L. Quorum sensing in *Escherichia coli*, *Salmonella typhimurium* and *Vibrio harveyi*: a new family of genes responsible for autoinducer production. *Proc. Natl. Acad. Sci. U.S.A.* **1999**, *96*, 1639-1644.

6. (a) Miller, M. B.; Skorupski, K.; Lenz, D. H.; Taylor, R. K.; Bassler, B. L. Parallel quorum sensing systems converge to regulate virulence in *Vibrio cholerae*. *Cell.* **2002**, *110*, 303-314. (b) Chen, X.; Schauder, S.; Potier, N.; Van Dorsselaer, A.; Pelczer, I.; Bassler, B. L.; Hughson, F. M. Structural identification of a bacterial quorum-sensing signal containing boron. *Nature.* **2002,** *415*, 545-549.

7. Miller, S. T.; Xavier, K. B.; Campagna, S. R.; Taga, M. E.; Semmelhack, M. F.; Bassler, B. L.; Hughson, F. M. *Salmonella typhimurium* recognizes a chemically distinct form of the bacterial quorum-sensing signal AI-2. *Mol. Cell.* **2004**, *15*, 677-687.

8. (a) Lewis, H. A.; Furlong, E. B.; Laubert, B.; Eroshkina, G. A.; Batiyenko, Y.; Adams, J. M.; Bergseid, M. G.; Marsh, C. D.; Peat, T. S.; Sanderson, W. E.; Sauder, J. M.; Buchanan, S. G. A structural genomics approach to the study of quorum sensing: crystal structures of three LuxS orthologs. *Struc.*. **2001**, *9*, 527-537. (b) Das, S. K. S.; Scott. E; Baker, P.J; Ruzheinikov, S.N; Foster, S; Hartley, A; Horsburgh, M.J; Rice, D.W. Cloning, purification, crystallization and preliminary crystallographic analysis of *Bacillus subtilis* LuxS. *Acta. Crystallogr. D. Biol. Crystallogr.* **2001**, *57*, 1324-5.

9. Zhu, J.; Dizin, E.; Hu, X.; Wavreille, A.-S.; Park, J.; Pei, D. *S*-ribosylhomocysteinase (LuxS) is a mononuclear iron protein. *Biochem.* **2003**, *42*, 4717-4726.

10. Rajan, R.; Zhu, J.; Hu, X.; Pei, D.; Bell, C. E. Crystal structure of *S*-ribosylhomocysteinase (LuxS) in complex with a catalytic 2-ketone intermediate. *Biochem.* **2005**, *44*, 3745-3753.

11. (a) Hardie, K. R.; Cooksley, C.; Green, A. D.; Winzer, K. Autoinducer-2 activity in *Escherichia coli* culture supernatants can be actively reduced despite maintenance of an active synthase, LuxS. *Microbiol.* **2003**, *149*, 715-728. (b) Ruzheinikov, S. N.; Das, S. K.; Sedelnikova, S. E.; Hartley, A.; Foster, S. J.; Horsburgh, M. J.; Cox, A. G.; McCleod, C. W.;

Mekhalfia, A.; Blackburn, G. M.; Rice, D. W.; Baker, P. J. The 1.2 Å structure of a novel quorum-sensing protein, *Bacillus subtilis* LuxS. *J. Mol. Biol.* **2001**, *313*, 111-122.

12. (a) Giglione, C.; Pierre, M.; Meinnel, T. Peptide deformylase as a target for new generation, broad spectrum antimicrobial agents. *Mol. Microbiol.* **2000**, *36*, 1197-1205. (b) Baldwin, E. T.; Harris, M. S.; Yem, A. W.; Wolfe, C. L.; Vosters, A. F.; Curry, K. A.; Murray, R. W.; Bock, J. H.; Marshall, V. P.; Cialdella, J. I.; Merchant, M. H.; Choi, G.; Deibel, M. R. Crystal structure of type II peptide deformylase from *Staphylococcus aureus*. *J. Biol. Chem.* **2002**, *277*, 31163-31171. (c) Rajagopalan, P. T. R.; Pei, D. Oxygen-mediated inactivation of peptide deformylase. *J. Biol. Chem.* **1998**, *273*, 22305-22310.

13. (a) Pei, D.; Zhu, J. Mechanism of action of S-ribosylhomocysteinase (LuxS). *Curr. Opin. Chem.Biol.* **2004**, *8*, 492-497. (b) Zhu, J.; Knottenbelt, S.; Kirk, M. L.; Pei, D. Catalytic mechanism of *S*-ribosylhomocysteinase: ionization state of active-site residues. *Biochem.* **2006**, *45*, 12195-12203. (c) Zhu, J.; Patel, R.; Pei, D. Catalytic mechanism of *S*-ribosylhomocysteinase (LuxS): stereochemical course and kinetic isotope effect of proton transfer reactions. *Biochem.* **2004**, *43*, 10166-10172.

14. Lowery, C. A.; Dickerson, T. J.; Janda, K. D., Interspecies and interkingdom communication mediated by bacterial quorum sensing. *Chem. Soc. Rev.* **2008**, *37*, 1337-1346.

15. Malanovic, N.; Streith, I.; Wolinski, H.; Rechberger, G.; Kohlwein, S. D.; Tehlivets, O. *S*-adenosyl-L-homocysteine hydrolase, key enzyme of methylation metabolism, regulates phosphatidylcholine synthesis and triacylglycerol homeostasis in yeast. *J. Biol. Chem.* **2008**, *283*, 23989-23999.

16. Vendeville, A.; Winzer, K.; Heurlier, K.; Tang, C. M.; Hardie, K. R. Making 'sense' of metabolism: autoinducer-2, LuxS and pathogenic bacteria. *Nat. Rev. Micro.* **2005**, *3*, 383-396.

17. Semmelhack, M. F.; Campagna, S. R.; Federle, M. J.; Bassler, B. L. An expeditious synthesis of DPD and boron binding studies. *Org. Lett.* **2005**, *7*, 569-572.

18. Bennett, J. M., K.; Kimmell, C. Synthesis and analysis of a versatile imine for the undergraduate organic chemistry laboratory. *J. Chem. Edu.* **2006**, *83*.

19. (a) Semmelhack, M. F.; Campagna, S. R.; Hwa, C.; Federle, M. J.; Bassler, B. L. Boron binding with the quorum sensing signal AI-2 and analogues. *Org. Lett.* **2004**, *6*, 2635-2637. (b) Meijler, M. M.; Hom, L. G.; Kaufmann, G. F.; McKenzie, K. M.; Sun, C.; Moss, J. A.; Matsushita, M.; Janda, K. D. Synthesis and biological validation of a ubiquitous quorum-sensing molecule. *Ang. Chem. Int. Edi.* **2004**, *43*, 2106-2108.

20. (a) Rasmussen, T. B.; Givskov, M. Quorum-sensing inhibitors as anti-pathogenic drugs. *Int. J. Med.Microbiol.* **2006**, *296*, 149-161. (b) Givskov, M.; de Nys, R.; Manefield, M.; Gram, L.; Maximilien, R.; Eberl, L.; Molin, S.; Steinberg, P. D.; Kjelleberg, S. Eukaryotic interference with homoserine lactone-mediated prokaryotic signalling. *J. Bac.* **1996**, *178*, 6618-22. (c) Rasmussen, T. B.; Skindersoe, M. E.; Bjarnsholt, T.; Phipps, R. K.; Christensen, K. B.; Jensen, P. O.; Andersen, J. B.; Koch, B.; Larsen, T. O.; Hentzer, M.;

Eberl, L.; Hoiby, N.; Givskov, M. Identity and effects of quorum-sensing inhibitors produced by *Penicillium* species. *Microbiol.* **2005**, *151*, 1325-1340.

21. Shen, G.; Rajan, R.; Zhu, J.; Bell, C. E.; Pei, D. Design and synthesis of substrate and intermediate analogue inhibitors of *S*-ribosylhomocysteinase. *J. Med. Chem.* **2006**, *49*, 3003-3011.

22. (a) Camarasa, M. J.; Velazquez, S.; San-Felix, A.; Perez-Perez, M. J.; Bonache, M. C.; Castro, S. D. TSAO Derivatives, inhibitors of HIV-1 reverse transcriptase dimerization: recent progress. *Curr. Pharma. Desi.* **2006**, *12*, 1895-1907. (b) Gupta, S.; Dua, R.; Camarasa, M.J.; Velazquez, S.; Nhonthachit, P.; Fransen, S.; McCann, D.; Petropolus, D.; Parkin, N.; Huang, W. Novel electrophoretic tag based *in vitro* assay to quantify dimerization of p66/p51 subunits of HIV-I reverse transcriptase (RT). **2007**, *23*. (c) Kolodziejski, P. J.; Koo, J.-S.; Eissa, N. T. Regulation of inducible nitric oxide synthase by rapid cellular turnover and cotranslational down-regulation by dimerization inhibitors. *Proc. Natl. Acad. Sci.* **2004**, *101*, 18141-18146. (d) McMillan M. A.K.; Auld D.S.; Baldwin J.J.; Blasko E.; Browne L.J.; Chelsky D.; Davey D.; Dolle R.E.; Eagen K.A.; Erickson S.; Feldman R.I.; Glaser C.B.; Mallari C.; Morrissey M.M.; Ohlmeyer M.H.J.; Pan G.; Parkinson J.K.; Phillips G.B.; Polokoff M.A.; Sigal N.H.; Vergona R.; Whitlow M.; Young T.A.; Devlin J.A. Allosteric inhibitors of inducible nitric oxide synthase dimerization discovered via combinatorial chemistry. *Proc. Natl. Acad. Sci. U.S.A.* **2000**, 1506-1511.

23. (a) Chen, W.; Weiss, N. M.; Sorger, P.K. Classic and contemporary approaches to modelling biochemical reactions. *Genes. Dev.* **2010,** *24*, 1861-1875. (b) Malladi, V. L. A.; Sobczak, A. J.; Meyer, T. M.; Pei, D.; Wnuk, S. F. Inhibition of LuxS by *S*-ribosylhomocysteine analogues containing a [4-aza] ribose ring. *Bioorg. & amp; Med.Chem.* **2011**, *19*, 5507-5519.

24. Boyne, A. F.; Ellman, G. L. A methodology for analysis of tissue sulfhydryl components. *Ana. Biochem.* **1972**, *46*, 639-653.

25. Alfaro, J. F.; Zhang, T.; Wynn, D. P.; Karschner, E. L.; Zhou, Z. S. Synthesis of LuxS inhibitors targeting bacterial cell-cell communication. *Org. Lett.* **2004**, *6*, 3043-3046.

26. (a) Koh, Y.; Matsumi, S.; Das, D.; Amano, M; Davis, A.D.; Li, J.; Leschenko, S.; Baldridge, A.; Shloda, T.; Yarchoan, R.; Ghosh, K. A.; Mitsuya, H. Potent inhibition of HIV-1 replication by novel non-peptidyl small molecule inhibitors of protease dimerization. *J. Biol. Chem.* **2007**, *282*, 28709-28720. (b) Ason, B.; Handayani, R.; Williams, C. R.; Bertram, J. G.; Hingorani, M. M.; O'Donnell, M.; Goodman, M. F.; Bloom, L. B. Mechanism of loading the *Escherichia coli* DNA polymerase III β sliding clamp on DNA. *J. Biol. Chem.* **2003**, *278*, 10033-10040. (c) Lee, H. H. Crystallization and preliminary X-ray crystallographic analysis of enoyl-acyl carrier protein reductase from *Helicobacter pylori*. *Acta. Crystallogr. D. Biol. Crystallogr.* **2002**, *58*, 1071-1073.

27. Liu, R. Synthesis of SRH and C3 analogs as potential LuxS inhibitors. M.S., University of San Francisco, San Francisco, CA, 2012.

28. Zhang, Z. M.; Gentile, T. R.; Migdall, A. L.; Datla, R. U. Transmittance measurements for filters of optical density between one and ten. *Appl. Opt.* **1997**, *36*, 8889-8895.

29. March, S. C.; Parikh, I.; Cuatrecasas, P. A simplified method for cyanogen bromide activation of agarose for affinity chromatography. *Ana. Biochem.* **1974**, *60*, 149-152.

30. Marion M, B. A rapid and sensitive method for the quantitation of microgram quantities of protein utilizing the principle of protein-dye binding. *Ana. Biochem.* **1976**, *72*, 248-254.

31. Krohn, R. I. The colorimetric detection and quantitation of total protein. *Curr. Prot. F. Ana. Chem.* **2001**.

32. Rüchel, R.; Steere, R. L.; Erbe, E. F. Transmission-electron microscopic observations of freeze-etched polyacrylamide gels. *J. Chrom. A* **1978**, *166*, 563-575.

33. Flavell, R.A.; Scott, D. L.; Bandle, E. F., Weissmann, C. Site-directed mutagenesis: effect of an extracistronic mutation on the *in vitro* propagation of bacteriophage Qbeta RNA. *Proc. Natl. Acad. Sci. U S A.* **1975**, *72*, 367–371.

34. Reiterer, F.; Nachtmann, F.; Knapp, G.; Spitzy, H. Fluorimetric determination of tyrosine and iodinated thyronines as the fluorescamine derivatives. *Micro. Acta.* **1978**, *69*, 115-124.

35. Wnuk, S. F.; Robert, J.; Sobczak, A. J.; Meyers, B. P.; Malladi, V. L. A.; Zhu, J.; Gopishetty, B.; Pei, D. Inhibition of *S*-ribosylhomocysteinase (LuxS) by substrate analogues modified at the ribosyl C3 position. *Bioorg. & Med. Chem.* **2009**, *17*, 6699-6706.

36. Chen, W.; Niepel, M.; Sorger, P. Classic and contemporary approaches to modeling biochemical reactions. *Gene. Dev.* **2010**, *24*, 1861-75.

37. Mathis, G. Probing molecular interactions with homogeneous techniques based on rare earth cryptates and fluorescence energy transfer. *Cli.Chem.* **1995**, *41*, 1391-7.

38. Aoyama, T. T. T.; Kodomari, M. A convenient synthesis of thioacetates and thiobenzoates using silica-gel supported potassium thioacetate. *Syn. Comm.* **2003**, *33*, 3817-3824.

39. Liu, H.; Naismith, J. An efficient one-step site-directed deletion, insertion, single and multiple-site plasmid mutagenesis protocol. *BMC. Biotech.* **2008**, *8*, 91.

40. Zhu, J.; Pei, D. A LuxP-based fluorescent sensor for bacterial autoinducer II. *ACS Chem.Biol.* **2008**, *3*, 110-119.